

## Durham E-Theses

---

*Some experimental and theoretical aspects of structure  
and bonding in a series of polyalkyl acrylates and  
methacrylates studied by ESCA*

Thomas, Herbert Ronald

### How to cite:

---

Thomas, Herbert Ronald (1975) *Some experimental and theoretical aspects of structure and bonding in a series of polyalkyl acrylates and methacrylates studied by ESCA*, Durham theses, Durham University. Available at Durham E-Theses Online: <http://etheses.dur.ac.uk/8904/>

### Use policy

---

The full-text may be used and/or reproduced, and given to third parties in any format or medium, without prior permission or charge, for personal research or study, educational, or not-for-profit purposes provided that:

- a full bibliographic reference is made to the original source
- a [link](#) is made to the metadata record in Durham E-Theses
- the full-text is not changed in any way

The full-text must not be sold in any format or medium without the formal permission of the copyright holders.

Please consult the [full Durham E-Theses policy](#) for further details.

UNIVERSITY OF DURHAM

A Thesis entitled

Some Experimental and Theoretical Aspects of Structure  
and Bonding in a Series of Polyalkyl Acrylates and  
Methacrylates Studied by ESCA

Submitted by

Herbert Ronald Thomas

A candidate for the Degree of Master of Science  
1975



### ACKNOWLEDGEMENTS

The work described in this thesis was carried out under the supervision of Dr. D.T. Clark and I would like to extend my sincere appreciation for his encouragement and inexhaustible assistance throughout this work. I am indebted to Xerox Corporation, Webster, New York for their generous financial support for my family and I, and to S.R.C. for provision of equipment.

I particularly wish to thank the following individuals within Xerox Corporation: Dr. C.B. Duke, Dr. J. Goldfrank, Dr. M. Shahin and Dr. M. Smith, without whose efforts this work would not have been possible.

Thanks are also due to the staff of the University of Durham Computer Unit and to the individuals of the workshop whose able workmanship provided the special apparatus necessary for this work.

## ABSTRACT

The core and valence levels of a series of polyalkyl-acrylates and polyalkyl, and aryl methacrylates have been studied by ESCA. From an analysis of the individual component peaks for the  $C_{1s}$  and  $O_{1s}$  core levels and from a comparison of the relative area ratios it is shown that ESCA may be applied to the study of the immediate surface compositions of these acrylic systems. The results presented suggest that on the ESCA depth profiling scale the technique statistically samples the repeat units with no evidence for preferential orientation of the side chains at the surface. For some systems ESCA provided evidence for a degree of surface oxidation and hydrocarbon contamination. The valence levels of the acrylic polymers are shown to be characteristic of the particular polymer and can be used for identification of the isomeric configuration of the alkyl groups.

The measured absolute and relative binding energies of the core levels of the polymer systems have been compared with a series of simple model compounds and different conformational configurations of models of polyacrylic acid and polymethyl-acrylate within the semi-empirical CNDO/2 SCF MO formalism using the charge potential model.

## C O N T E N T S

	<u>Page</u>
<u>CHAPTER 1. Electron Spectroscopy for Chemical Applications (ESCA)</u>	1
(i) General Introduction	1
(ii) General Information on Electron Spectroscopy	2
(a) Ultraviolet Photoelectron Spectroscopy	2
(b) Auger Electron Spectroscopy	3
(c) X-ray Photoelectron Spectroscopy	8
(iii) Fundamental Electronic Processes Involved in ESCA	10
(iv) Basic Features of ESCA	15
(a) Core Electron Binding Energies	15
(b) Valence Electron Binding Energies	23
(c) Multiplet Splittings	25
(d) Spin-Orbit Splitting and Electrostatic Splitting	26
(e) Shake-up and Shake-off Processes	29
(f) Escape Depths	32
(g) Line Shape Analysis in ESCA	33
(v) ESCA Instrumentation	33
(a) X-Ray Equipment	35
(b) Source Chamber	37
(c) Analyzer Chamber	39
(d) Electron Detector	41
<u>CHAPTER 2. Studies of Structure and Bonding in Polymers through the Application of ESCA</u>	43
(i) General Information	43

	<u>Page</u>
(ii) Sample Preparation and Polymer Nomenclature	44
(a) Powders	45
(b) Solution Cast Films	45
(c) Pressed or Extruded Films	45
(d) 'In situ' Polymerized Films	46
(iii) Static Studies on Polymers with ESCA	50
(a) Chemical Composition	50
(b) Structural Details	55
(c) Fine Structural Details	59
(iv) Dynamic Studies on Polymer Systems	63
(a) Surface Treatments	63
General Introduction to Experimental Sections	67
<u>CHAPTER 3. Core and Valence Energy Levels of a Series of Poly-alkylacrylates</u>	69
(i) General Introduction	69
(ii) Experimental	71
(a) Samples	71
(b) Sample Preparation	72
(c) Post-treatment of Polyisopropyl Acrylate	73
(d) Instrumentation	74
(iii) Theoretical	75
(iv) Results and Discussion for Model Compounds	76
(a) Core Levels of Model Compounds	76
(1) Experimental	76
(2) Theoretical	80
(b) Valence Levels of Model Compounds	85

	<u>Page</u>
(v) Results and Discussion for Polyacrylates	88
(a) Experimental	88
Polymer Compositions and Absolute and Relative Binding Energies of Core Levels	88
(b) Theoretical Models for the Quantitative Interpretation of Absolute and Relative Binding Energies	94
(c) Valence Levels of Polyacrylates	103
(vi) Polyalkyl Acrylates for which the Surface Composition is Different from the Bulk	105
(vii) ESCA Studies of Adsorption at Surfaces	113
 <u>CHAPTER 4. Studies of Structure and Bonding in a Series of Poly-alkyl, and -aryl Methacrylates through the Application of ESCA</u>	 116
(i) Introduction	116
(ii) Experimental	118
(a) Samples	118
(b) Sample Preparation	120
(c) Post-treatment of Polyisopropyl Methacrylate	120
(d) Instrumentation	121
(iii) Theoretical	121
(iv) Results and Discussion for Polyalkylmethacrylates	121
(a) Experimental	121
(b) Valence Levels of Polymethacrylates	131
(v) ESCA Studies of Adsorption at Surfaces	131
 APPENDIX A	
 APPENDIX B	
 REFERENCES	

CHAPTER 1

Electron Spectroscopy for Chemical Applications (ESCA)

## CHAPTER 1

### Electron Spectroscopy for Chemical Applications (ESCA)

#### (i) General Introduction.

In electron spectroscopy the interaction of a mono-energetic beam of exciting radiation with a molecule results in the ejection of electrons from the molecule whereupon the binding energies (B.E.'s) of the electrons are determined. Today there are essentially three types of exciting radiation used; u.v. light, electrons and X-rays. There are, as in most areas of spectroscopy, advantages and disadvantages to each technique.

U.V. excitation has the advantage over the other techniques in that much higher resolution can be obtained but is limited to the low B.E. electrons found in the valence levels. This technique, commonly referred to as photoelectron spectroscopy (UPS) is usually limited to vapour phase analysis<sup>1</sup> but solids have been investigated.<sup>2</sup>

Electron excitation has been used to study both vapours and solids and is normally referred to as Auger spectroscopy,<sup>3</sup> and can be viewed as a study of 'secondary electrons'. Auger spectroscopy has the advantage of possessing a continuously variable energy, in which the electron beam can be focussed but has the disadvantage of a low signal to background ratio when compared to the other two techniques. Recent findings have also shown the electron beam to be destructive to the surfaces studied thereby giving results which are not representative of the original surface.<sup>4</sup>

X-ray excitation has the advantage that the core and valence levels for all atoms, excluding H and He, where there is no distinction between core and valence levels, can be studied and furthermore solids, gases and liquids can be conveniently studied. This technique, which is the topic of this thesis, using soft X-rays (e.g.  $Mg_{K\alpha_{1,2}} = 1253.7$  eV,  $Al_{K\alpha_{1,2}} = 1486.6$  eV) is known as ESCA<sup>5,6</sup> (Electron Spectroscopy for Chemical Applications) or XPS (X-ray Photoelectron Spectroscopy).

Chapter 1 of this thesis is concerned with the theory of electron spectroscopy and the instrumentation utilized in ESCA experiments.

Chapter 2 is a review of the current literature on the applications of ESCA to structure and bonding in polymers and presents the objectives of the experimental portion of this thesis.

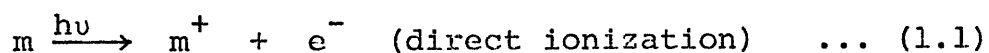
Chapters 3 and 4 are ESCA studies and theoretical treatments of a series of polyacrylates and polymethacrylates respectively.

(ii) General Information on Electron Spectroscopy.

Electron spectroscopy is the study of the energy of electrons ejected from a molecule by the influence of a mono-energetic beam of radiation directed on the molecule. There are in practice today three types of radiation used to study the electronic structure of molecules: (a) u.v. radiation, (b) electron beams and (c) X-rays.

(a) The excitation of the electronic structure with u.v. radiation is commonly referred to as UPS (Ultraviolet Photoelectron Spectroscopy) and makes use generally of the

He(I) and He(II) resonance lines as light sources with photon energies of 21.2 eV and 40.8 eV respectively, although Kr (10.3 eV) and Hg (4.89 eV) are also available. This technique was introduced by D.W. Turner and M.I. Al-Joboury at Imperial College, London in 1961<sup>1</sup> and is used to study essentially the valence levels of a molecule, where the fundamental processes that eject electrons are:



Because the inherent line width in UPS is of the order of 5 m eV, (HeI), under high resolution, vibrational fine structure accompanying valence level photoionizations of H<sub>2</sub>, H<sub>2</sub>O and D<sub>2</sub>O has been observed by L. Asbrink and J.W. Kabalais;<sup>7,8</sup> such resolution is presently not possible by either Auger or ESCA.

(b) Auger Electron Spectroscopy (AES) as conventionally applied is based on the analysis of the energy of electrons that are ejected from a sample as a consequence of excitation by primary electron beams typically ~ 2 kV. The electrons that are of principal interest are those resulting from 'Auger' processes and the electrons possess characteristic energies which are directly related to the energy level in the atoms from which they are ejected. This technique is truly a surface analysis technique in that the penetration depth for the exciting electrons is only about 5 atomic layers.<sup>3</sup> Auger spectroscopy may be viewed as a two step process involving the ejection of an electron from an inner shell by a photon

or electron. When electrons are used as the radiation source the incident electron is emitted along with the inner shell electron and when photons are used as the energy source only the inner shell electron is ejected.

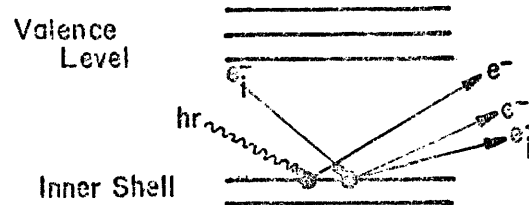


Figure 1.1. Inner Shell Photoionization during Auger Process.

The second step involves an electron dropping down from a higher level to the vacancy in the inner shell with the simultaneous emission of an X-ray or a second electron (the study of emitted X-rays is referred to as X-ray fluorescence spectroscopy and will be discussed later). When the electrons drop from a valence shell to fill the inner shell vacancy the chemical shifts involved are related to both outer and inner shells and in a few suitable cases information can be gained on the binding energies of both shells.

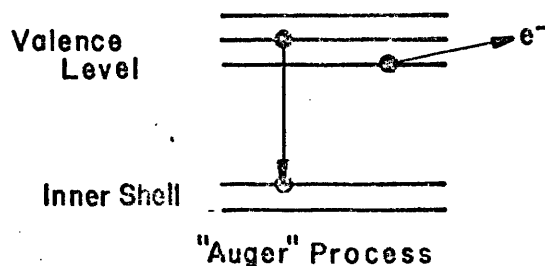


Figure 1.2. Secondary Electron Emission during Auger Process.

Where the electronic vacancy in the inner shell is filled by an electron from another inner shell the Auger spectra is useful for analysis of inner shell transitions. Transitions of this type are very efficient and lead to very short lifetimes with well resolved spectra.

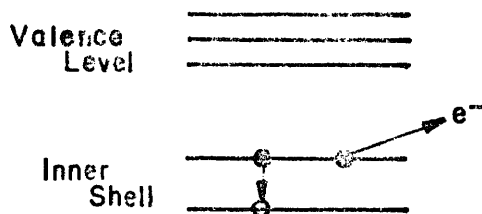


Figure 1.3. Inner Shell Emission during Auger Process.

For a general Auger transition which involves any set of levels KLM, a peak should appear at:

$$E(Z) = E_K - E_L - E_M (Z + \Delta) - \phi_A \quad \dots (1.3)$$

where: Z is the atomic number

$\Delta = 1$  (due to the extra positive charge from the loss of an electron)

$\phi_A$  is the work function of the analyzer

$E_K$  is the energy from a K level transition

$E_L$  is the energy from a L level transition

$E_M$  is the energy from a M level transition

This equation (1.3) can, however, lead to errors in some cases because the final state of the doubly ionized atom must be defined. The additional definition is needed because the energies involved in the transitions in the Auger process are governed by the coupling scheme amongst electronic wave-functions in the initial (single ionization) as well as the

final (double ionization) electronic configuration. LS coupling dominates for light elements and jj coupling for heavy elements. The rate of emission of Auger electrons is determined, essentially, by the K shell ionization rate. The other mode of de-excitation, X-ray emission, is essentially very inefficient<sup>9</sup> for the lighter elements and is negligible for energies less than 500 eV, while Auger efficiency is approximately comparable to X-ray emission at about 2000 eV. The relative efficiencies between X-ray fluorescence and Auger current decrease for the low atomic number elements and Auger current is relatively constant with Z when lower energy transitions are involved for the heavy elements.

The decrease in X-ray fluorescence with decreasing energy is due to the fact that it is an electromagnetic (dipole) process and depends mostly on the acceleration of the orbiting electron. The Auger process, however, is dependent upon the electrostatic forces accompanied by a vacancy in the inner shell.

Essentially there are three types of chemical information which may in principle be obtained from Auger spectra. However, it should be pointed out that the extraction of this information is by no means straightforward since differences in energy levels are involved. The first is the chemical shift due to the shifts of the inner shell energy levels arising from changes in valence electron distributions. The second type of information pertains to the valence levels themselves. The valence bond spectra are usually quite pronounced due to the redistribution (relaxation) of electrons

upon formation of a new electronic configuration. The third type of information that is obtained is much more vague and is referred to as 'molecular orbital energy spectra' and is of course also involved with part of the valence levels. If the molecular orbitals are known for a specific compound then the valence energy levels can be compared. This technique although it has the limitation that to-date molecular orbitals cannot be assigned to specific energy levels the symmetry of its component wave functions can be used to 'infer' point group symmetry of an atom in a crystal to locate it within a unit cell.<sup>10</sup>

Under ideal conditions minute amounts of surface atoms have been detected, down to the range of  $10^6$  atoms/cm.<sup>3</sup> at the surface. However, recent evidence has shown that the surfaces of materials studied are altered due to radiation damage from the electron beam,<sup>4</sup> these findings, being relatively new (July 1975), will not be elaborated on at this time.

The emission of X-rays instead of electrons leads to X-ray fluorescence (secondary-emission analysis) and is an excellent means of qualitative analysis for constituents of atomic number greater than eight (8). Concentrations down to 0.1% for most elements and 0.01% for elements around Fe, Co, Ni have been detected. X-ray emission tables exist<sup>11</sup> which enable a particular element to be observed at a position of its strongest lines, and then all of its lines can be identified in the spectrum once its presence is known. Figure 1.4 is a plot of the X-ray fluorescence yield and

Auger electron yields in the K shell as a function of atomic number (Z) for the light elements in the periodic table.

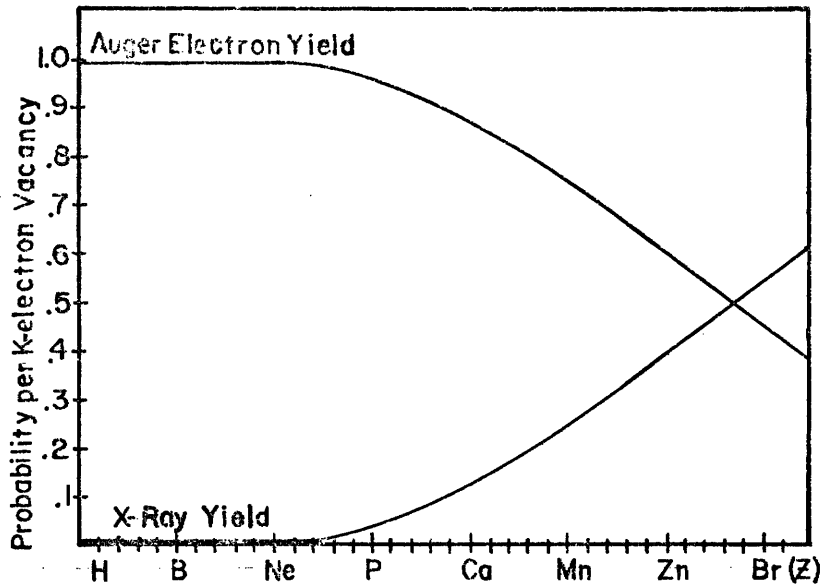


Figure 1.4. X-ray Fluorescence Yield and Auger Electron Yield in the K-shell as a Function of Atomic Number.

(c) The third source of radiation used to excite the electronic structure is X-ray radiation and it is the application of this process that is the topic of this thesis. This technique was originally developed in the early 1950's by Siegbahn and co-workers at the Institute of Physics, Uppsala University, Sweden, and in 1970 the first commercial instrument was made available. The technique was well documented in the first ESCA book<sup>5</sup> and the name ESCA was coined by Siegbahn for 'Electron Spectroscopy for Chemical Applications'. The ESCA technique is also known by other names, given below:

- (1) X-ray Photoelectron Spectroscopy (XPS).
- (2) High Energy Photoelectron Spectroscopy (HEPS).

(3) Induced Electron Emission Spectroscopy (IEES).

(4) Photoelectron Spectroscopy of the Inner Shell (PESIS).

Several of the more important features of ESCA are given below followed by detailed discussions on specific topics of ESCA:

- (1) The sample may be solid, liquid or gas and sample sizes are small being 1 mg. solid, 0.1  $\mu$ l. liquid and 0.5 cc. (STP) of a gas.
- (2) The technique is for all practical purposes non-destructive in that the X-ray flux is quite small ( $\sim 0.1$  millirad/sec.).<sup>12</sup> This is especially advantageous over Auger spectroscopy where the electron beam produces many surface changes, particularly in polymeric systems where cross-linking and degradation can occur.
- (3) The technique is independent of the spin properties of the nucleus and can be used to study any element of the periodic table with the exception of H and He where there is no distinction between the core and valence levels.
- (4) The technique has a comparable sensitivity to most other analytical techniques as illustrated in Table 1.1.
- (5) The information obtained from the spectrum is directly related to the molecular structure and the theoretical interpretation is relatively straightforward. Information is obtained on both the inner shell and the valence levels of the molecule enabling

a reasonably thorough analysis of the electronic structure of the molecule.

Table 1.1.

Sensitivities of Various Analytical Techniques

Technique	Surface	Bulk	Minimum Detectable Quantity (g.)
(a) Infrared		✓	$10^{-6}$
(b) Atomic absorption		✓	$10^{-9} \rightarrow 10^{-12}$
(c) Vapour phase chromatography		✓	$10^{-3} \rightarrow 10^{-7}$
(d) High pressure liquid chromatography		✓	$10^{-6} \rightarrow 10^{-9}$
(e) Electron spectroscopy for chemical appl.	✓		$10^{-10}$
(f) Mass spectroscopy		✓	$10^{-10} \rightarrow 10^{-15}$
(g) Neutron activation	✓		$10^{-12}$
(h) Ion-scattering spectrometry	✓		$10^{-15}$
(i) X-ray fluorescence	✓		$10^{-7}$
(j) Auger spectroscopy	✓		$10^{-14}$
(k) Secondary ion scattering spectrometry	✓		$10^{-13}$

(iii) Fundamental Electronic Processes Involved in ESCA.

In ESCA the samples being studied are irradiated with a monoenergetic beam of soft X-rays with photon energies typically being utilized:  $Mg_{K\alpha_{1,2}}$  (1253.7 eV),  $Al_{K\alpha_{1,2}}$  (1486.6 eV),  $Cu_{K\alpha}$  (8078 eV) and  $Cr_{K\alpha}$  (5415 eV).

Electrons in the molecule having binding energies less than the photon energy may be photoemitted, which allows for the study of both inner shell and valence energy levels. There are also electronic relaxation processes accompanying the loss of an electron (photoionization) which will be discussed later.

The total kinetic energy of an emitted photoelectron (KE, which may include the contributions from the vibrational, rotational and translational motions, as well as electronic) is given by the equation:

$$\text{K.E.} = h\nu - \text{B.E.} - E_r \quad \dots (1.4)$$

where  $h\nu$  is the energy of the incident photon (where  $h$  is Planck's constant and  $\nu$  is the frequency of the X-ray radiation), B.E. is the binding energy of the emitted electron which is defined as the positive energy required to remove an electron to infinity with zero kinetic energy, and  $E_r$  the recoil energy of the atom. Siegbahn, et al.<sup>6</sup> have calculated that the recoil energy of atoms decreases with increasing atomic number, e.g. H = 0.9 eV, Li = 0.1 eV, Na = 0.04 eV, K = 0.02 eV and Rb = 0.01 eV. Therefore it is evident that the  $E_r$  term only has significance for the lighter elements, when compared with the instrumental linewidths obtained with the present study of elements from carbon upwards in the periodic table. With the present resolution of typical ESCA spectra the excitations from the translational, vibrational and rotational motions are seldom observed, therefore only various electronic energy states are studied.

Therefore, the equation for a free molecule reduces to equation (1.5) below:

$$\text{K.E.} = h\nu - \text{B.E.} \quad \dots (1.5)$$

For samples studied in the gas phase a convenient energy reference is the vacuum level which corresponds to the relevant ion and electron being at infinite separation. In a solid sample the 'given' electronic levels are broadened into bands and a potential barrier exists at the surface. It is important to understand the relationship that exists between the B.E.'s observed experimentally by ESCA on solids vs. free molecules when compared with values calculated theoretically by ab initio and semi-empirical LCAO-MO-SCF treatments. Solid samples fall into essentially two classes: (1) conducting samples, such as metals, in electrical contact with the spectrometer and (2) insulating samples, such as polymers, which may not be in electrical contact.

The most convenient reference level for conducting samples is the Fermi level.<sup>6</sup> In a metal this level, sometimes referred to as the 'electron chemical potential' is defined as the highest occupied level.

The work function,  $\phi_s$ , for a solid is defined as the energy gap between the free electron level and the Fermi level in the solid. The vacuum levels for the solid sample and the spectrometer may however be different and the electron will experience either a retarding or accelerating potential equal to  $\phi_s - \phi_{\text{spec}}$  where  $\phi_{\text{spec}}$  is the work function of the spectrometer. In ESCA it is the K.E. of the electron when it enters the analyzer that is measured and taking zero binding energy to be the Fermi level of the sample the following equation results,

$$\text{B.E.} = h\nu - \text{K.E.} - \phi_{\text{spec}} \quad \dots (1.6)$$

Therefore the binding energy when referred to the Fermi level does not vary for samples but only depends upon the  $\phi_{\text{spec}}$  and remains a constant for all levels.

It is evident that for conducting samples in electrical contact with the spectrometer the Fermi level serves as a convenient reference level. For insulating samples, such as polymers, the Fermi level is not so well defined and usually lies somewhere between the filled valence levels and the empty conduction band.<sup>6</sup>

Equation (1.6) assumes equilibrium conditions during the ejection of an electron, which may or may not occur when the resistance of the sample is high compared with the electrical currents needed to replace the electron vacancies due to photoemission.

Several investigations have shown that the primary photoelectrons are rapidly slowed down by the interaction with matter and can generate intense currents of slow 'secondary' electron clouds at the surface of the sample.<sup>13-15</sup> These secondaries play an important role in establishing the electrical equilibrium at the surface of the sample and have been found to be approximately 20% of the photoelectron flux in a conducting sample and 99% of the flux in an insulating sample.<sup>13</sup>

A phenomenon related to the reference level of an insulating sample is the positive charging of the surface of a sample as a consequence of photoemission. This 'sample charging' is due to the inability of the sample to replace electrons at the surface from the surroundings in contact with

the sample, either through the bulk or across the surface. This sample charging results in a net retardation of photoemitted electrons from the surface and therefore larger binding energies are measured. This sample charging effects all photoemitted electrons by the same retardation voltage therefore shifting all the energies by an equal amount.<sup>16</sup> The extent of charging depends on a number of factors, such as temperature, surface and bulk conductivities of the sample, and electron and photon fluxes. Typical shifts for systems studied in this work were of the order of one to four eV.

If the sample has a uniformly distributed positive potential at the surface, then the energy equation for a solid becomes,

$$\text{K.E.} = h\nu - \text{B.E. (s)} - \phi_s - \Delta \quad \dots (1.7)$$

where  $\Delta$  is the energy shift due to the positive sample charge.

If either a non-uniform distribution or non-equivalent positive potential (often referred to as 'differential sample charging') occurs across the surface of the sample, one can see from equation (1.7) that for core levels of atoms of different charge that the electrons will encounter different retardation potentials at the surface and a broadening of the primary photoelectron peak will result. A more detailed consideration of this charging effect will be discussed in the second chapter on the applications of ESCA to polymers.

An effect observed on the primary photoelectron peak in the ESCA spectrum is a tailing to the higher B.E. (lower K.E.) of the peak. This effect is due to the inelastically scattered

electrons in which very small losses have occurred in photoemission from the bulk of the sample. The depth for which elastic photoemission occurs in solids has been estimated to be between  $50\text{\AA}$  and  $100\text{\AA}$  by depositing successive monolayers of an organic material on a metallic substrate and monitoring the disappearance of the primary photoelectron peaks of the substrate.<sup>6</sup> This phenomenon has been cleverly exploited in the 'depth profiling' of fluorinated polyethylene samples by monitoring the apparent 'escape depth' (elastic photoemission peaks) of different energy levels of atoms and correlating it to the depth of fluorination of the polymeric surface.<sup>17</sup> This technique will be discussed in detail in the second chapter on polymers.

(iv) Basic Features of ESCA.

(a) Core Electron Binding Energies.

The binding energy of a core level electron, in theory, is the difference in energy between the ground state molecule and the hole state. This energy difference varies for each atom and is characteristic for the particular element, thereby affording a technique to study all the elements (except for H and He) of the periodic table.<sup>5</sup> Listed below in Table 1.2. are the approximate core electron binding energies of the first row elements.

Table 1.2.

First Row Element Core Electron Binding Energies

	Li	Be	B	C	N	O	F	Ne
1s level in eV	55	111	188	284	399	532	686	867

The X-ray excitation of these core level electrons is amply done in ESCA since the typical  $K_{\alpha}$  radiation can penetrate well below the vacuum level. For core level electrons which are more tightly bound than can be studied by the  $K_{\alpha}$  X-ray typically used, there are core levels less bound that can be studied and the second row elements are shown in Table 1.3. with the typical core level binding energies.

Table 1.3.

Second Row Element Core Type Electron Binding Energies

eV	Na	Mg	Al	Si	P	S	Cl	A
1s	1072	1305	1560	1839	2149	2472	2823	3203
2s	63	89	118	149	189	229	270	320
2p <sub>1/2</sub>	31	52	74	100	136	165	202	247
2p <sub>3/2</sub>	31	52	73	99	135	164	200	245

It is readily seen that when using either  $Mg_{K_{\alpha 1,2}}$  (1253.7 eV) or  $Al_{K_{\alpha 1,2}}$  (1486.6 eV) that even in the second row elements, from aluminium on, the 1s levels are too tightly bound and higher levels must be chosen for study. When a choice of levels to be studied is made there are certain considerations which should be taken into account:

- (1) The core level should have a high cross section for photoionization, which results in a high intensity spectrum.
- (2) The escape depth of the photoemitted electron must be sufficient to allow reasonable depth study on the sample.

- (3) Levels should not be chosen where the binding energies of electrons from other elements at different levels will interfere with the one being studied e.g. the 1s level of B at 188 eV and the 2s level of P at 189 eV.
- (4) The linewidths should be sufficiently narrow so as not to obscure subtle chemical shifts such as the case where cross sections are similar for identical levels of different elements but linewidths are not, due to hole state lifetimes.
- (5) The peak should be well removed from high background signals, such as tails caused by inelastically scattered electrons, so that the signal to noise ratio is sufficiently high. A typical well resolved spectrum is shown in Figure 1.5a. where the conditions above are satisfied, and one where they are not, Figure 1.5b.

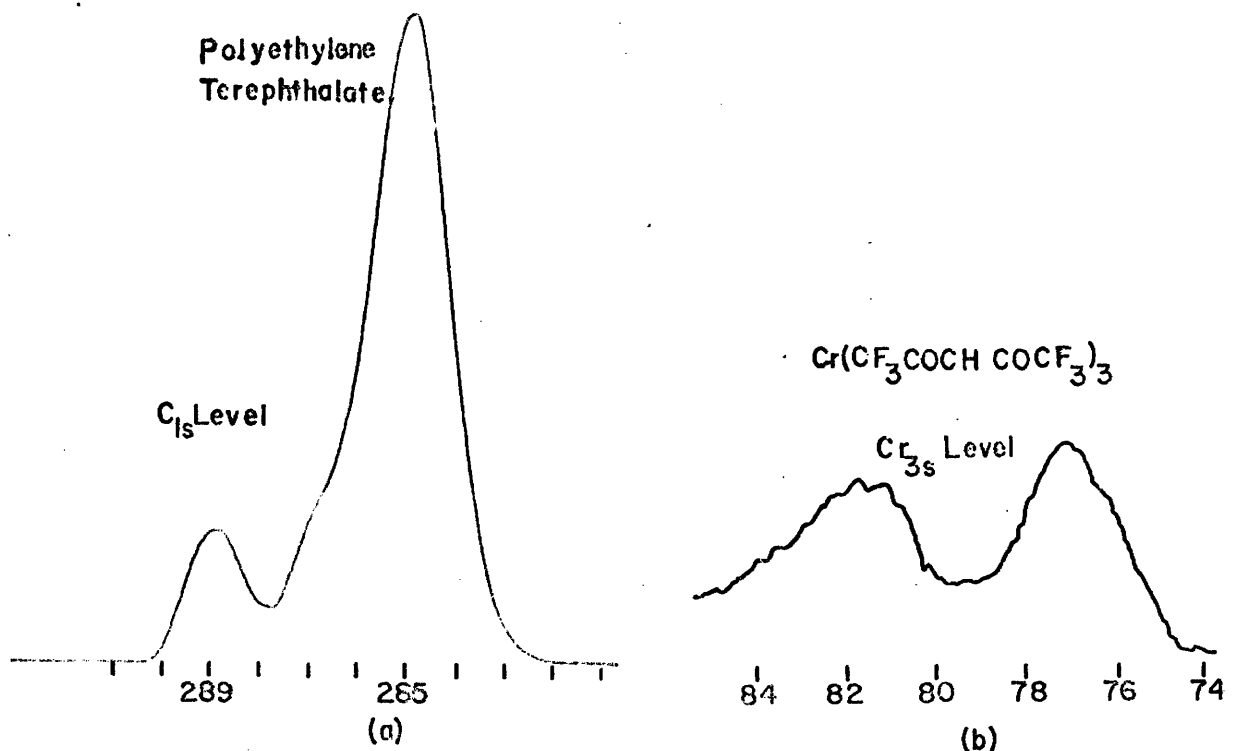


Figure 1.5. Typical Well-resolved (a) and Un-resolved (b) ESCA Spectra.

As can be seen from Figure 1.5a. for a given core level the peak intensities are proportional to the relative number of atoms in their particular environments. In some cases allowance must be made for reduction of the peak intensity due to shake-up and shake-off but this will be discussed later.

One of the most important measurements made in ESCA is the shift in core levels on atoms in different chemical environments and these relative shifts rather than the absolute binding energies are what theoreticians attempt to interpretate.

The theoretical treatment of absolute and relative binding energies involves computation of energy differences between the neutral molecule and relevant core ionized species. Such calculations have predominantly been within the Hartree-Fock formalism and therefore neglect correlation energy and relativistic effects. Fortunately in the particular case of levels which are localized, relativistic and correlation energy correction are atomic in nature and therefore contribute very little to differences in binding energy for a given core level. Calculations within the Hartree Fock formalism can account quantitatively for the substantial electronic reorganization accompanying core ionizations.

Koopmans' theorem<sup>18</sup> ignores the fact that the electrons remaining in atomic shells after photoionization relax as the photoelectron is emitted, providing stabilization energy for the ion.

Approximate relaxation energies have been calculated by Gelius<sup>19</sup> for many atoms in the early part of the periodic table

and it has been shown that their magnitude is approximately 75 - 85% of the square root of the final energy of the ions.

Therefore in practice these types of calculations are carried out within the Hartree-Fock model which neglects both relativistic and electron correlation effects. Figure 1.6. demonstrates the relationship between the experimental, Koopmans' theorem (where the assumption that the initial one-electron orbitals,  $\phi_i$ , making up the electron wave function  $\psi(n)$  are identical to the final orbitals  $\phi_i'$  making up the  $n-1$  electron wavefunction  $\psi_{(n-1)}^F$ ) and binding energies calculated as energy differences).

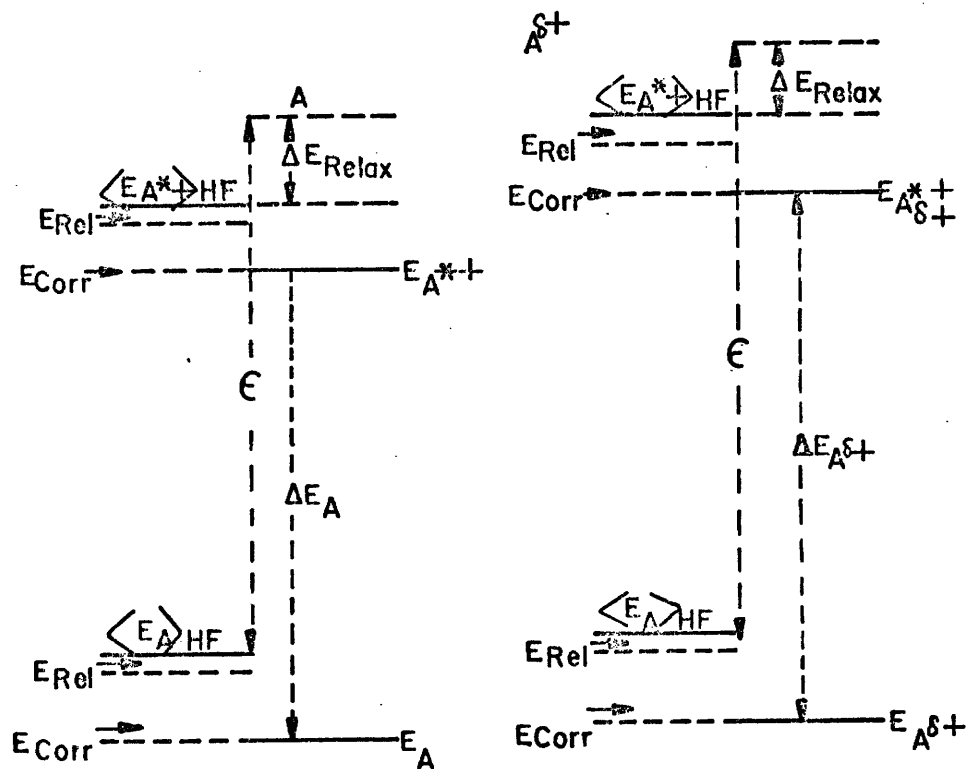


Figure 1.6. Energy Relationship Between Calculated and Experimental Binding Energies and Koopmans' Theorem.

The applications of molecular orbital calculations with Koopmans' theorem upon the interpretation of ESCA spectrum was examined by Clark<sup>20</sup> and the following was shown.

The shift in core electron binding energy from Figure 1.6. is:

$$\Delta B.E. = \Delta E_A^{\delta+} - \Delta E_A \quad \dots (1.8)$$

where:

$$\Delta E_A = (\epsilon_{HF}^A - \Delta E_{RELAX}) + (E_{CORR}^A - E_{CORR}^{A*+}) + (E_{REL}^A - E_{REL}^{A*+}) \quad \dots (1.9)$$

$\Delta E_{RELAX}$  = energy associated with the relaxation of an ionized atom due to electronic reorganization accompanying photoionization.

$E_{CORR}$  = electron correlation energy effect

$E_{REL}$  = relativistic energy effect

therefore

$$\begin{aligned} \Delta B.E. &= \Delta(\Delta E_{HF}^{A\delta+} - \Delta E_{HF}^A) + \Delta(\Delta E_{CORR}^{A\delta+} - \Delta E_{CORR}^A) \\ &+ \Delta(\Delta E_{REL}^{A\delta+} - \Delta E_{REL}^A) \\ &= \Delta(\epsilon^{A\delta+} - \epsilon^A)_{HF} + \Delta(\Delta E^{A\delta+} - \Delta E^A)_{CORR} \\ &+ \Delta(\Delta E^{A\delta+} - \Delta E^A)_{RELAX} + \Delta(\Delta E^{A\delta+} - \Delta E^A)_{REL} \quad \dots (1.10) \end{aligned}$$

As previously discussed since the molecular orbital calculations ignore the relativistic and electron correlation effects if we assume that, (1) the molecules have similar valence electron distributions and (2) the relaxation energies. ( $E_{RELAX}$ ) are 'nearly'\* the same, we can set these terms to zero.

---

\* It has been shown that this approximation is not entirely accurate in that in an extensive series of compounds studied by Clark, et al.,<sup>21-22</sup> covering a number of core levels and a variety of bonding situations differences in the relaxation energies for carbon 1s levels in both saturated and unsaturated systems covered a range of ~1.5 eV. It was found that in the series studied relaxation energies were lowest for the core levels corresponding to the highest binding energy.

$$\Delta(\Delta E)_{\text{CORR}} \sim 0$$

$$\Delta(\Delta E)_{\text{REL}} \sim 0$$

$$\Delta(\Delta E)_{\text{RELAX}} \sim 0$$

and we have the shift in binding energy at the Hartree-Fock limit:

$$\Delta \text{B.E.} = \Delta(\epsilon^{\text{A}\delta+} - \epsilon^{\text{A}})_{\text{HF}} \quad \dots (1.11)$$

therefore, for a series of closely related molecules, Koopmans' theorem describes adequately the shift in binding energies for core levels but does not hold when valence level relaxation energies do not remain constant in the series.

Chemical shifts in ESCA were first interpreted in terms of an ionic model by Siegbahn and co-workers.<sup>6</sup> If a charge is removed from, or added to the valence level of a molecule, as in the formation of a covalent bond or ion, the electrostatic potential within the valence shell is changed. If an amount<sup>9</sup> of charge is removed from the valence electron distribution of an atom to infinity, the potential energy is lower by the amount:

$$\Delta E = \frac{q}{r} \quad \dots (1.12)$$

where  $r$  is the radius of the valence shell. When the electron is not removed to infinity but to a finite distance,  $R$ , from the molecule, the lowering of the potential energy (shift) is given by

$$\Delta E = \left(\frac{1}{r} - \frac{1}{R}\right)q \quad \dots (1.13)$$

although in the ionic crystal model the lattice effects have to be calculated. As far as core level electrons are concerned, neighbouring ions can, to a first approximation, be regarded as

point charges since the orbital overlap is negligibly small. Therefore, for the crystal model, a summation of the potentials from the point charges in the crystal will determine the binding energy of the core electron. In this model, the crystal potential  $V_i$  at the centre of atom  $i$  is:

$$V_i = \sum_{j \neq i} \frac{q_j}{r_{ij}} \quad \dots (1.14)$$

where  $r_{ij}$  are the centre-to-centre inter-ionic distances and  $q_j$  is the charge anion  $j$ .

This model was extended to covalent compounds<sup>5</sup> and the change in potential as a consequence of the redistribution of the valence electrons on the formation of a bond can be divided into two components: (a) the component associated with the change of the valence electron population on the atom and (b) the component associated with a two centre interaction, originating from the electron distribution in the remainder of the molecule, which is considered as point charges distributed throughout the molecule. Therefore the binding energies,  $E_i$ , are:

$$E_i = E^0 + kq_i + \sum_{j \neq i} \frac{q_j}{r_{ij}} \quad \dots (1.15)$$

where  $q_i$  is the charge on atom  $i$

$k$  is the average interaction between a core and valence electron on the atom

$r_{ij}$  are the interatomic distances

$E^0$  is a reference level binding energy

The assumption of a point charge model is equivalent to assuming that there is no overlap between the core electron density on atom  $i$  and the valence electron densities on the other atoms in the molecule. This assumption is the basis for the utilization of the CNDO/2 molecular orbital calculations in relating ESCA chemical shifts. In fact the relationship 1.15 may be derived theoretically from an expansion of Koopmans' theorem in the zero differential overlap approximation. Such an analysis shows that the one centre parameter  $k$  is approximately equal to the coulomb repulsion between a core and valence electron on atom  $i$ .

(b) Valence Electron Binding Energies.

The use of a high energy photon source enables a study of not only the core levels but also the whole of the valence energy level region and this distinguishes ESCA from UPS in that for the latter the photon sources which are most commonly employed (viz. He(I) and He(II)) only allow the study of the higher occupied orbitals. In studying metals the use of a high energy photon source also minimizes the modulation arising from final state effects and hence gives a close experimental measure of the density of states.

It has recently been shown that the relative intensities of various peaks in the valence electron spectrum vary with differences in the incident excitation energy, not only between X-ray and U.V. but between various X-ray energies.<sup>23</sup> These effects are attributed to the cross-section differences involved in the various electronic states in the valence band region.

Figure 1.7. demonstrates the striking difference between X-ray and U.V. valence band studies on carbon monoxide.

Figure 1.7a. is the valence band using  $Mg_{K\alpha_{1,2}}$  (1253.7 eV) excitation and 1.7b. is the valence band using He(II) (40.8 eV) excitation (corrections for energy reference levels have been made, note that the direction of increasing energy is opposite in the two spectra).

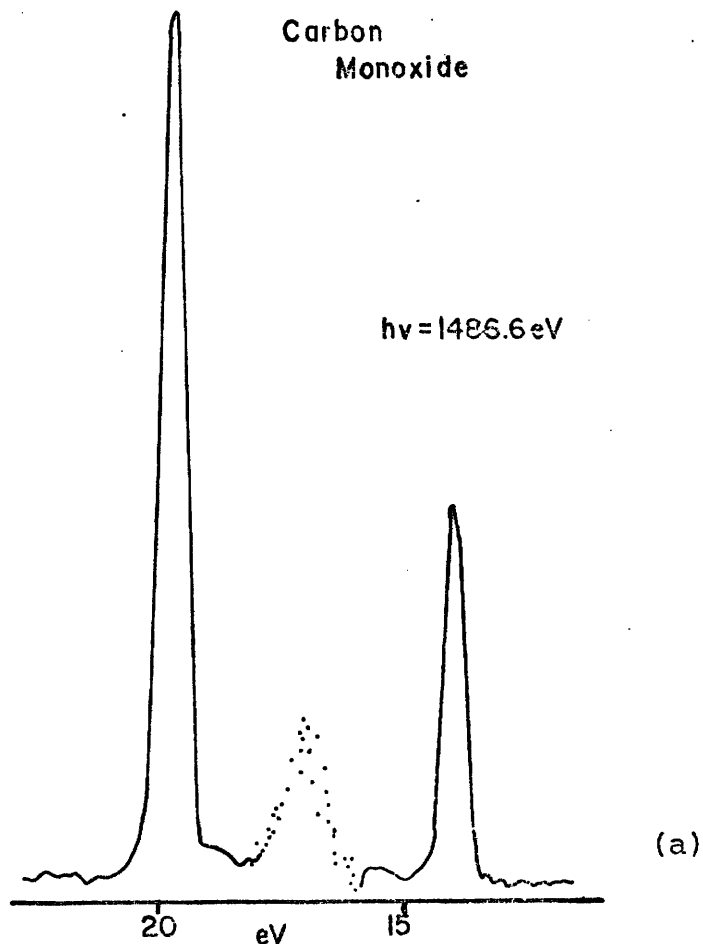
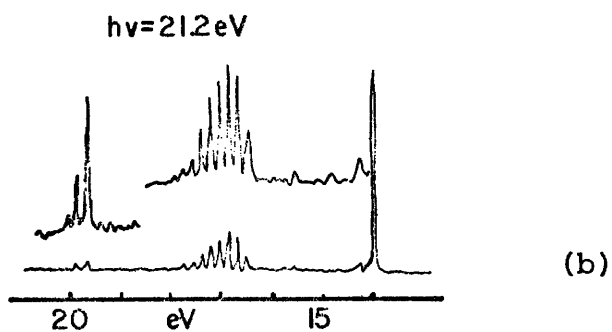


Figure 1.7. Valence Energy Levels from Carbon Monoxide Using  $Mg_{K\alpha_{1,2}}$  (1253.7 eV) and He(II) 40.8 eV Radiation Sources.

In many cases involving isomeric systems where the core level spectra are essentially the same, the 'fingerprint' nature of the valence energy levels can be extremely useful for structural assignment. This aspect of valence band studies will be discussed later in Chapter 2 on polymers.

(c) Multiplet Splittings.

The chemical shifts in binding energies discussed in previous sections can be attributed to differences in the electronic environments of the relevant atoms. Multiplet splittings on the other hand arises for paramagnetic systems and indeed the phenomenon of multiplet splittings accompanying core ionization was predicted for transition metal ions<sup>24</sup> in advance of the experimental observations by Fadley, et al.<sup>25</sup> A simpler example is provided by Siegbahn<sup>5</sup> on NO and O<sub>2</sub>. In their study on N<sub>2</sub>, NO and O<sub>2</sub> molecules they found that the N<sub>2</sub> molecule did not possess core level splitting since the core level (1s) after photoemission was degenerate with respect to spin. Whereby NO and O<sub>2</sub> core levels were split, e.g. upon photoemission from a core level in oxygen or nitrogen in NO the molecular ion NO<sup>+</sup> was left in either a triplet or singlet state respectively. The splitting observed in the 1s spectrum can be attributed to the exchange interaction between the core electrons and the two unpaired 2π electrons having different energies. The O<sub>2</sub> molecule has a similar molecular orbital structure but has two unpaired electrons in its outer π-type orbital. Figure 1.8. describes the orbital levels in N<sub>2</sub>, NO and O<sub>2</sub> and Figure 1.9. the ESCA 1s levels of the molecules.

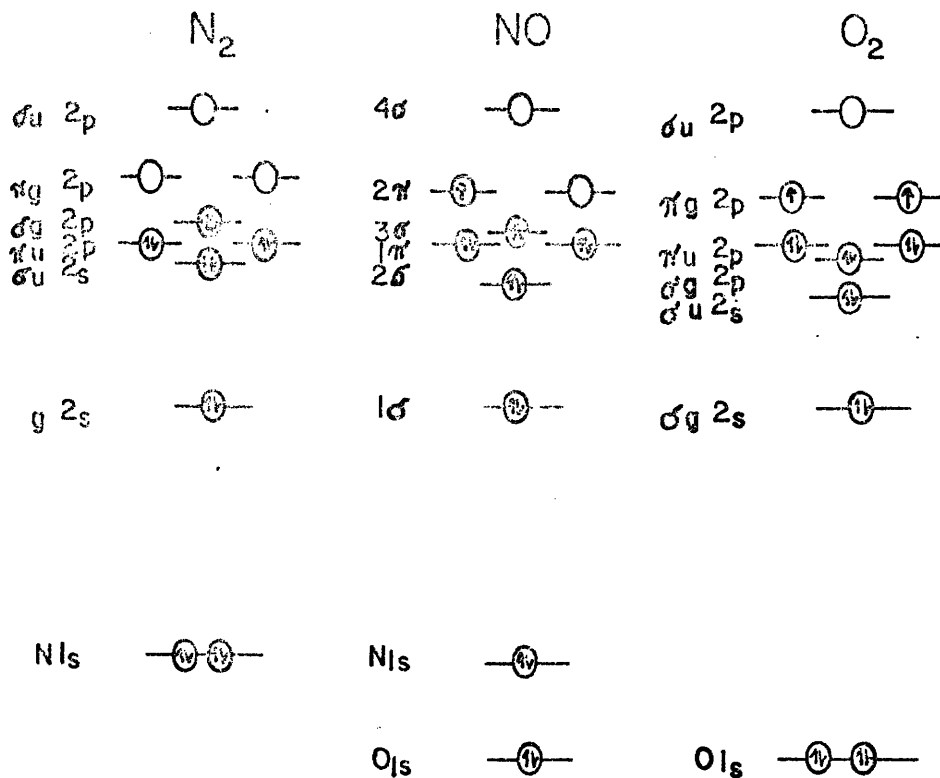


Figure 1.8. Level Diagrams of  $N_2$ ,  $NO$  and  $O_2$ .

(d) Spin-Orbit Splitting and Electrostatic Splitting.

Another splitting phenomenon observed is that arising from coupling between the spin and the angular momenta, which result in two final states. When photoionization occurs from other than an s type orbital a doublet structure is observed in the ESCA spectrum.<sup>6</sup> This doublet arises from coupling between the spin and orbital angular momenta which gives rise to the possibility of two values of the total quantum number (J) for the hole state formed. The intensities of the peaks in the doublet are proportional to the ratio of the degeneracies of the states  $(2J + 1)$ . Table 1.4. list the intensity ratios for different levels and an ESCA spectrum of the  $4F_{5/2, 7/2}$  doublet of Au is shown in Figure 1.10.

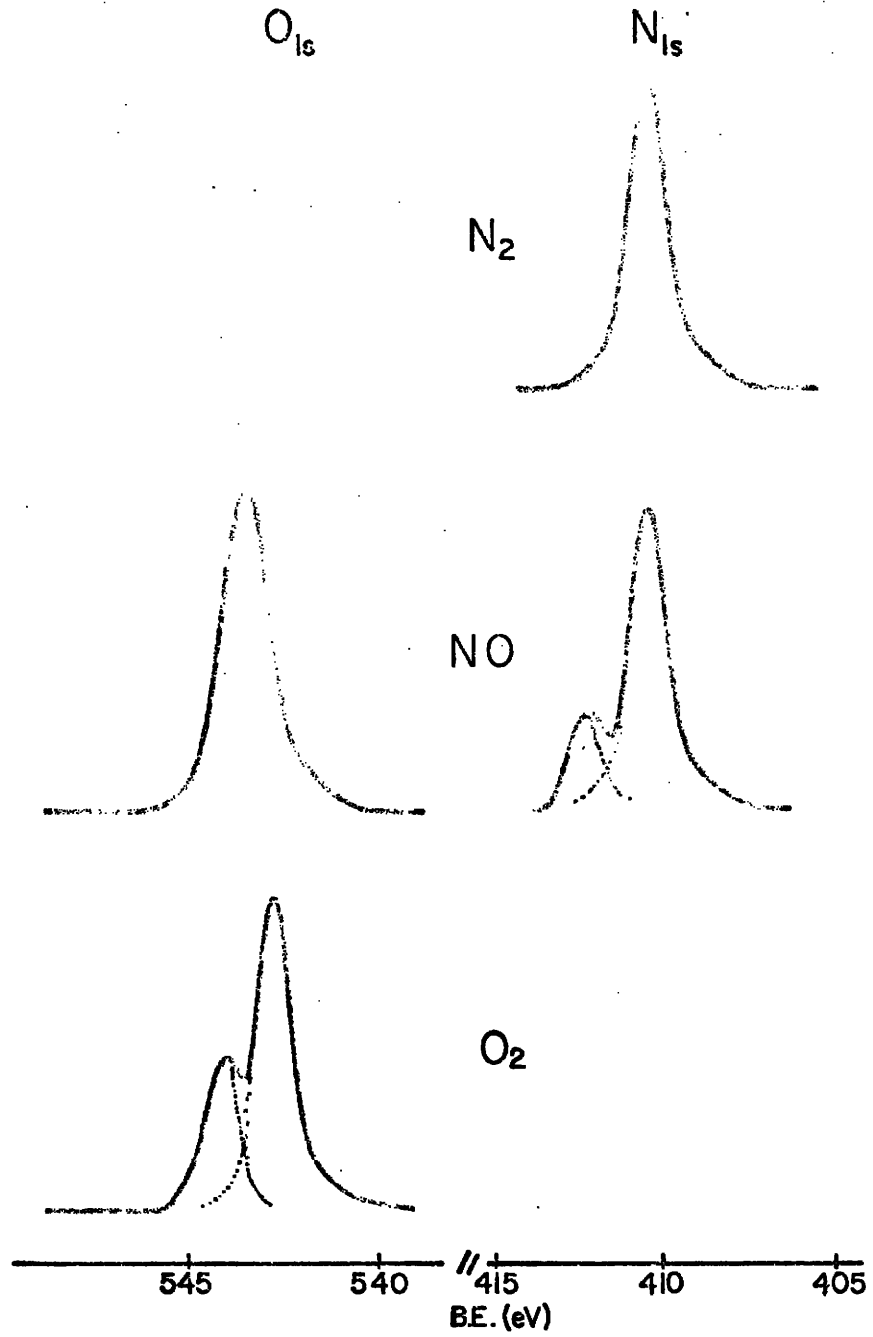


Figure 1.9. ESCA Spectra from  $N_2$ , NO and  $O_2$  showing Multiplet Splitting.

Table 1.4.

Intensity Ratios For Different Levels

Orbital quantum number		Total quantum number		Intensity Ratio
		J	(p + s)	(2J+1)/(2J+1)
s	0	$\frac{1}{2}$		No splitting
p	1	$\frac{1}{2}$	$\frac{3}{2}$	1:2
d	2	$\frac{3}{2}$	$\frac{5}{2}$	2:3
f	3	$\frac{5}{2}$	$\frac{7}{2}$	3:4

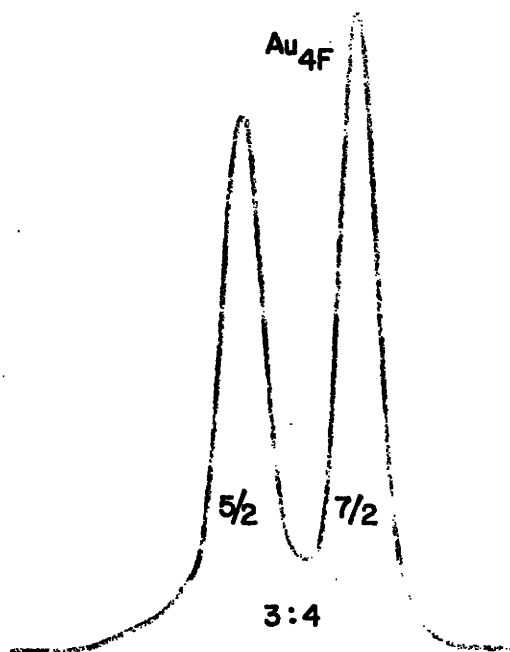


Figure 1.10. Spin-Orbit Split Doublet of the Au<sub>4f</sub> Level.

An electrostatic splitting in the  $5p_{3/2}$  levels of some gold compounds has been observed by Novakov and Hollander<sup>24-25</sup> and has been attributed to the interaction of the internal electrostatic field with the  $M = \pm \frac{1}{2}$  and  $M = \pm \frac{3}{2}$  substrates of the  $5p_{3/2}$  electron levels. Figure 1.11. illustrates the effects attributed to electrostatic splitting (internal electric field gradients) in  $U_{\text{METAL}}$ .

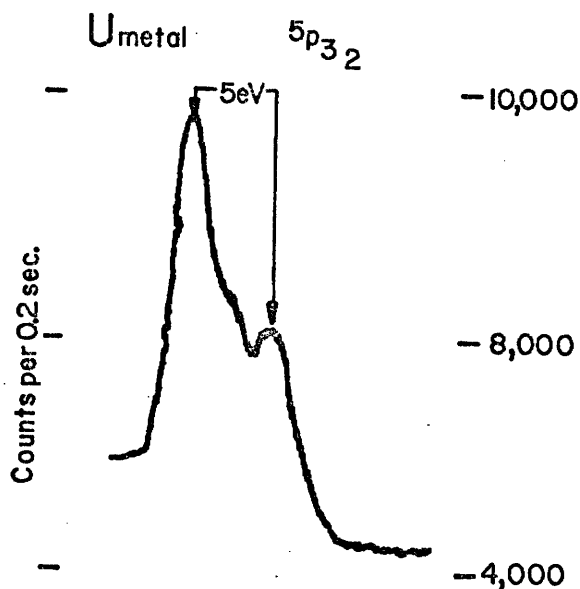


Figure 1.11. Electrostatic Splitting in the  $5p_{3/2}$  Level of  $U_{\text{METAL}}$ .

(e) Shake-up and Shake-off Processes.

It is apparent in the ESCA spectrum of numerous compounds that additional processes are taking place apart from the primary photoionization process manifesting itself in a single peak. Often peaks of much smaller intensity are found on the high B.E. side of the primary peak and they are a consequence of so-called 'multi-electron processes' commonly referred to as 'shake-up' and 'shake-off'.

These multi-electron processes occur mostly by a two-electron process in which two transitions are identified;<sup>28</sup>

(1) shake-up, where the second electron is excited to a higher bound state or (2) shake-off where the second electron is excited to an unbound continuum.

These processes derive their energy from the single electron process and will therefore lower the K.E. of the primary photoelectron. Therefore a revision is needed to equation (1.5) to account for these multi-electron processes:

$$\text{K.E.} = h\nu - \text{B.E.} - \bar{E} \quad \dots (1.16)$$

where  $\bar{E}$  is the energy of the multi-electron process.

The probability of shake-up involves the overlap of two orbitals and the selection rules governing the shake-up excitation are of the monopole type:

$$\Delta J = \Delta L = \Delta S = \Delta M_J = \Delta M_L = \Delta M_S = 0 \quad \dots (1.17)$$

and the probability for the shake-off process increases from zero for a value of  $h\nu$  equal to the single-electron binding energy to a constant value for  $h\nu$  equal to a few times this value.<sup>29</sup>

With a conventional ESCA spectrometer as employed in this work using an unmonochromatized X-ray source, the background arising from inelastic scattering processes and the bremsstrahlung generally obscure the low intensity features such as shake-off processes making them difficult to detect.

Theoretical treatments of the multi-electron processes are found in the literature and a review of models based on

the 'sudden approximation' concept is presented by Manne and Aberg.<sup>30</sup> Figure 1.12. is a schematic of the two multi-electron processes discussed above.

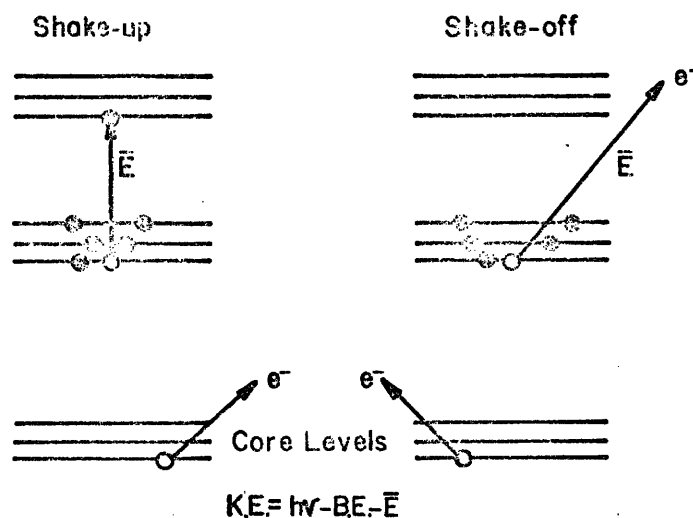


Figure 1.12. Schematic of the Shake-up and Shake-off Processes.

Figure 1.13. is a typical example of the shake-up satellite found in an ESCA spectrum, in this case poly-1-vinylnaphthalene. Shake-off processes are much less intense than the shake-up and are found to lower K.E.

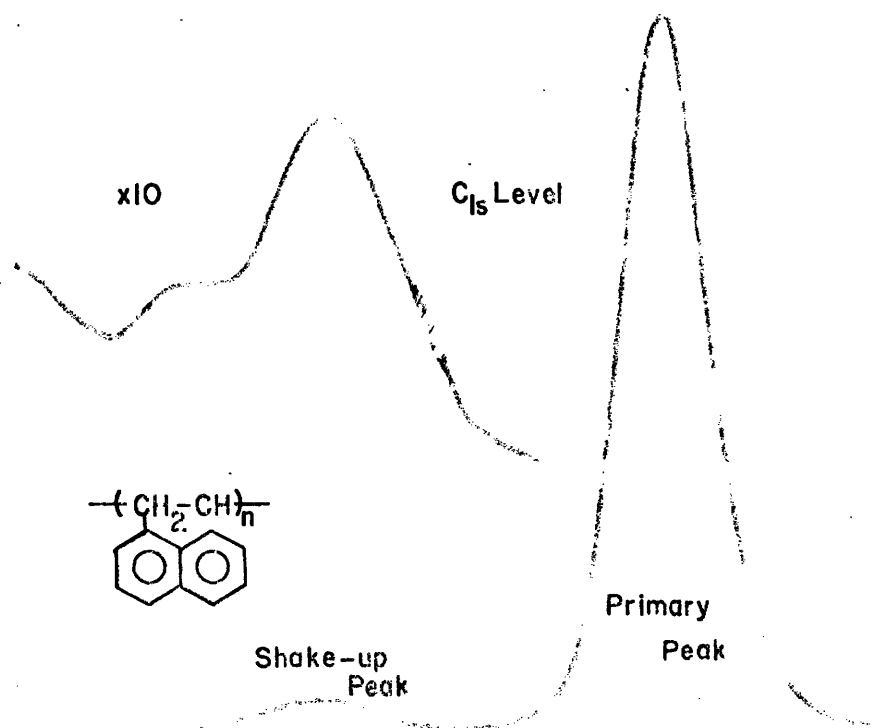


Figure 1.13. ESCA Spectrum of Poly-1-vinylnaphthalene Indicated Shake-up Peak and Primary Photoionization Peak.

(f) Escape Depths.

The escape depth ('mean free path', is the depth at which  $1/e$  of the emitted electrons have not suffered any energy loss)<sup>17</sup> is dependent upon essentially two major factors, (1) the electronic level being studied and (2) the X-ray excitation energy. Siegbahn, et al.<sup>6</sup> demonstrated by dip-coating monolayers of pure iodostearic acid on chromium plated brass that electrons from the  $I_{3d_{5/2}}$  level were emitted from less than the top  $100\text{\AA}$  of the monolayer films. Figure 1.14. is the  $I_{3d_{5/2}}$  spectrum from the study where the multilayers are  $40\text{\AA}$ ,  $120\text{\AA}$  and  $400\text{\AA}$  thick respectively with an iodine concentration of one per area of  $10\text{\AA}^2$ .

As the double layers were increased the counting rate (proportional to concentration) did not increase linearly. For instance when the thickness has reached  $400\text{\AA}$  the intensity had only increased by a factor of 3.5 over the  $40\text{\AA}$  sample. This indicates the photoelectrons were emitted from depths of less than  $100\text{\AA}$ . Clark, et al.<sup>17</sup> has presented a detailed analysis of the fluorination of polyethylene using escape depth information to determine the depth of fluorination in the film and this aspect of escape depth analysis will be discussed later in Chapter 2 on polymers.

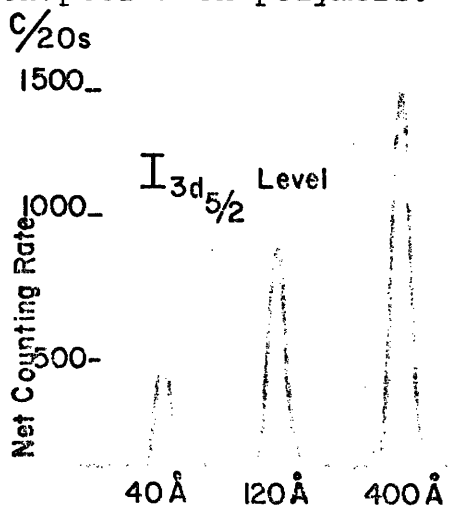


Figure 1.14. The  $3d_{5/2}$  Level from Iodine in Three Different Multilayer Samples.

(g) Line Shape Analysis in ESCA.

Complex peaks containing multi-contributions can often be resolved into their individual components by deconvolution; in this study a Du Pont 310 curve resolver (analogue computer) was used. Gaussian curve shapes are often assumed, but other shapes can be set on the curve resolver. Since when assuming a gaussian shape an infinite number of gaussian curves can be fit to the complex peak a prior knowledge of line widths, chemical shifts and approximate stoichiometry are required to obtain the unique solution to the deconvolution of the spectra. These line widths and chemical shifts are obtained through the studies of a vast number of similar well characterized compounds under identical experimental conditions. The curve resolver also has the facility for integration of peak areas and therefore relative area ratios, when cross sections are taken into account, can determine elemental and group ratios in compounds. Figure 1.15. is a complex spectra that has been deconvoluted into its individual components with area ratios shown.

(v) ESCA Instrumentation.

Since the introduction of the first commercial instrument in 1970 several designs have been placed on the market. This study was carried out on an A.E.I. ES200A spectrometer of which the essential components are shown in Figure 1.16. The three main features of the apparatus are the:

- (a) X-ray equipment,
- (b) Source chamber,
- (c) Analyzer chamber.



(a) X-Ray Equipment.

The equipment consists of a Marconi-Elliott type GX5 high voltage generator that may be operated in the vacuum pressure region  $< 10^{-5}$  torr. The most commonly used X-ray sources, as previously discussed, are  $Mg_{K\alpha_{1,2}}$  and  $Al_{K\alpha_{1,2}}$  radiation (in this study  $Mg_{K\alpha_{1,2}}$  was the source of choice). Typical conditions for the power input are 12 kV and 15 ma which produce photon fluxes in the region of  $\sim 0.1$  milli rad./sec. Component linewidths for the X-ray source in the particular cases of Mg and Al targets are about .7 eV and .9 eV respectively and can be reduced by monochromatization.<sup>5,6</sup>

A typical X-ray spectra is shown in Figure 1.17. where it represents the energy content per unit wavelength internal emitted by an X-ray tube with a  $^{74}W$  anode.<sup>31</sup> It is obvious that the spectrum is composed of a set of sharp lines superimposed on a continuum.

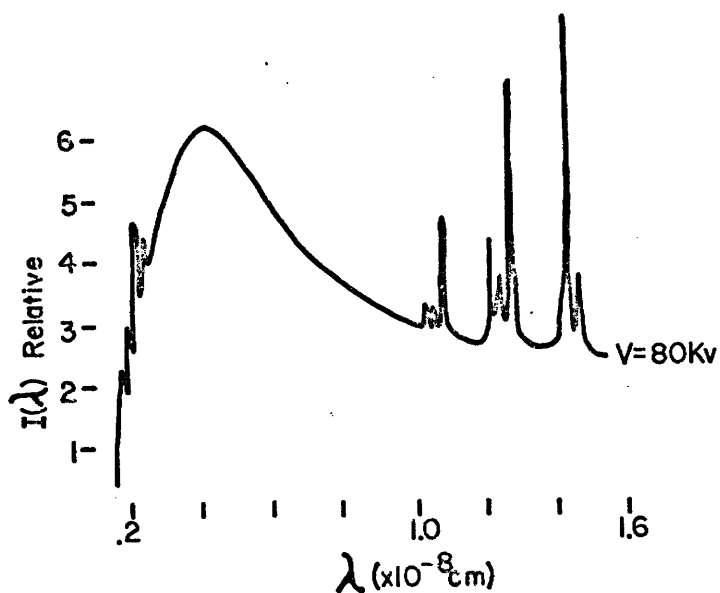


Figure 1.17. Typical X-ray Spectrum

The continuum's shape depends only on the energy of the incident electrons on the anode, not on the nature of the anode and the  $\lambda_0$  cutoff at short wavelengths is inversely proportional to the electron K.E., and follows the equation:

$$h\nu_0 = E \quad \dots (1.20)$$

where  $h$  is Plank's constant. The total X-ray energy per electron,  $E_T$ , is proportional to the integral over  $\lambda$  of the continuum and obeys the equation:

$$E_T = kZE^2 \quad \dots (1.21)$$

where  $k \sim 0.7 \times 10^{-4}$  for  $E_T$  and  $E$  in MeV where  $Z$  is the atomic number of the anode. The fraction of the electron kinetic energy converted into X-ray energy is:

$$E_T/E = kZE \quad \dots (1.22)$$

For a typical case of  $Z = 90$  and  $E = 0.05$  MeV,  $E_T/E$  is only about 0.3%.

The characteristic line spectra depend only on the atomic number of the anode and not on the incident electrons, however line spectra are obtained only when the electron K.E. satisfies the relation:

$$E > E_T = h\nu = hc/\lambda \quad \dots (1.23)$$

where  $\nu$  is the frequency and  $\lambda$  the wavelength in question.

The total X-ray energy emitted in a particular line increases with incident electron K.E. according to the empirical relation,

$$I \propto (E - E_T)^n \quad \dots (1.24)$$

when  $n \sim 1.5$ .

The line spectra of interest from the Al and Mg anodes normally used in ESCA are from the so-called K series (spectroscopic notation for  $n = 1$ ) transitions and particularly the  $K\alpha_{1,2}$  lines. However, the unmonochromatized spectra of the  $Mg_{K\alpha}$  radiation contain the continuum and particularly the  $K(\alpha_7, \alpha_3, \alpha_4, \alpha_5, \alpha_6$  and  $K\beta)$  where the  $K\alpha_3$  satellite is 9.5% relative intensity from the primary  $K\alpha_{1,2}$  lines (8.4 eV higher K.E.) and the  $K\alpha_4$  satellite is 4.5% relative intensity from the primary  $K\alpha_{1,2}$  lines (10.1 eV higher K.E.).

$Al_{K\alpha}$  radiation can be monochromatized with a crystal diffraction technique,<sup>5</sup> to eliminate the gross satellites (and the continuum) and be left with the  $K\alpha_{1,2}$  lines. (Unfortunately monochromatization of the  $Mg_{K\alpha}$  lines is not presently possible with crystal diffraction since no suitable crystal is currently available with the proper lattice spacing.)

For  $Al_{K\alpha}$  essentially three techniques are available, (a) 'dispersion-compensation', (b) 'slit-filtering' and (c) fine-focussing, all using crystal diffraction of the X-ray radiation and these techniques will attain ultimate linewidths of 0.2 eV.

Another system described by Gelius<sup>32</sup> uses a rotating anode (about 5-10,000 r.p.m.) which is characterized by a fine-focussing X-ray line, high power electron gun and several spherically bent quartz crystals for monochromatization of the  $Al_{K\alpha}$  radiation. Figure 1.18. illustrates these techniques.

(b) Source Chamber.

The spectrometer source chamber, or sample region, contains the X-ray source aperture, seven access ports for sample

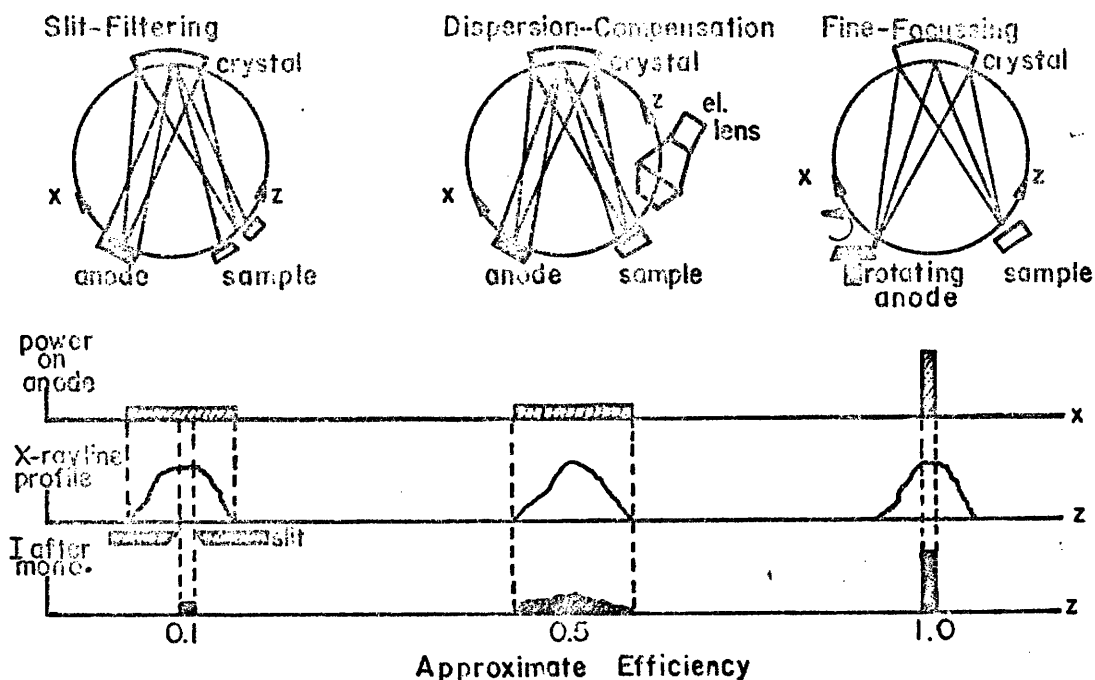


Figure 1.18. Techniques for Monochromatization of X-Rays.

introduction and various pre- or post-treatments, and a retarding lens system into the analyzer Chamber.

The X-ray source aperture is simply an aluminium window (.003" thick) which separates the X-ray generator from the sample and ensures that electrons scattered from the X-ray target or from the electron generating filament do not enter the source chamber.

The access ports allow for attachment of various sample probes which permit the study of liquids (via a reservoir shaft), volatile solids (via a direct inlet shaft with vapour condensed on an insertion shaft at low temperatures), gases (via a gas valve with studies directly from the gas phase) and non-volatile solids such as films, powders, fibres, etc. (via a plate shaft equipped with heating and cooling temperature control). Typical operating pressures are  $10^{-7}$  torr or better although under ideal conditions better than  $10^{-9}$  torr is attainable.

(c) Analyzer Chamber.

The analyzer on the A.E.I. ES200A is a hemispherical double focussing electrostatic analyzer, which was originally described by Purcell<sup>33</sup> in 1938, enclosed within two mu-metal shields for magnetic shielding. The resolution of the hemispherical analyzer is based upon three variables:

- (1) mean radius of the hemispheres, R,
- (2) width of the entrance slit,
- (3) width of the exit slit.

Therefore the resolution,  $\Delta E/E$ , where E is the energy of the electrons is

$$\Delta E/E = R/W \quad \dots (1.25)$$

where W = combined widths of entrance and exit slits.

It is quite easily seen that to improve the resolution three terms can be varied:

- (1) reduce the slit width, which has the effect of reducing the signal intensity,
- (2) increase the hemispherical radius, which increases engineering cost and complexity and pumping requirements,
- (3) retard the electrons before entering the analyzer so as to reduce their K.E.

With reasonable compromises made on the slit width to obtain sufficient signal intensities and the hemispherical sizes to prevent mechanical distortion and high engineering cost and practical vacuum pump sizes the ES200A retards the electrons before they enter the analyzer by passing them through a lens assembly. This lens system actually serves a double purpose:

- (1) The lens system allows the analyzer to be located at a convenient distance physically from the source chamber which permits a maximum flexibility in sample handling.
- (2) A retarding potential on the electrons allows more flexibility on the resolution requirements of the analyzer.<sup>34</sup>

The electrons passing through the analyzer can be focussed at the collector by either of two methods:

- (1) Electronically scanning the retarding potential applied to the lens while keeping the hemispherical potential constant, or
- (2) Simultaneously scanning the retarding potential applied to the lens and the hemispherical potential and keeping a constant ratio between the two, which is the technique used on this ES200A.

The overall resolution  $\Delta E_m/E$ , of the system also depends upon contributions from sources other than the analyzer.

- (1) The width of the X-ray radiation line,  $\Delta E_x$ .
- (2) The natural width of the electron energy distribution in the level being studied,  $\Delta E_1$ .
- (3) The line broadening due to spectrometer irregularities, which can vary with electron emission energy,  $E$  and slit widths,  $\Delta E_s$ .
- (4) The line broadening due to solid state effects in the sample,  $\Delta E_{ss}$ .

Therefore the overall resolution is given the equation:

$$(\Delta E_m)^2 = (\Delta E_x)^2 + (\Delta E_l)^2 + (\Delta E_s)^2 + (\Delta E_{ss})^2 \quad \dots (1.26)$$

(This relationship is strictly valid only for gaussian line-shapes.) A variable on the ES200A is the collector slit width which can be adjusted at 0.2, 0.1 or 0.03 inches depending on the resolution and sensitivity desired.

(d) Electron Detector.

The detector contains a collector aperture (exit slit), described above, which pass the selected K.E. electrons into an electron multiplier. The output pulses from the channel multiplier are amplified and fed into a data handling system. The signals into the data handling system generate the ESCA spectra by one of two methods:

- (1) The continuous scan, where the electrostatic field is increased from the present starting K.E. continuously while the signals from the multiplier are monitored by a rate meter. When the signal to background ratio is sufficiently high a graph of the electron counts per second versus the K.E. of the electrons is plotted directly onto an X-Y recorder.
- (2) The step scans, where the field is increased by preset increments (typically 0.1 eV) and at each increment the (a) counts may be measured for a fixed length of time or (b) a fixed number of counts may be timed. The data obtained from the step scans is stored in a multichannel analyzer and many scans can

be made on a sample to average any random fluctuations in background. Using this technique the signal to noise ratio goes up as the square root of the number of scans, although care must be taken to avoid long term sample changes, such as hydrocarbon surface build-up, where the first scans are not typical of the last scans. Wide scans encompassing the entire range from zero K.E. to the K.E. of the X-ray source as well as narrow scan ranges for specific studies are available.

CHAPTER 2

Studies of Structure and Bonding in Polymers through the  
Application of ESCA

CHAPTER 2

Studies of Structure and Bonding in Polymers through the  
Application of ESCA

(i) General Introduction.

The application of ESCA to the structure and bonding in polymer systems to date has mainly concentrated on fluoropolymer systems. There are basically two reasons for this focus of attention:

- (1) The large chemical shift in the core levels of carbon ( $C_{1s}$ ) induced by fluorine presents the best case for sorting out the information from the ESCA spectrum on the areas of application to polymers.
- (2) The importance of the fluoropolymer systems both technologically and academically and their comparative difficulty of analysis by other common spectroscopic techniques, due to their insolubility and intactability, lend themselves to study by ESCA.

By far the greater part of the effort on the applications of ESCA to polymer studies has been carried out by Clark at the University of Durham and there are essentially two areas that have been investigated in the structure and bonding of polymers.

(A) Static Studies.

- (1) Chemical Compositions.
  - (a) elemental compositions.
  - (b) % comonomers in copolymers.

- (2) Structural Details.
    - (a) structural repeat units in copolymers, e.g. random, alternating or block repeat units.
    - (b) domain structures in block copolymers.
  - (3) Fine Structural Details.
    - (a) structural isomerism, e.g. cis, trans etc.
    - (b) shake-up studies on unsaturated systems.
    - (c) charge distributions in polymers.
  - (4) Valence Bond Studies on Polymer Systems.
- (B) Dynamic Studies.
- (1) Surface Treatments
    - (a) casing.
    - (b) fluorination.
  - (2) Thermal and Photochemical Degradation.
  - (3) Depth Profiling of Surfaces.
  - (4) Oxidative Degradation of Polymers.

Each of these topics will be covered in detail in this chapter but before the discussion a clarification is needed on the ways in which polymer samples are prepared for ESCA examination and the definitions of polymer terminology to be used throughout the remainder of this thesis.

(ii) Sample Preparation and Polymer Nomenclature.

There are a few methods which have been found to be convenient for preparing samples for examination by ESCA. These are (a) the direct study of suitably mounted powder samples, (b) solution cast films, (c) pressed or extruded films and (d) 'in situ' polymerized films. Each of these techniques will be discussed separately.

(a) Powders.

When the polymer sample is available as a powder, which if often the case, it is convenient to examine it by applying the powder to a double sided tape which possesses nominal heat resistance ('Scotch Brand' electrical tape #75, 3M Company, works quite well and is a silicone type polymer), and apply the tape directly to the sample probe. Caution of course must be taken to avoid incomplete coverage of the tape which would result in extraneous signals observed from the tape backing. Samples prepared in this way generally tend to have lower signal/noise ratios than do smooth films and the primary photo-ionization peaks tend to have broader full width at half maximum (FWHM) than do films.

(b) Solution Cast Films.

When the polymers are sufficiently soluble, thin films may be solution cast onto a suitable backing, such as clean Au sheet and mounted onto the sample probe. Conventional dip or bar coating procedures are adequate for the coating process. Care must be taken to use clean coating apparatus and pure solvents to avoid the segregation of impurities at the surface during evaporation of the solvent. For easily oxidized polymers the coating procedure should be carried out under an inert gas for the evaporation of the solvent and for systems where H-bonding is a problem complete removal of extraneous water is imperative.

(c) Pressed or Extruded Films.

To eliminate the contaminations possibly introduced by solvent casting for appropriate polymers it is convenient to study them as pressed or extruded films. For polymers with low Tg's, such as elastomers, it is often possible to 'melt' a

small amount of polymer onto a suitable substrate and allow it to spread as a thin film. (In the case of the polyacrylates discussed in Chapter 3 this was the method used for nearly all the samples.) When films are prepared from powders or pellets it is often convenient to press the film between clean aluminium foil at temperatures and pressures appropriate to avoid degradation of the polymer sample, often also done under an inert gas atmosphere to avoid oxidation.

(d) 'In situ' Polymerized Films.

A very convenient and often contamination free method of studying polymer films is by carrying out the polymerization on the probe tip by various methods such as U.V. or  $e^-$  irradiation, plasmas (glow-discharge polymerization) or pyrolysis of appropriate monomers, such as the paracyclophane series.

It is convenient to note here also that since most polymers are inherently good insulators, the thin films studied are generally speaking not in electrical contact with the spectrometer. This will result in sample charging, as discussed in Chapter 1, and therefore referencing the energy scale back to the Fermi level becomes necessary. There are two methods which readily accomplish this:

- (1) Either allow hydrocarbon build-up from the extraneous atmosphere in the spectrometer source to build-up on the sample and monitor the  $C_{1s}$  level at  $\sim 285$  eV.
- (2) Deposit a thin film of Au on the sample and monitor the  $4f_{7/2}$  level at  $\sim 84$  eV. In the A.E.I. ES200A used in this study with an unmonochromatized X-ray source, retarding lens system, double focussing

hemispherical electrostatic analyzer and associated slit system the charging is not serious and only corrections of a few eV are needed.

The difficulty in the characterization of polymers, particularly in the case of their surfaces, arises from the fact that polymers are not as well-defined as simple non-macromolecular compounds. The gross chemical structure of polymers can be simple as in the case of linear homopolymers, or complex as in the case of branched or cross-linked copolymers. As an example consider representative systems based on polyvinyl toluene and these are shown in Figure 2.1.

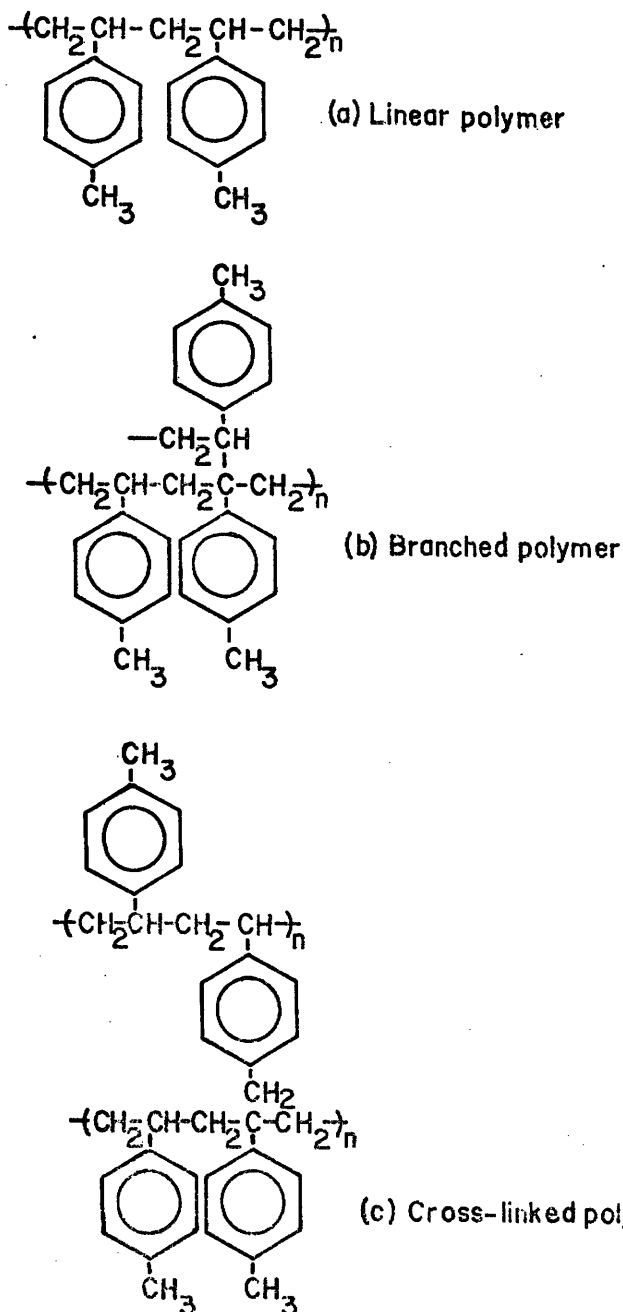


Figure 2.1. Structure Assignments to Polyvinyl Toluene.

These differences in gross structure all based on the same basic building block give rise to a tremendous variation in the physical, chemical, mechanical and electrical properties of the system.

It is often the case that for a given polymer system the structure of the bulk is substantially different than that of the surface. For example since solids communicate with the rest of the universe by way of their surfaces it is possible to produce a crosslinked surface while maintaining the integrity of the bulk. A technique which is capable therefore of monitoring differences in structure between the surface and the bulk is obviously of considerable relevance in many fields of academic and technical importance.

Along with gross structural differences in polymers, there are also isomeric differences arising from unsymmetrical monomers and the resultant structures are shown in Figure 2.2.

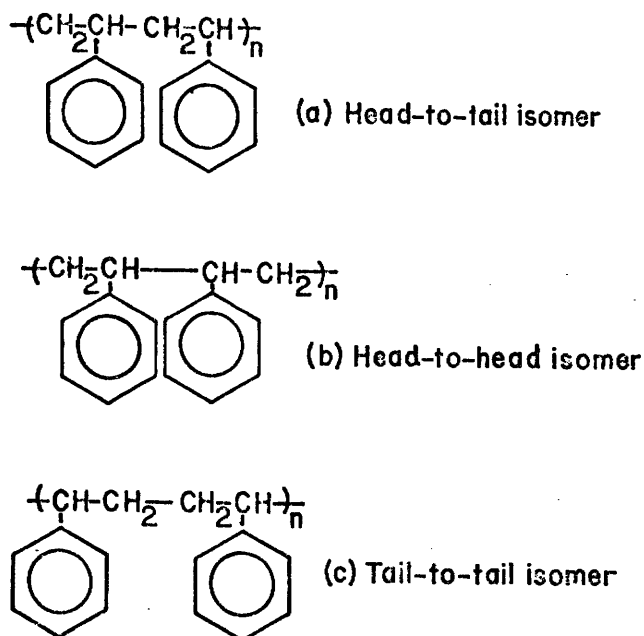


Figure 2.2. Isomeric Assignments to Polystyrene.

Not only can structural isomerism occur in polymers, but also stereoisomerism (CIS-TRANS) as shown in Figure 2.3.

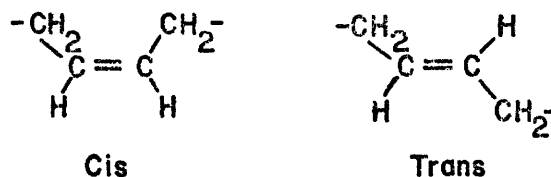


Figure 2.3. Stereoisomerism Assignments to Polymers.

Tacticity is another type of stereoisomerism and is classified into three categories as shown in Figure 2.4.

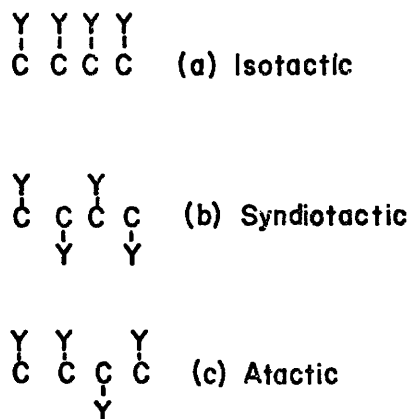


Figure 2.4. Tacticity Assignments to Polymers.

Copolymers have other types of structural assignments and can be made such as random, alternating, graft or block copolymers as shown in Figure 2.5.

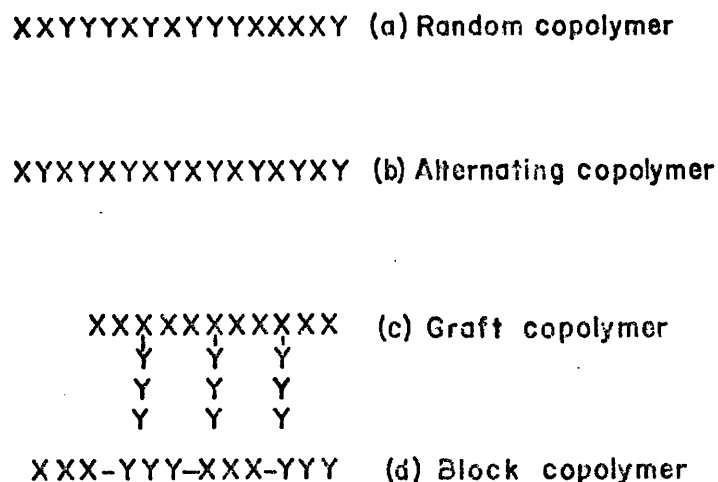


Figure 2.5. Structure Assignments to Copolymers.

(iii) Static Studies on Polymers with ESCA.

(a) Chemical Composition.

(1) It is quite apparent that ESCA is a valuable tool for the identification of the surface elements on a polymer sample and is a routine procedure and easily attained. A wide scan through the energy spectrum on a sample will afford identification of the elements present by the use of appropriate tables. A wide scan of the surface of a polymer film is shown in Figure 2.6. with elemental identification on the spectrum.

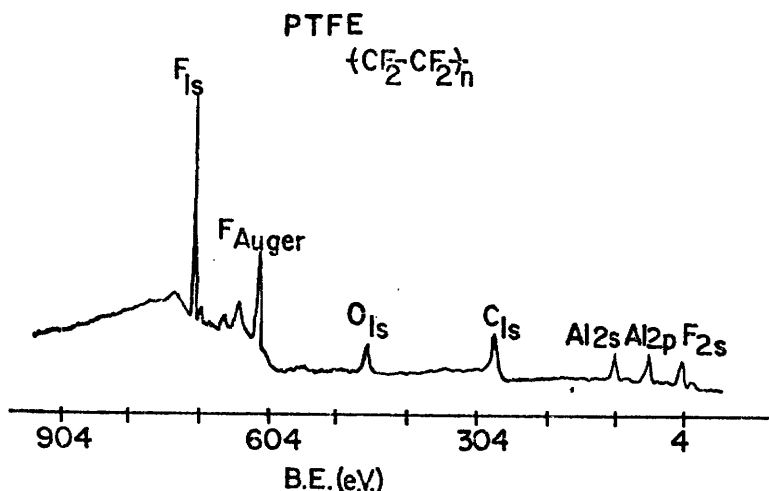


Figure 2.6. Wide Scan ESCA Spectrum of PTFE Pressed Between Al Foil.

(2) Percent Comonomers in Copolymers.

Before a discussion on the determination of percent comonomers in a copolymer can ensue a brief discussion on the qualitative and quantitative nature of the substituent effect on core binding energy in polymers must be treated.

The simplest system to begin with of course is the simple homopolymers of the fluoroethylenes, for which the complications

due to branching, end groups and structural abnormalities are minimal.

The measurement of the core levels of a polymer typically take about  $\frac{1}{2}$  hour whereas under normal operating conditions hydrocarbon build-up is noticeable after several hours. Therefore, as discussed earlier, the reference level for the energy scale is determined by measuring the core levels of the polymer immediately upon introduction into the spectrometer and then allowing time for hydrocarbon build-up, the spectrum is recorded to observe the appearance of an extra peak, as shown in Figure 2.7.

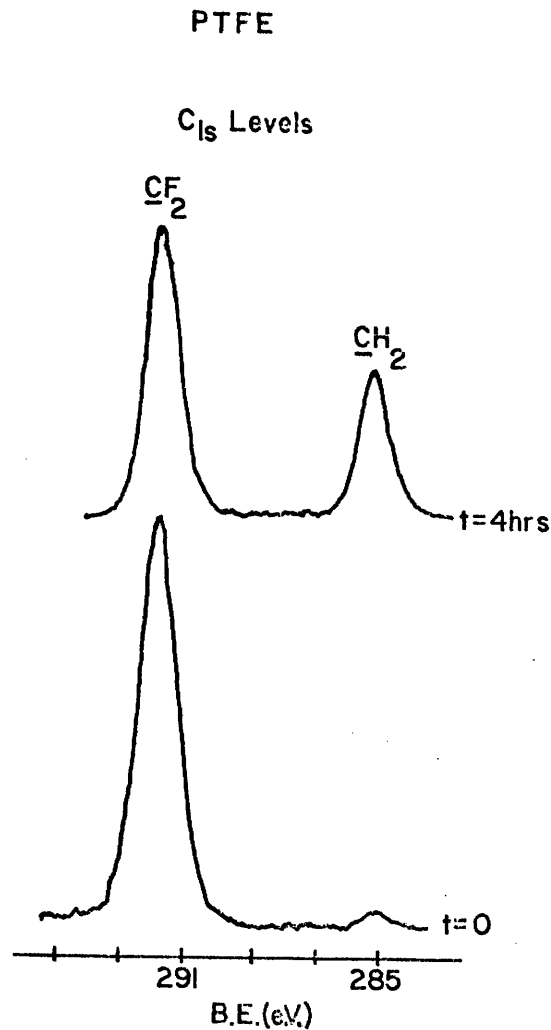


Figure 2.7.  $C_{1s}$  Levels of PTFE Film at 0 Time and 4 Hours  
in Source to Demonstrate Hydrocarbon Reference Level.

In a series of polymers studied by Clark,<sup>35</sup> et al., the binding energies for the  $C_{1s}$  and  $F_{1s}$  levels were identified and Table 2.1. list the data pertaining to the polymers and Figure 2.8. demonstrates the substituent effect in the  $C_{1s}$  levels of the homopolymers studied.

Table 2.1.

Binding Energies of the Homopolymers of Ethylene and the Fluoro-ethylenes.

	$C_{1s}$	$\Delta(C_{1s})$	$F_{1s}$	$\Delta(F_{1s})$
$(CH_2-CH_2)_n$	285.0	(0)	-	-
$(CFH-CH_2)_n$ <u>-CFH-</u>	288.0	3.0	689.3	(0)
<u>-CH<sub>2</sub>-</u>	285.9	0.9	-	-
$(CFH-CFH)_n$	288.4	3.4	689.3	(0)
$(CF_2-CH_2)_n$ <u>-CF<sub>2</sub>-</u>	290.8	5.8	689.6	0.3
<u>-CH<sub>2</sub>-</u>	286.3	1.3	-	-
$(CF_2-CFH)_n$ <u>-CF<sub>2</sub>-</u>	291.6	6.6	690.1	0.8
<u>-CFH-</u>	289.3	4.3	690.1	0.8
$(CF_2-CF_2)_n$	292.2	7.2	690.2	0.9

By taking the appropriate pairs of polymers it was possible to assign structural features to the peaks in the spectrum and investigate the primary and secondary effects of hydrogen replacement, and it was shown that there is a rapid fall off in the  $C_{1s}$  B.E. as a function of the fluorine substituted.

It is important also to determine the intensity ratios for the core levels in the simple homopolymer systems due to the



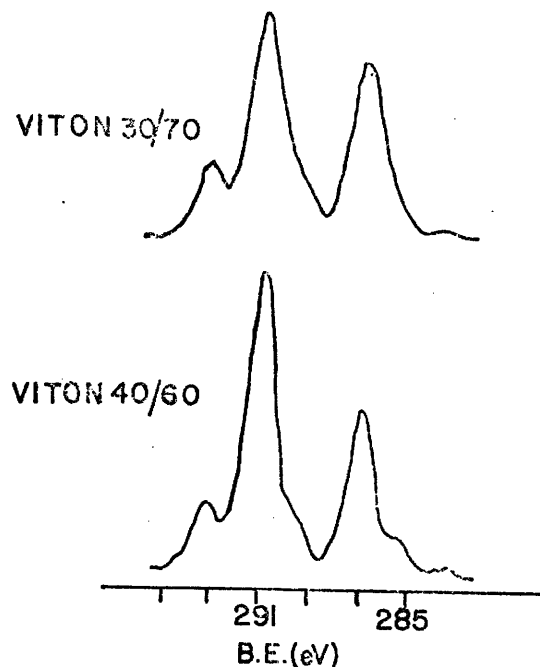


Figure 2.9. C<sub>1s</sub> Levels of Viton Copolymers.

The procedure as applied by Clark was to measure the area of the  $\underline{\text{CF}}_3$  peak, the total area of the ( $\underline{\text{CF}}_2 + \underline{\text{CF}}$ ) peak and the area of the  $\underline{\text{CH}}_2$  peak when the spectrum was deconvoluted into its individual components.

Three different techniques were used to compute the comonomer ratios as an internal check on the reliability of the methods. Essentially they were:

- (1) Based on the stoichiometry of the HFP unit the mole % of HFP must be three times the peak area due to  $\underline{\text{CF}}_3$ .
- (2) The peak area due to  $\underline{\text{CF}}_2$  and  $\underline{\text{CF}}$  is made up of half the total C<sub>1s</sub> peak area due to  $\underline{\text{VF}}_2$  ( $\frac{1}{2} \underline{\text{VF}}_2$ ) and two thirds the total C<sub>1s</sub> peak due to HFP.
- (3) The peak area due to  $\underline{\text{CH}}_2$  is half the total area due to  $\underline{\text{CF}}_2$ , therefore the mole % of HFP is

$$\text{mole \% HFP} = 100 - (2X \% \text{ peak area due to } \underline{\text{CH}}_2) \dots (2.1)$$

Table 2.2. gives the results of the three methods of calculations.

Table 2.2.

% HFP Incorporation Calculated by Three Methods

	Method of Calculation		
	(i)	(ii)	(iii)
Sample 40/60	39	42	40
Sample 30/70	33	30	32

(b) Structural Details.

(1) The ability of ESCA for the determination of the structural details of a polymer is best illustrated by the application to the copolymer of ethylene/tetrafluoroethylene.<sup>37</sup> A series of the copolymers was studied and the  $C_{1s}$  and  $F_{1s}$  levels of the copolymers are shown in Figure 2.10.

From the ESCA data the copolymer compositions may be calculated from the relative ratios of the high to low B.E. peaks in the  $C_{1s}$  levels (attributed to  $\underline{CF}_2$  and  $\underline{CH}_2$  respectively) and also from the overall  $C_{1s}/F_{1s}$  intensity ratios, using data from homopolymers as discussed in the previous section.

It was shown that using these two methods of calculating the composition that they were in good agreement with bulk analytical methods (C and F elemental analysis) and also demonstrated that the samples were uniform at the surface due to the good agreement of the two sets of data.

Once the compositions are established, structural details are the next order of assignment. The studies on the homopolymers of fluorinated ethylenes revealed that structural

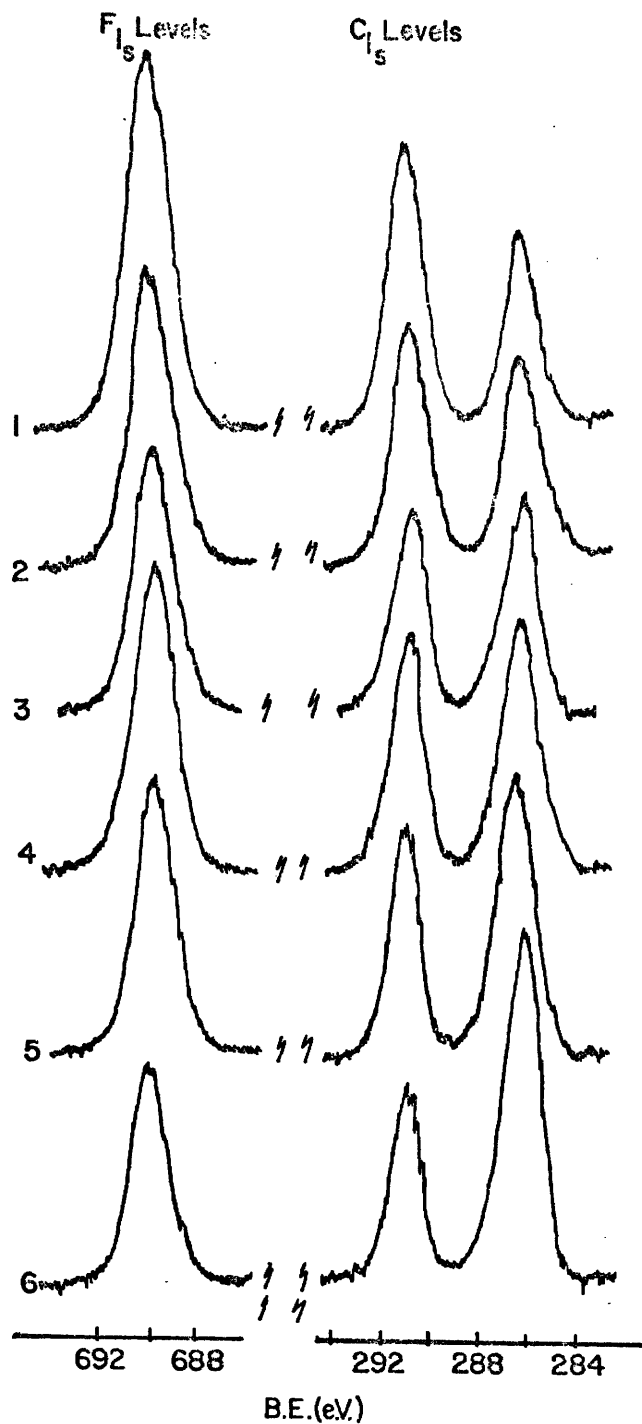


Figure 2.10. Fluorine-1s and Carbon-1s Spectra for Ethylene-tetrafluoroethylene Copolymers.

information is most readily obtained from the absolute B.E.'s and chemical shifts in the C<sub>1s</sub> core levels. The chemical shift

on the  $C_{1s}$  levels is understood qualitatively in terms of the simple substituent effect discussed in the previous section and quantitatively in terms of the charge potential model discussed in the first chapter and will be further discussed in this chapter on the charge distribution in polymers. The chemical shifts lead to a clear distinction between the extreme cases of block-vs-alternating structure from the  $C_{1s}$  B.E.'s expected for a block sequence of ethylene and tetrafluoroethylene from the  $C_{1s}$  B.E. for the homopolymers. For an alternating structure the  $C_{1s}$  B.E.'s observed for PVF<sub>2</sub> based on substituent effects and the calculations with the charge potential model on simple systems would predict the B.E.'s unique for this system.

Therefore if either the block or the alternating structure predominate the  $C_{1s}$  levels would show this and as Figure 2.10. clearly demonstrates an alternating structure was found due to the expected chemical shift of  $\sim 4.7$  eV versus a shift of  $\sim 7.2$  eV expected for a block structure.

Further examination of the spectra revealed two features where the total linewidths (FWHM) were greater than the (FWHM) for the respective homopolymers (2.0 eV - vs. - 1.3 eV  $\pm$  0.1 eV) and where the peak shapes were asymmetric. These two observations indicated that the spectra were envelopes of a number of overlapping peaks arising from different molecular environments. With a complex deconvolution of the spectra, theoretical calculations on expected B.E.'s from a series of model compounds using pentad sequences of the two monomers and assignments of triads for the monomer from the pentad sequence

calculations, Clark was able to obtain good agreement between the physical and general spectroscopic properties of the ethylene-tetrafluoroethylene copolymer.

(2) The domain structure found in AB block copolymers of dimethylsiloxane and styrene was investigated<sup>38</sup> by using the different sampling depths for photoemitted electrons.  $I_{\alpha}$  values for the  $O_{1s}$ ,  $C_{1s}$ ,  $Si_{2s}$  and  $S_{2p}$  core levels were established. It was found that ESCA revealed a surface structure dominated by the polydimethylsiloxane which indicated that most likely, due to the free energy of the surface, the siloxane component was prevalent. It was also found that domain structures could be radically changed from dimethylsiloxane droplets in styrene to styrene droplets in dimethylsiloxane by casting from different solvents. Figure 2.11. shows the ESCA spectra of films of polystyrene, copolymer cast from cyclohexane, copolymer cast from styrene and polydimethylsiloxane from top to bottom respectively.

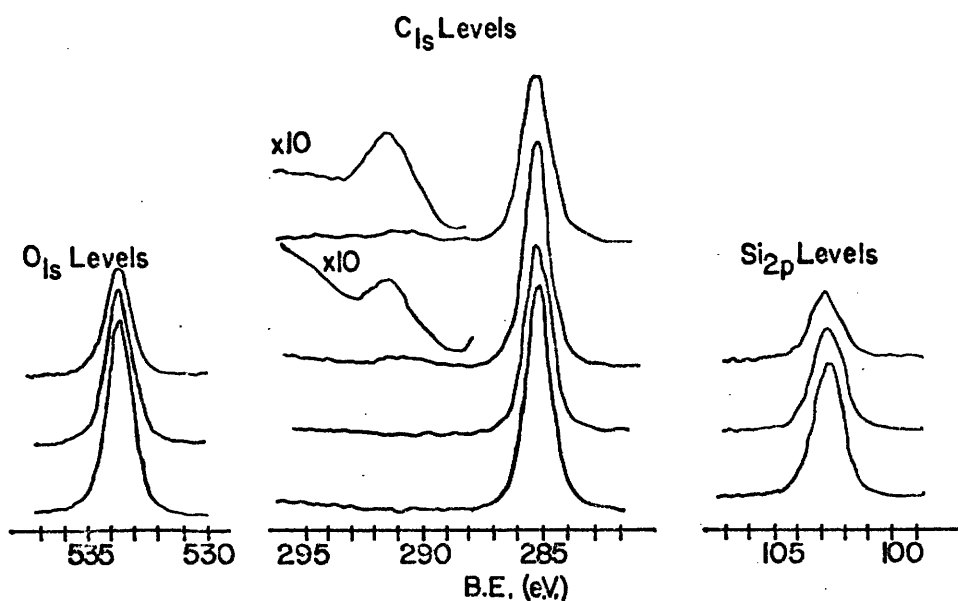
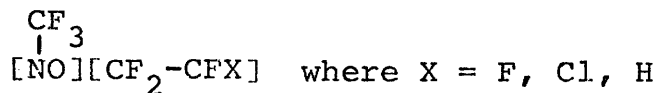


Figure. 2.11.  $C_{1s}$ ,  $O_{1s}$  and  $C_{1s}$  Levels for Solution Cast Films of Dimethylsiloxane/Styrene AB Block Copolymers, Polystyrene and Polydimethylsiloxane.

(c) Fine Structural Details.

(1) The complex analysis of the structural isomerism in a nitroso rubber copolymer



was carried out<sup>39</sup> and the  $C_{1s}$  levels for three of the rubbers are shown in Figure 2.12.

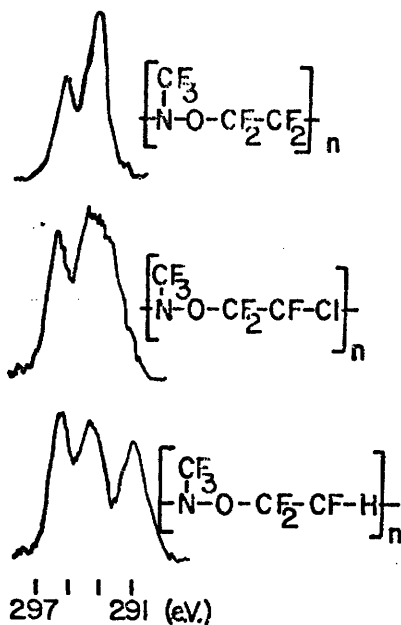
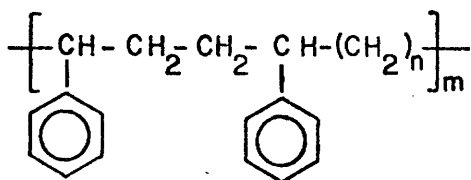


Figure 2.12.  $C_{1s}$  Levels in a Series of Nitroso Rubbers.

The assignments of the peaks, based on previous knowledge from homopolymer and copolymer systems, is straightforward, and the chemical shifts assigned in terms of the simple substituent effect. Once the alternating sequence of the copolymer was identified, by methods discussed previously, an investigation into the possibility of detecting structural isomerism was made. By the application of simple compounds with the charge potential model and complex deconvolutions of the spectra, assignments were made on the structural isomerism.

(2) The shake-up phenomena in a series of para-substituted polystyrenes and simple polymer systems has been investigated<sup>40</sup> and has been compared with other spectroscopic data, with theoretical calculations within the sudden approximation equivalent cores model and, CNDO SCF MO formalism identifying the shake-up arising from  $\pi \rightarrow \pi^*$  transitions involving the highest occupied and lowest unoccupied orbitals of the pendant aromatic systems. The polymers studied included polystyrene, polydiphenylsiloxane, poly-1-vinylnaphthalene, poly-2-vinylnaphthalene, poly-acenaphthalene and polyvinylcarbazole and it was shown that the shake-up structure was characteristic of a given pendant group. Although the simple model calculations have a tendency to predict transition probabilities lower than found experimentally the success of the models in predicting trends and arriving semi-quantitatively at results on substituent effects in the substituted polystyrenes provides a firm basis for extension of this work.

The unique application of the shake-up phenomena in the study of a series of alkane-styrene copolymers further demonstrated the potential utility of this method of analysis.<sup>41</sup> The study of the copolymers



where  $n = 0, 1, 3, 5, 6, 10,$

provided evidence that a trend existed between the shake-up intensity and the chain length of the alkane component, and that the structure of the shake-up satellites and the energy separation remain essentially constant. Figure 2.13. illustrates the effect of decreasing shake-up intensity with increasing alkane chain length.

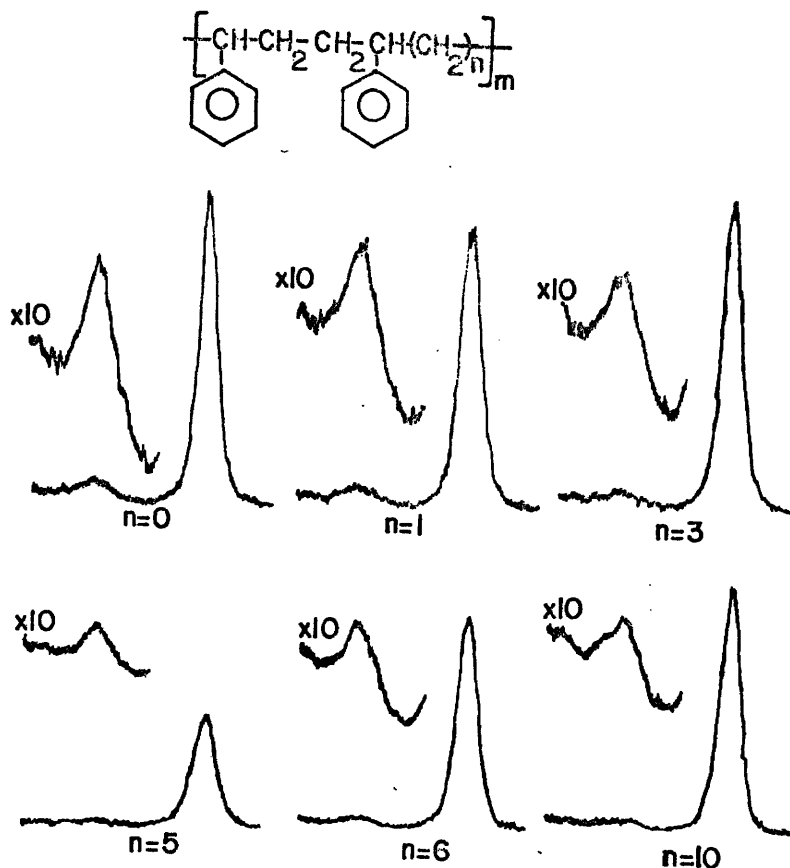


Figure 2.13.  $C_{1s}$  Levels in a Series of n-alkane /Styrene Copolymers.

(3) The charge potential model, as discussed in Chapter 1, can be applied to polymers when the parameters  $k$  and  $E^0$  are established for all the relevant core levels of the polymer systems being studied. It is possible to invent the model to obtain the experimental charge distributions within a polymer system. This method has the obvious application of being able to calculate the charge distributions in large models that are impracticable

for conventional molecular orbital calculations and comparing it to experimentally found B.E.'s. Figure 2.14. illustrates the experimental charge distributions found in polyvinylidene fluoride and polytrifluoroethylene model systems.

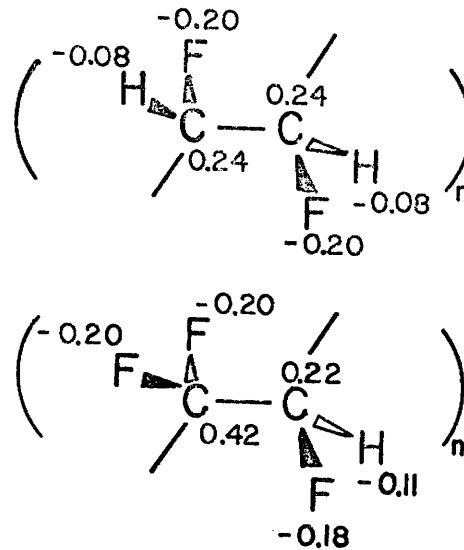


Figure 2.14. Experimental Charge Distributions for Polyvinylidene Fluoride and Polytrifluoro-Ethylene.

(4) The valence levels of polymers are of relevance to the detailed interpretation of the overall electrical properties of polymers. In the case of simple molecules the study of the valence levels by ESCA has the disadvantages, as discussed in Chapter 1, when compared to UPS in that the cross sections are generally lower in ESCA and the resolution is much poorer (see Figure 1.7.).

When studying polymer systems these disadvantages are offset in that since there are so many vibrational modes possible, resolution becomes less of a problem. Also, with ESCA, all the

valence levels can be studied whereas with UPS only the higher occupied levels can be studied and with electron energies of 0 - 21 eV (HeI) and 0 - 70 eV (He II). In UPS this is the region of rapidly varying escape depth where surface contamination would be critical, whereas this is much less so with X-ray photon energies. Figure 2.15. illustrates typical valence band spectra for a series of polymers.

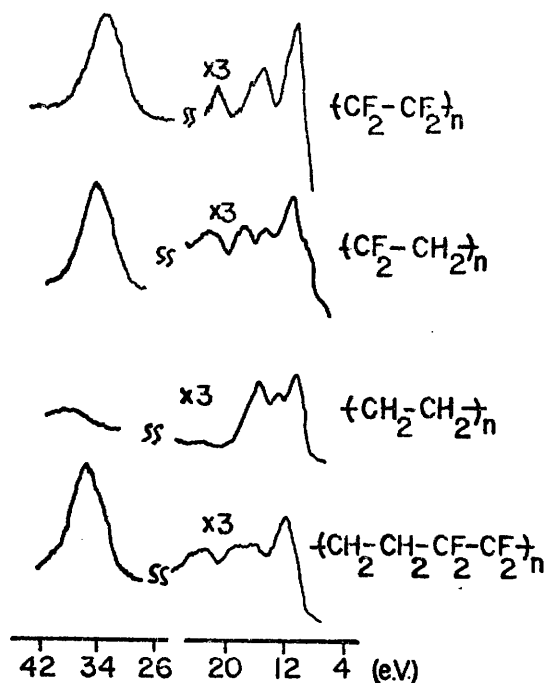


Figure 2.15. Valence Band Spectra for a Series of Polymers.

(iv) Dynamic Studies on Polymer Systems.

(a) Surface Treatments.

(1) Crosslinking by activated species of inert gases (CASING), where a polymer is exposed to activated species of inert gas is a particularly good application of ESCA to polymer chemistry. Studies have been made on copolymers of ethylene/tetrafluoroethylene where the films were irradiated with a low energy (2 kV) beam of argon ions for successive periods of 5

seconds and the  $C_{1s}$  and  $F_{1s}$  core levels monitored.<sup>42</sup> Figure 2.16. quite clearly demonstrates the effects on the top surface of the ion bombardment. Possible mechanisms for the process were proposed and the most likely steps chosen based on the ESCA information available.

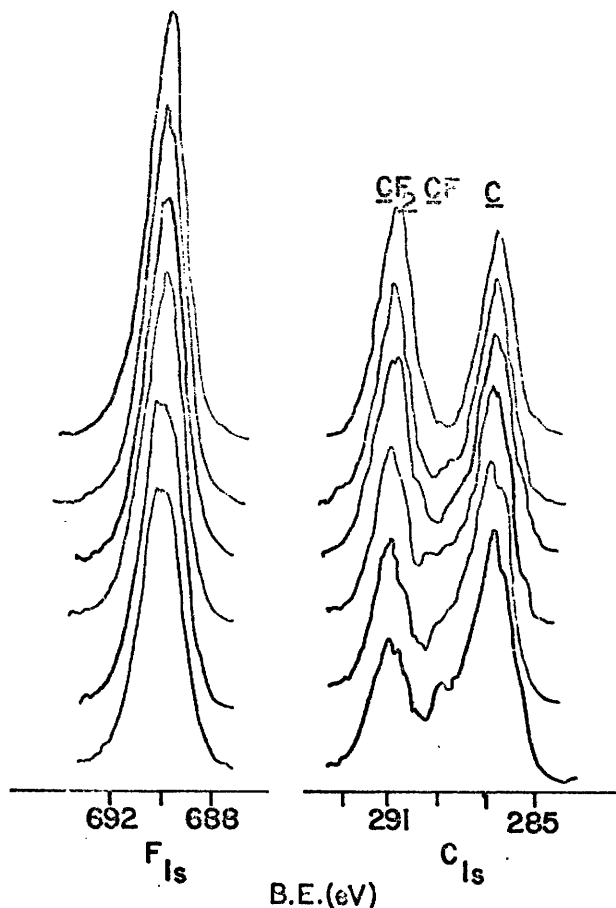


Figure 2.16. Effects of Argon Ion Treatment on Ethylene-Tetrafluoroethylene Copolymers.

(2) The surface fluorination of polyethylene was examined<sup>20</sup> and a very detailed analysis of the spectra confirmed the technique to establish a quite complete picture of the early stages of the surface fluorination process.

Although a detailed description of the analysis is beyond the scope of this summary the results of the investigation were based upon two methods of analysis. The first method was based upon the equation (2.2.).

$$\frac{y}{K} - 1 = \frac{y}{K} e^{-d/\Omega_3} - e^{-e/\Omega_1} \quad \dots \quad (2.2)$$

where  $y$  = measured area ratios for  $F_{1s}$  and  $F_{2s}$  peaks from ESCA spectrum.

$K$  = infinity values for escape depths of infinitely thick films measured from homopolymers.

$\Omega_3$  = electron mean free path appropriate to  $F_{2s}$  levels

$\Omega_1$  = " " " " " "  $F_{1s}$  levels

where a grid of computed values for the right-hand side of equation (2.2.) was prepared to values of  $\underline{d}$  in the range 2 - 41 Å at 1 Å intervals and ratio  $\Omega_3/\Omega_1$  from 1 to 2 in 0.1 increments. The computations for 40 values of  $\underline{d}$  and 11 values for each ratio of  $\Omega_3/\Omega_1$  generates 24,200 data points. These tables were used in the analysis of five fluorinated films and fluorinated film thicknesses were computed to be 3.5, 6, 16, 30 and 36 Å respectively for the five films.

An alternate procedure using the  $C_{1s}$  levels determined the depth of fluorination of the film and Table 2.3. illustrates the comparison between the two methods.

Table 2.3.

Calculated Thickness of Fluorinated Film (d)

Experiment	$d, \text{Å}$		Average
	From $C_{1s}$ spectra	From $F_{1s}/F_{2s}$ spectra	
1	5.5	3.5	4.5
2	9.0	6.0	7.5
3	15.0	16.0	15.5
4	24.0	30.0	27.0
5	46.0	36.0	41.0

The remaining points: thermal and photochemical degradation, depth profiling of surfaces and oxidative degradation of polymers have not been investigated to any great length but it is obvious from the points made throughout this summary that these areas have great potential for investigation by ESCA, and that real-time studies and process control will become a reality as more sophisticated instrumentation becomes available.

General Introduction to Experimental Sections.

Polymers derived from acrylate and methacrylate monomers are of some considerable importance industrially and as such have been exhaustively studied both from an academic and technological standpoint. A review of the literature on 'acrylic polymers' reveals a voluminous amount of work concentrating in such areas as the mechanical, electrical and thermal properties of the polymers, particularly from an engineering standpoint. Impact strengths, flexural strengths, heat distortion temperatures, coefficients of thermal expansion, dielectric constants are just a few of the many engineering properties well characterized and full reported in the literature on acrylic polymers.<sup>43</sup>

A close scrutiny of the literature on the chemical properties of the acrylic polymers reveals that a good deal is known about the kinetics and mechanisms of the polymerizations and the tacticities of the resulting polymers. The characterization of these polymer systems has been carried out, to a very large degree, on the solution phase properties concentrating on such problems as weight average molecular weight, chain entanglement, dielectric relaxation constants for the side chains, light scattering data, optical rotation, stereochemical regularity, etc.<sup>44,45</sup>

Scattered publications appear infrequently on the solid state properties of the acrylic polymers,<sup>46</sup> and these are most often studies on either the morphology, or the relaxation and conformational properties of the side chains. These studies essentially concern the bulk polymer.

It is quite apparent that since solids communicate with their environment by way of their surfaces that a very important area of investigation which hereto appears virtually untouched, is the characterization of the immediate surface of polymers. Properties at the surface such as chain conformation, tacticity, oxidation, degradation, side chain orientation and propensity for hydrogen bonding are all important aspects of the acrylic polymers which will determine their usefulness in technological applications.

The third chapter presents an investigation of a series of polyalkyl acrylates concentrating on the areas described above, along with a theoretical analysis of model compounds and model systems for the tacticity of the polymer systems.

The fourth chapter is a study of a series of poly-alkyl and -aryl methacrylates and includes studies on oxidation, orientation of side chains and hydrogen bonding at the surface.

CHAPTER 3

Core and Valence Energy Levels of a Series of Polyalkyl-  
acrylates

## CHAPTER 3

### Core and Valence Energy Levels of a Series of Poly- alkylacrylates.

#### (i) General Introduction.

Previous work on the ESCA of Polymers<sup>17,35,37,39</sup> has shown how a detailed consideration of the absolute and relative binding energies and relative intensities of peaks corresponding to the direct photoionization of core levels in polymeric systems can provide valuable data on structure and bonding in general in polymeric systems. The investigations reported to date have largely pertained to fluorocarbon based polymers where the large electronegativity of the fluorine substituents give rise to a substantial span in binding energies for  $C_{1s}$  levels corresponding to substituted carbon atoms in widely differing electronic environments.<sup>42</sup> For systems in which the shifts in core binding energies are insufficiently large to be resolved (e.g. solely hydrocarbon based polymers) it has recently been shown<sup>40,41</sup> that it is still possible to derive information on structure and bonding in these systems from observations of the relative intensities and separation from the direct photoionization peak of the satellite peaks arising from shake-up transitions.

For fluorocarbon materials it was shown that surface modifications may readily be detected by ESCA and quantitative data obtained from an investigation of changes in relative peak intensities for core levels which cover a wide range in binding energies giving rise to substantial differences in escape depth dependencies and hence sampling depth.<sup>17</sup> Since many of the important physical, chemical, electrical and mechanical properties

depend on the structure and bonding in the outermost few tens of Angstroms of the surface, any technique which can clearly differentiate this region from the bulk is of some considerable importance.<sup>42</sup> ESCA will clearly become increasingly important in establishing whether structure and bonding at the surface of polymer samples is the same or different from the bulk and also in monitoring chemical and physical modifications which are initiated at the surface. One important example is surface oxidation which is clearly of relevance in any discussion of ageing and weathering of materials.

This chapter and the following report an ESCA investigation of the core and valence energy levels of an extensive series of polyacrylates and polymethacrylates. These materials form an interesting comparison with the series previously investigated and fit logically into the systematic studies on the application of ESCA to polymer chemistry. Thus, the range of substituent effects is considerably smaller than in previously studied fluorocarbon based polymer series,<sup>42</sup> and the span in escape depth dependencies is also somewhat less. While there has been a considerable effort expended in studying aspects of the structure and bonding of simple polyalkyl acrylates by a variety of spectroscopic techniques, it is clear that there is paucity of data pertaining to the surface and subsurface structure of the solid systems, since most of the previous work refers to the polymers in solution.<sup>44-46</sup> This study therefore has attempted to remedy this situation and has been addressed to the following.

From studies of the absolute and relative binding energies of the core levels and the relative peak intensities the

- 71 -

composition can be established for these materials and draw comparisons with data pertaining to the bulk.<sup>17,35,37,39</sup> This is obviously of relevance in establishing whether specific orientation of alkyl groups occur at the surface as a function of the length of the side chain and if surface oxidation or cross linked features are apparent. To draw comparisons with the bulk an I.R. study was also undertaken. A subsidiary objective of some considerable importance was a parallel study to investigate the extension of theoretical models for quantifying the data pertaining to both absolute and relative binding energies and to confirm the assignment of core levels. This has also allowed an investigation of the possibility of using ESCA for studying structural isomerisms in these systems. For comparison purposes some simple model systems were investigated from both an experimental and theoretical standpoint. The data derived from these studies has also proved particularly useful in elaborating the main features of the valence bands of the two series of polymers.

(ii) Experimental.

(a) Samples.

As an aid to the interpretation of the data pertaining to the polymer systems a series of model compounds were studied as listed in Table 3.1. Methanol, ethanol, acetone and diethylether were obtained as spectroscopic grade solvents while the esters were reagent grade materials which were shown by g.l.c. to be >98% purity. The polymers, also listed in Table 3.1. were commercially available samples obtained from Cellomer Associates Inc., P.O. Box 311, Webster, N.Y. and were used directly in preparing samples for the ESCA investigation. Except as noted

Table 3.1.

Model Compounds and Polyalkyl Acrylate Samples Studied in this Work Showing the Tg's for the Latter.

Model Compounds	Polyacrylate Homopolymers	Typical Tg's (°C)
Methanol	Polyacrylic acid	+106
Ethanol	Polymethyl acrylate	+ 9
Acetone	Polyethyl acrylate	- 20
Diethyl ether	Polyisopropyl acrylate	- 3
Ethyl formate	Poly-n-butyl acrylate	- 49
Ethyl acetate	Polyisobutyl acrylate	- 24
Isopropyl acetate	Poly-t-butyl acrylate	- 21
Isobutyl acetate	Poly-2-ethylhexyl acrylate	- 55
Ethyl acetoacetate	Poly-n-decyl acrylate	~ - 45
	Poly-n-lauryl acrylate	- 65
	Polyhexadecyl acrylate	+ 15
	Polyoctadecyl acrylate	~+ 40

(See Appendix A for I.R. Spectra of Polymers).

in the ensuing discussion, infrared analysis confirmed the overall purity of the samples and where comparisons were available, agreed with spectra in the literature.

(b) Sample Preparation.

The model compounds, all relatively low boiling liquids, were studied in the form of thin films condensed onto a cooled gold substrate directly in the spectrometer source. To accomplish this, samples (0.1  $\mu$ l) were injected into a reservoir shaft (~ 500 cc.'s in volume) which was attached to the source region of the spectrometer by means of an insertion lock system. The samples were leaked through a metrosil plug in the reservoir shaft and the directed jet of vapour impinged onto the cooled

gold substrate mounted onto a sample probe. The reservoir temperature was typically  $\sim 30^{\circ}\text{C}$  and that of the cooled probe tip  $\sim -100^{\circ}\text{C}$ . By studying these samples as thin films on gold sufficient charge carriers are available such that sample charging is obviated allowing direct calibration of the energy scale.

The low Tg's for the majority of the polyalkyl acrylates studied, facilitated the preparation of samples as thin films coated onto gold substrates, the latter being attached directly to the sample probe by means of double sided Scotch tape. Polyacrylic acid in the form of a fine powder was coated onto double sided Scotch tape directly attached to the spectrometer probe while for polyoctadecyl acrylate a small amount of the sample was deposited onto a gold substrate attached to the sample probe which was then slowly raised in temperature from ambient to  $\sim 40^{\circ}\text{C}$ . By this means the sample spread evenly as a thin film onto the substrate.

(c) Post-treatment of Polyisopropyl Acrylate.

The study of the adsorption of a series of 'hydrogen bonding species' at the surface of polyisopropyl acrylate was accomplished by exposing the polymer (which had been previously coated onto a gold substrate to about  $100\ \mu$  thick), to the appropriate material. In this study the compounds selected were HF,  $\text{H}_2\text{O}$  and  $\text{NH}_3$  in the order of decreasing propensity for hydrogen bonding. The polymer sample was exposed to a stream of HF into atmospheric pressure for several minutes and the sample then transferred to the spectrometer, the spectra being recorded after pump down to the required operating base pressure

(an operation requiring ~ 5 minutes). The H<sub>2</sub>O treatment was accomplished simply by wiping the surface of the polymer with a wet tissue and the sample then inserted into the spectrometer for analysis. The NH<sub>3</sub> treatment was accomplished by exposing the polymer sample to the atmosphere of NH<sub>3</sub> in a closed container of .88% ammonia for half an hour. The sample was then removed from the container and introduced into the spectrometer for analysis.

In the particular cases of polyisopropyl, polyoctadecyl, poly-2-ethyl hexyl and poly-n-decyl acrylates qualitative studies were made of wettabilities. Contact angles for sessile drops of water on the polymer films were measured from enlargements of photographs taken with rear illumination.<sup>47</sup> No attempt was made to quantify the results because of the crude nature of the experiments, however as noted in the text a clear distinction was apparent between those samples which were unoxidized at the surface and those which were oxidized.

(d) Instrumentation.

Spectra were recorded with an A.E.I. ES200A spectrometer using MgK $\alpha_{1,2}$  exciting radiation. Typical operating conditions were: X-ray gun; 12 kV, 15 mA; pressure in the sample chamber, ca. 10<sup>-8</sup> torr. Under the experimental conditions employed, the gold 4f<sub>7/2</sub> level at 84 eV used for calibration, had a full width at half maximum (FWHM) of 1.2 eV. No evidence was obtained for radiation damage to the sample from long term exposure to the X-ray beam.

The infrared spectra were recorded on a Perkin Elmer 577 Grating Infrared Spectrometer and wide scan spectra from 2.5

to 40  $\mu$  were complemented by high resolution spectra in the C-H and C=O stretching regions from 2.5 to 5.5  $\mu$ .

Overlapping peaks were resolved into their individual components by use of a DuPont 310 curve resolver (an analogue computer). The detailed deconvolutions were based on a knowledge of linewidths determined from the model compounds. Previous studies<sup>17</sup> have shown<sup>42</sup> that for individual components of the core level spectra for the O<sub>1s</sub> and C<sub>1s</sub> levels the lineshapes approximate fairly closely to gaussian.

(iii) Theoretical.

The data pertaining to the model compounds have been interpreted at three levels of sophistication. For the smallest systems Ab Initio calculations have been carried out on both the neutral and ionized systems and the assignment of levels confirmed by reference to binding energies computed as energy differences from Koopmans' Theorem<sup>18,22</sup> and from the charge potential model.<sup>5</sup> These calculations were carried out using the ATMOL series of programs implemented on an IBM 370/195 computer.<sup>48</sup> The basis sets employed were STO 431G expansions using the relevant best atom exponents for the appropriate core and valence orbitals for carbon, oxygen and hydrogen.<sup>49,50</sup>

For the larger model systems and for the polymer models, calculations were carried out within the all valence electron CNDO/2 SCF MO formalism<sup>50</sup> employing the charge potential model. These computations were carried out on an IBM 360/67 computer and for a typical convergence limit of  $10^{-3}$  a.u. in the total energy calculations on the largest model systems studied (35 atoms, 86 basis functions) required  $\sim$  10 minutes of cpu time for 10 iterations.

(iv) Results and Discussion for Model Compounds.

(a) Core Levels of Model Compounds.

(1) Experimental.

The primary sources of ESCA data which have been extensively utilized to date are absolute and relative binding energies and relative peaks areas.<sup>17,35,37,39,42</sup> As a preliminary to a detailed investigation of the polyacrylates it was necessary therefore to study a series of simple molecules as model systems to provide a firm basis for the interpretation of the data. Direct measurements of the relative area ratios for the  $O_{1s}$  and  $C_{1s}$  levels of homogeneous thick films of the condensed model compounds plotted against the stoichiometric ratios provides an excellent straight line (Fig. 3.1) correlation

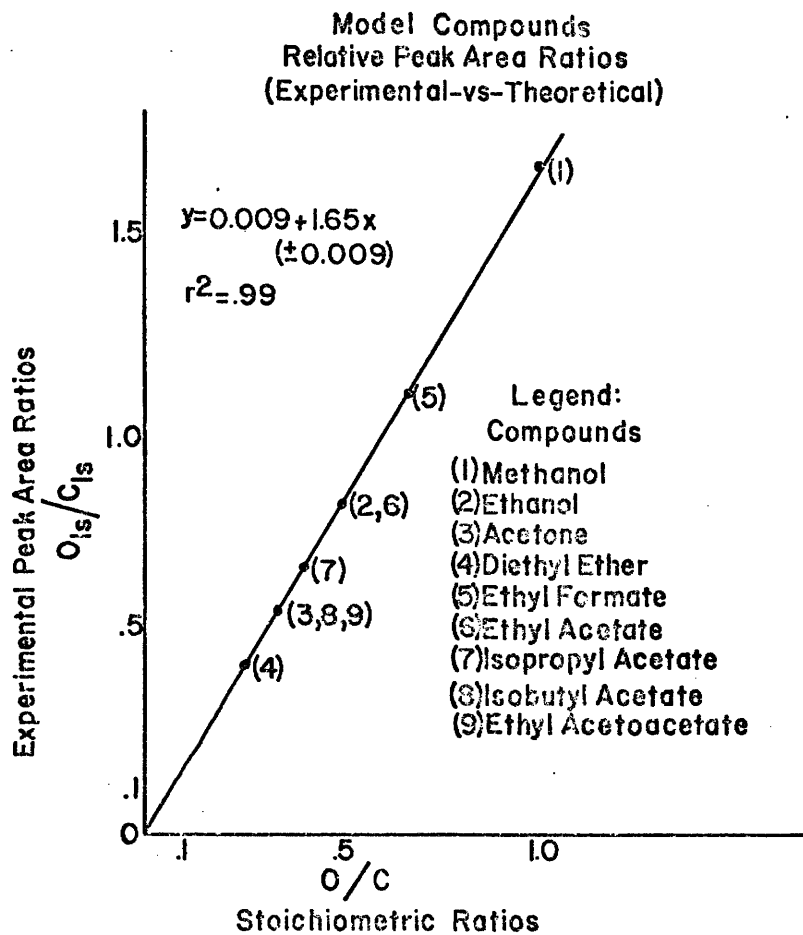


Figure 3.1. Plot of Measured  $O_{1s}/C_{1s}$  Area Ratios Versus Stoichiometric Ratios for Model Compounds.

the slope being  $1.65 \pm 0.009$  ( $r^2 = .99$ ). This therefore provides the required sensitivity factors for the  $C_{1s}$  with respect to  $O_{1s}$  core levels, these factors of course being instrument dependent since they depend not only on the relative cross sections for photoionization but also on spectrometer factors such as sensitivity of the detector for electrons of different kinetic energy, etc. Having obtained an experimentally determined correction factor for the relative peak areas as a function of stoichiometry, a discussion of the relative and absolute binding energies for various structural features is warranted. Well resolved spectra were obtained in all cases and by careful calibration of linewidth, (FWHM) and lineshape, incompletely resolved peaks could be unambiguously deconvoluted within very narrow error limits (typically  $\pm 0.2$  eV) and the relevant data are recorded in Table 3.2.

To enable a direct comparison to be drawn with the experimental data for the polymers to be discussed in a later section, representative spectra of some simple alkyl acetates are shown in Fig. 3.2.

In each case core levels corresponding to carbon atoms not directly bonded to oxygen had binding energies centred  $\sim 285.0$  eV and have therefore been omitted from the table. Taking this as the energy reference it is clear that the shift in binding energy for a given carbon is characteristic of the chemical environment. For carbon atoms singly bonded to oxygen (e.g. alcohols, ethers and simple esters) the binding energies and shifts are highly characteristic, being  $286.6 \pm 0.1$  eV and  $1.6 \pm 0.1$  eV respectively. The carbon atoms doubly bonded to oxygen fall

Table 3.2.

Experimentally Determined Binding Energies for Model Compounds

Molecule	Experimental Binding Energies in eV					
	1s Levels				2s Levels	
	-C-O-	C=O	C=O	-O-C	O <sub>2s</sub>	C <sub>2s</sub>
CH <sub>3</sub> OH	533.6	-	-	286.6	25.6	16
CH <sub>3</sub> CH <sub>2</sub> OH	533.6	-	-	286.6	25.5	16
CH <sub>3</sub> COCH <sub>3</sub>	-	533.6	287.9	-	25.2	13
CH <sub>3</sub> CH <sub>2</sub> OCH <sub>2</sub> CH <sub>3</sub>	533.6	-	-	286.5	26.5	16
HCOOCH <sub>2</sub> CH <sub>3</sub>	534.5	533.3	289.3	286.6	26.7	14
CH <sub>3</sub> COOCH <sub>2</sub> CH <sub>3</sub>	534.4	533.6	289.0	286.6	26.0	16
CH <sub>3</sub> COOCH(CH <sub>3</sub> ) <sub>2</sub>	534.5	533.5	289.2	286.7	26.0	16
CH <sub>3</sub> COOCH <sub>2</sub> CH(CH <sub>3</sub> ) <sub>2</sub>	534.4	533.2	289.2	286.7	26.0	16
CH <sub>3</sub> COCH <sub>2</sub> COOCH <sub>2</sub> CH <sub>3</sub>	534.4	533.1 533.6	288.9 287.2	286.3		

into two classes, namely simple carbonyl compounds and esters, the binding energies and shifts for the former being significantly lower than for the latter ( $287.9 \text{ eV} \pm 0.2 \text{ eV}$ ,  $2.9 \text{ eV} \pm 0.2 \text{ eV}$  and  $289.1 \pm 0.2 \text{ eV}$  and  $4.1 \pm 0.2 \text{ eV}$  respectively). The overall shifts in binding energies therefore are sufficiently large to allow a ready means of identification of a particular structural feature.

For the O<sub>1s</sub> levels the binding energies for the simple carbonyl compounds, alcohols and ether are essentially the same. By comparison, in the esters the singly and doubly bonded oxygen exhibit a substantial shift ( $1.2 \pm 0.2 \text{ eV}$ ) and the theoretical analysis presented below unambiguously assigns the higher binding energy component as arising from the singly bonded oxygen.

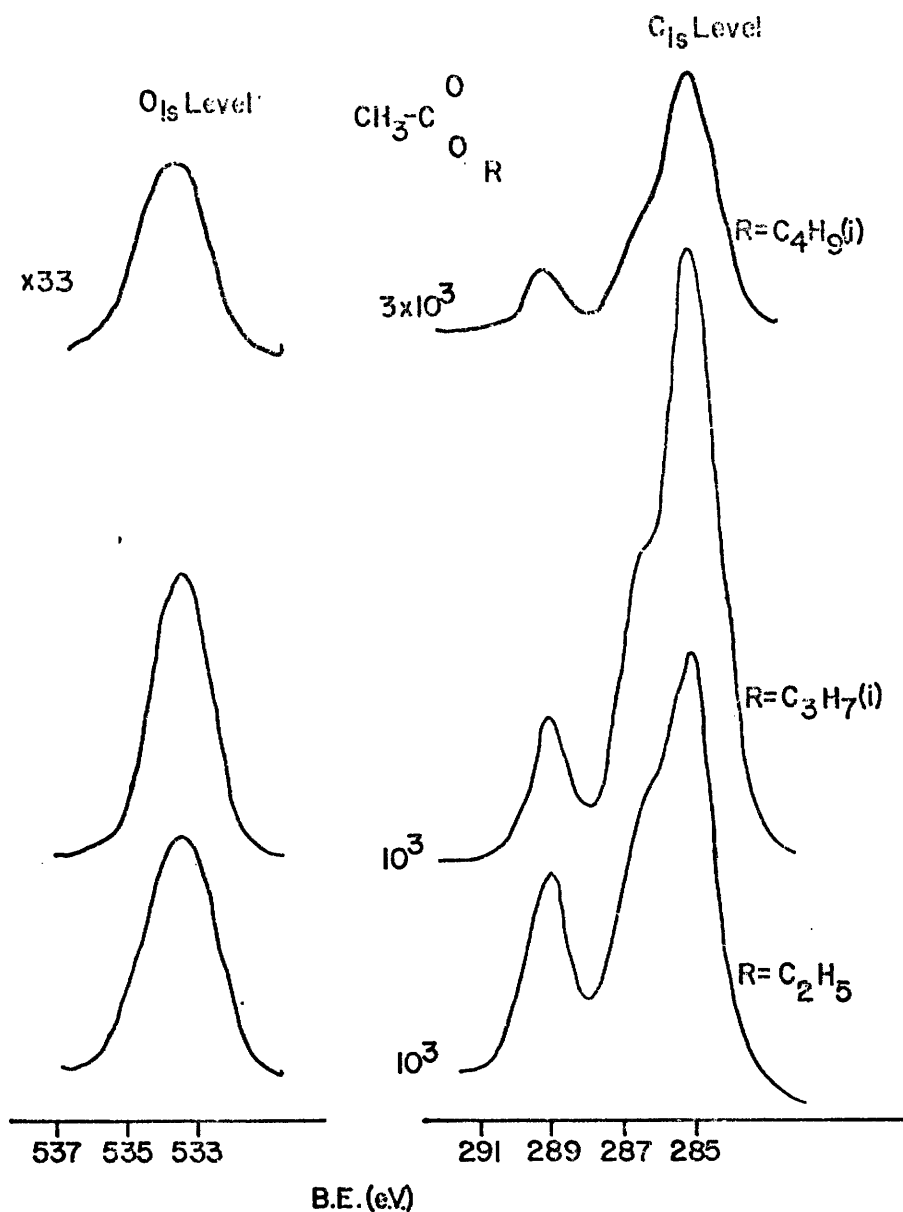


Figure 3.2. Core Level Spectra for Simple Alkyl Acetates.

Comparison of the absolute binding energies indicates that while the binding energy of the carbonyl type oxygen of the ester group is comparable to that of a simple carbonyl compound, that of the ester type oxygen is significantly higher than that of the alcohol from which it is derived. To check the overall internal consistency of this assignment data is also presented for ethylacetoacetate which under the conditions employed in these experiments exists almost solely (96%) in the keto form. The

oxygen 1s levels for this compound correspond to a superposition of those for an ester group and a simple ketone; the oxygen doubly bonded to carbon exhibiting a small shift ( $\sim 0.5$  eV) while the singly bonded oxygen of the ester group is at substantially higher binding energy and is directly comparable to that for the corresponding simple esters. A discussion of the  $C_{1s}$  levels for ethylacetoacetate will be given in a later section when surface oxidation of the polyacrylates is considered.

(2) Theoretical.

It has been shown that with careful calibration, with respect to simple model systems,<sup>17,35,37,39,42</sup> it is possible to quantitatively describe both absolute and relative binding energies for polymer systems. The analysis has been based on the so-called charge potential model<sup>5</sup> which may formally be derived from Koopmans' Theorem<sup>18</sup> in the zero differential approximation.<sup>36</sup> The model, relating charge distributions to molecular core binding energies is intuitively appealing to chemists and has the distinct advantage that in appropriate cases the model may be inverted enabling charge distribution to be obtained from experimentally determined binding energies.<sup>51</sup> In this model the binding energy ( $E_i$ ) of a given core level located in atom  $i$  is related to the charge distribution in the molecule as

$$E_i = E_i^O + kq_i + \sum_{j \neq i} \frac{q_j}{r_{ij}} \quad \dots (3.1)$$

where  $E_i$  is the experimentally determined binding energy for a given core level,

$E_i^O$  is a reference binding energy level,

$q_i$  is the charge on atom  $i$  on which the core hole is located

and  $k$  is a constant (approximately equal to the one-centre repulsion integral between a core and valence electron on atom  $i$ ).

As a necessary pre-requisite to the application of this model to the discussion of the data pertaining to the polyacrylates, studies were carried out on simple model compounds, the objectives being twofold. First, to confirm the assignment of core levels and second, to obtain values for the charge potential parameters  $E^0$  and  $k$  for the  $O_{1s}$  and  $C_{1s}$  core levels. Calculations of the requisite charge distributions were accomplished within the all valence electron CNDO/2 SCF MO formalism.<sup>17,35,37,39</sup> By plotting  $E - \sum \frac{q_j}{r_{ij}}$  (where  $E$  is the experimentally determined binding energy) versus  $q_i$  the charge on atom  $i$  on which the core hole is located,  $E^0$  and  $k$  for each core level may be determined as an intercept and slope respectively. Fig. 3.3. shows the correlation for the  $C_{1s}$  and  $O_{1s}$  levels and least squares analysis of the data yields values of 284.6 eV and 25.2 for  $E^0$  and  $k$  respectively for the  $C_{1s}$  levels, the correlation coefficient being 0.99. These values are in excellent agreement with those previously determined for simple fluorocarbon systems.<sup>52</sup> The relatively small range of binding energies leads to a considerable scatter in the data for the  $O_{1s}$  levels and the correlation coefficient (0.76) is therefore somewhat lower. Nonetheless the concomitant error limits still lead to an unambiguous assignment of the  $O_{1s}$  levels and this has been checked by carrying out detailed non-empirical LCAO SCF MO calculations of absolute binding energies from computations on the neutral molecules and the relevant hole states. Table 3.3 shows

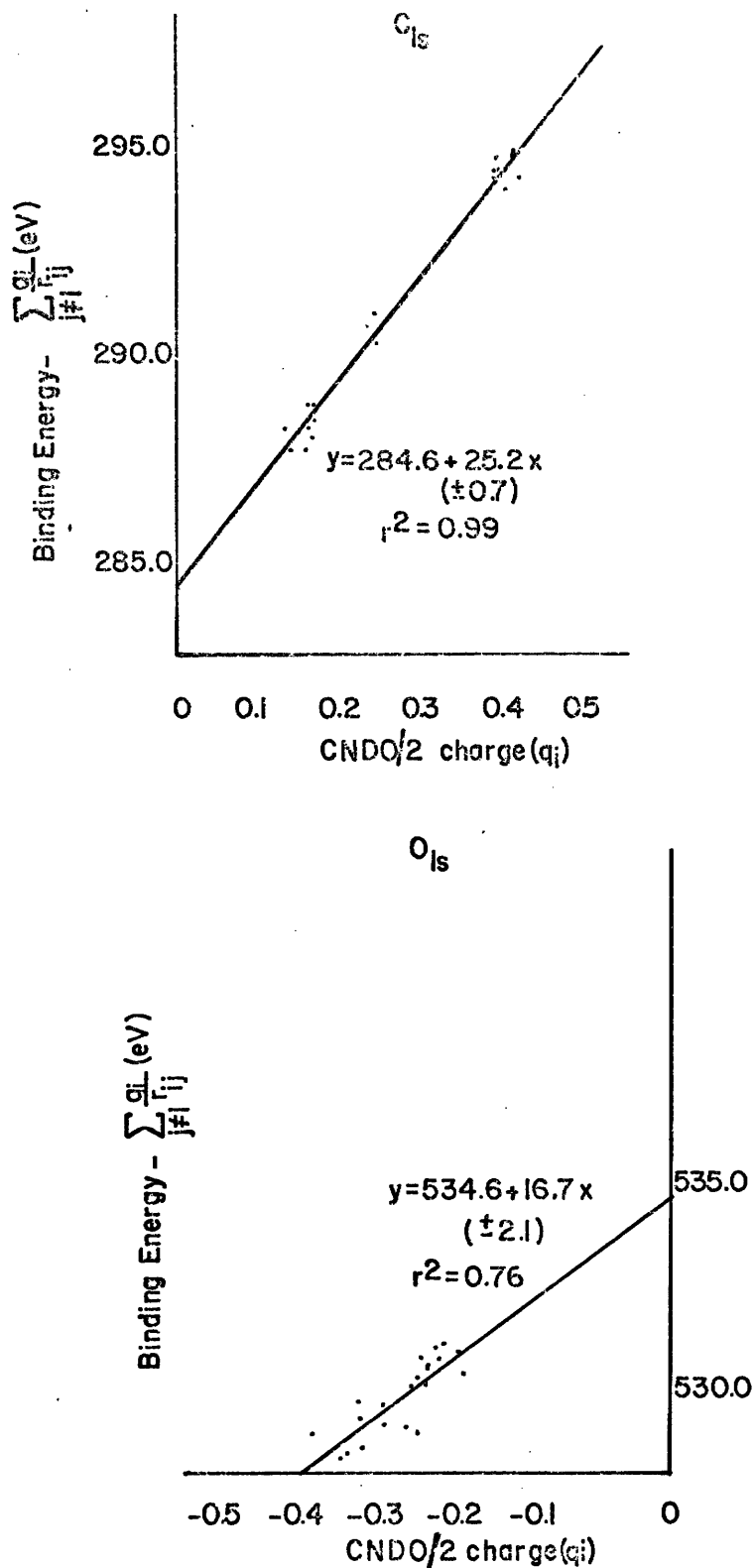


Figure 3.3. Charge Potential Correlations for the  $C_{1s}$  and  $O_{1s}$  Levels of Model Compounds.

Table 3.3.

Absolute Binding Energies for the  $C_{1s}$  and  $O_{1s}$  Levels of the  
Model Compounds from the Charge Potential Model

Molecule	Theoretical Binding Energies in eV			
	-C-O-	C=O	C=O	C-O-
CH <sub>3</sub> OH	533.7	-	-	286.5
CH <sub>3</sub> CH <sub>2</sub> OH	533.6	-	-	286.8
CH <sub>3</sub> COCH <sub>3</sub>	-	533.2	287.8	-
CH <sub>3</sub> CH <sub>2</sub> OCH <sub>2</sub> CH <sub>3</sub>	533.2	-	-	286.6
HCOOCH <sub>2</sub> CH <sub>3</sub>	534.4	533.2	289.1	287.4
CH <sub>3</sub> COOCH <sub>2</sub> CH <sub>3</sub>	534.2	532.9	289.1	287.2
CH <sub>3</sub> COOCH(CH <sub>3</sub> ) <sub>2</sub>	534.1	532.9	289.0	287.4
CH <sub>3</sub> COOCH <sub>2</sub> CH(CH <sub>3</sub> ) <sub>2</sub>	534.2	532.9	289.1	287.2
CH <sub>3</sub> COCH <sub>2</sub> COOCH <sub>2</sub> CH <sub>3</sub>	534.2	532.8	289.1	287.2
		533.1	288.0	

the calculated absolute binding energies obtained from the charge potential model using the values of  $k$  and  $E^0$  derived from Fig. 3.3. It is clear that both the absolute and relative binding energies are in excellent agreement with experiment and the assignments are further reinforced by the detailed non-empirical study, the results of which are detailed in Table 3.4.

The reference level for these calculations differs of course from that for the charge potential model which has been specifically calibrated with respect to measurements pertaining to the solid state where the convenient energy reference is the Fermi level whereas for the non-empirical calculations the reference is the vacuum level.<sup>36</sup> From studies on simple organic molecules in both the gas and solid phase, the difference in reference levels has been shown to be  $\sim 5$  eV which corresponds

Table 3.4.

Theoretically Calculated Absolute and Relative Binding Energies  
for some Core and Valence Levels of  $\text{CH}_3\text{OH}$ ,  $\text{CH}_2\text{O}$  and  $\text{HCOOH}$  as  
Simple Model Systems

	Molecule	Binding Energy					
		Calc.	Exptl. <sup>†</sup>	R.E. <sup>††</sup>	(a)	(b)	Exptl.
$\text{O}_{1s}$ Levels	$\text{CH}_3\text{OH}$	544.5	538.9	16.4	(0)	(0)	(0)
	$\text{HCHO}$	545.1	539.0	17.1	0.6	1.3	0.1
	$\text{H}-\text{C} \begin{array}{c} \text{O} \\   \end{array}$	544.3	538.3	17.2	-0.2	0.6	-0.6
	$\text{H}-\text{C} \begin{array}{c} \text{OH} \\   \end{array}$	546.3	540.1	16.5	1.8	1.9	1.2
$\text{C}_{1s}$ Levels	$\text{CH}_3\text{OH}$	295.5	292.3	11.2	(0)	(0)	(0)
	$\text{HCHO}$	297.8	293.9	10.6	2.3	1.7	1.6
	$\text{H}-\text{C} \begin{array}{c} \text{O} \\   \end{array}$	299.3	295.4	10.5	3.8	3.0	3.1
	$\text{H}-\text{C} \begin{array}{c} \text{OH} \\   \end{array}$						
$\text{O}_{2s}$ Levels	$\text{CH}_3\text{OH}$	34.3	~32	2.6	(0)	(0)	(0)
	$\text{HCHO}$	35.9	~34	2.8	1.6	1.9	~2
	$\text{HC} \begin{array}{c} \text{O} \\   \end{array}$	35.0	~31	2.2	0.7	0.4	~-1
	$\text{HC} \begin{array}{c} \text{OH} \\   \end{array}$	35.8	~33	4.1	1.5	3.1	~1
$\text{C}_{2s}$ Levels	$\text{CH}_3$	23.9	~23	1.1	(0)	(0)	(0)
	$\text{HCHO}$	22.2	-	0.9	-0.7	-2.0	-
	$\text{HC} \begin{array}{c} \text{O} \\   \end{array}$	22.7	~22	0.9	-1.2	-1.5	-1.0
	$\text{HC} \begin{array}{c} \text{OH} \\   \end{array}$						

<sup>†</sup> Experimental data for core levels from ref. (5).

The data for the  $\text{O}_{2s}$  and  $\text{C}_{2s}$  valence levels is taken from ref. (53).

<sup>††</sup> R.E. refers to relaxation energy accompanying photoionization Cf. Ref. (22).

approximately to the work function of the sample.<sup>36</sup>

Considering first the  $O_{1s}$  levels, the assignment of formic acid as prototype for systems containing carbonyl groups is unambiguous with the carbonyl oxygen being substantially lower in binding energy. This is also apparent from straightforward application of Koopmans' Theorem which neglects of course the substantial electronic reorganization concomitant with core ionization.<sup>22</sup> It is significant however that the relaxation energies are characteristic of the local electronic environment.<sup>22</sup> Thus the calculated relaxation energies for the formally singly and doubly bonded oxygens in formic acid (16.5 eV and 17.2 eV respectively) are substantially the same as those for the  $O_{1s}$  levels in methanol (16.4 eV) and formaldehyde (17.1 eV) respectively, although the calculated absolute binding energies differ significantly. The calculations also successfully reproduce the substantial increase in binding energy for the ester type oxygen, by comparison with the alcohol, and the smaller decrease in binding energy for the carbonyl oxygen in going from a carbonyl group to a carboxyl function. It is interesting to note that this feature is also reproduced in the  $O_{2s}$  valence levels and this point will be discussed later.

(b) Valence Levels of Model Compounds.

In other studies on polymeric systems it was shown that the substantial differences in escape depth dependence for deep lying valence levels which are core like in character (viz.  $F_{2s}$ ) with respect to tightly bound core levels, may usefully be employed for analytical depth profiling.<sup>17</sup> In the present context it is clear from the published data in the literature on

model compounds that it is only for the deep lying  $O_{2s}$  valence levels which are readily identifiable that this possibility for analytical depth profiling is a feasible proposition. (This is of course in addition to the depth profiling capability arising from differences in escape depth dependence for the  $O_{1s}$  and  $C_{1s}$  levels). Gas phase (HeII) data was briefly alluded to for simple model compounds<sup>53</sup> and the assignment of levels based on non-empirical LCAO SCF MO calculations. In going to a high energy photon source (e.g.  $MgK\alpha_{1,2}$   $h\nu = 1253.7$  eV), as employed in this work, the differential changes in cross section with photon energy are such that for first row elements the intensities of levels derived from orbitals which are largely 2s in character is considerably greater than that from orbitals which are largely of 2p character.<sup>54</sup> For systems containing relatively large alkyl groups it is also clear from the literature that the region of the spectra corresponding to photoionization from orbitals essentially derived from linear combinations of  $C_{2s}$  levels span a considerable energy range making a direct integration of their overall intensities for comparison with that of the core levels somewhat difficult.<sup>53</sup> In utilizing the valence energy region for information, with regard to composition as a function of depth, restrictions were made to using the  $O_{2s}$  levels, although it will become clear that the overall band profile for the valence levels as a whole constitutes a 'fingerprint' for the system.

The measured valence energy regions corresponding to the core levels of the model systems shown in Fig. 3.2. are reproduced in Fig. 3.4. Reference to theoretical calculations

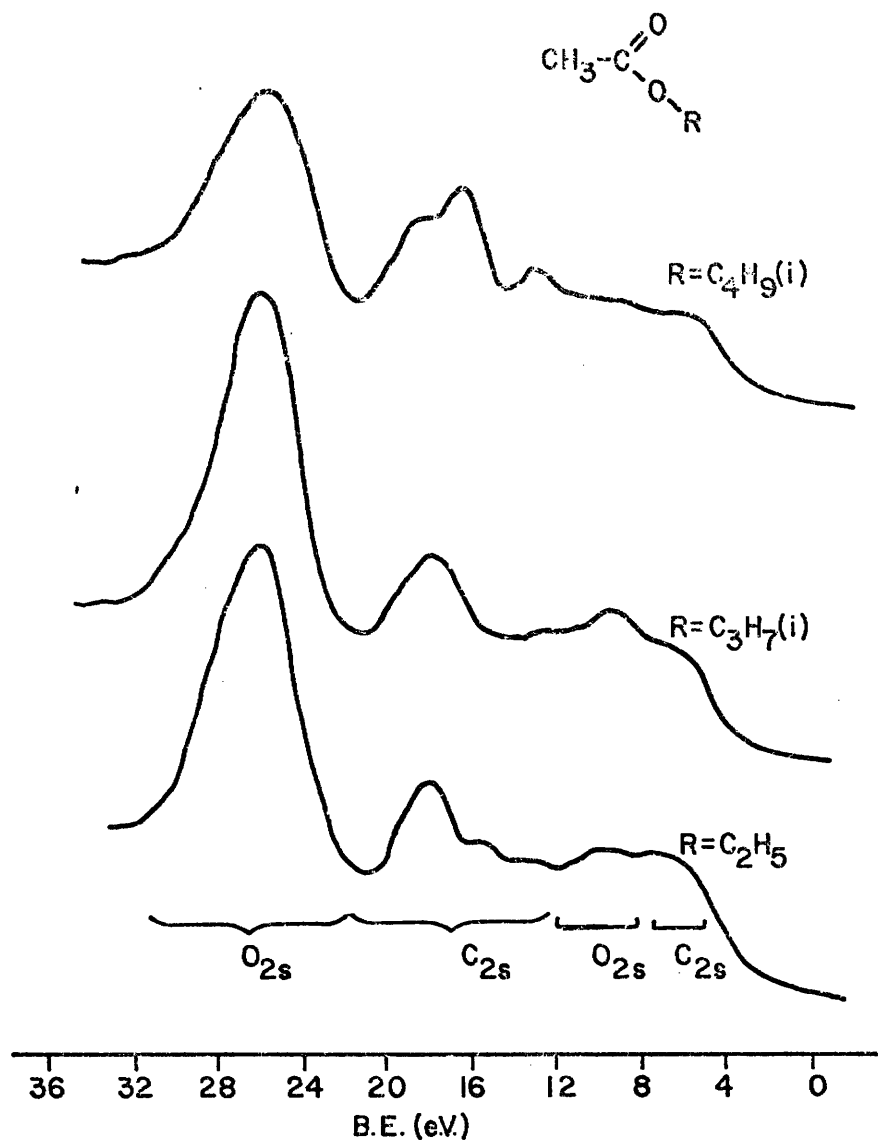


Figure 3.4. Measured valence energy levels for the alkylacetates whose core levels are shown in Fig. 3.2. The assignment of the energy levels indicated is solely qualitative and is included to convey the dominant characteristic of molecular orbitals in each region. In the energy range from 4 - 16 eV there is considerable overlap of characteristics and for this reason attention has been focussed primarily on the well resolved peak to high binding energy attributable to linear combination of the O<sub>2s</sub> levels.

and direct comparison with the experimental data on related systems unambiguously assigns the intense broad peak centred ~ 27 eV binding energy (solid phase Fermi Level as reference)

arising from molecular orbitals constituted primarily from linear combination of  $O_{2s}$  orbitals. The other regions corresponding very approximately to the assignment given (there is considerable overlap in each region) are distinctive and form a useful diagnostic feature for the alkyl component as will become apparent, however the considerable overlap make these levels less useful from the point of view of information with respect to analytical depth profiling. The difficulties involved in direct integration of the  $O_{2s}$  levels consequent upon the sloping baseline mean that the experimentally determined area ratios for the  $O_{1s}/O_{2s}$  levels are subject to a somewhat greater error than that for the  $O_{1s}/C_{1s}$  ratio as previously discussed. Analysis of the data for all the model compounds yields an  $O_{1s}/O_{2s}$  ratio of  $11 \pm 1$ . It should be emphasized however that this ratio, being instrument dependent, applies only to the particular experimental configuration used in this study. The approximate kinetic energies pertaining to photoemitted electrons from the  $O_{1s}$  and  $O_{2s}$  levels using a  $MgK\alpha_{1,2}$  photon source at  $\sim 720$  eV and  $\sim 1227$  eV respectively which from a consideration of a generalized curve of escape depth versus kinetic energy should correspond to significant differences in electron mean free paths.<sup>17,42</sup>

(v) Results and Discussion for Polyacrylates.

(a) Experimental.

Polymer compositions and absolute and relative binding energies of core levels

Preliminary experiments revealed that some of the polyacrylate samples studied as thin films on gold were oxidized.

Further experiments showed that the oxidation in some cases was limited to the surface of the samples but in others extended to the bulk. The evidence for this is most conveniently presented after a discussion of the results pertaining to the polymer samples where a variety of data established that the surface was representative of the bulk. The core level spectra for these samples are shown in Fig. 3.5. Considering firstly

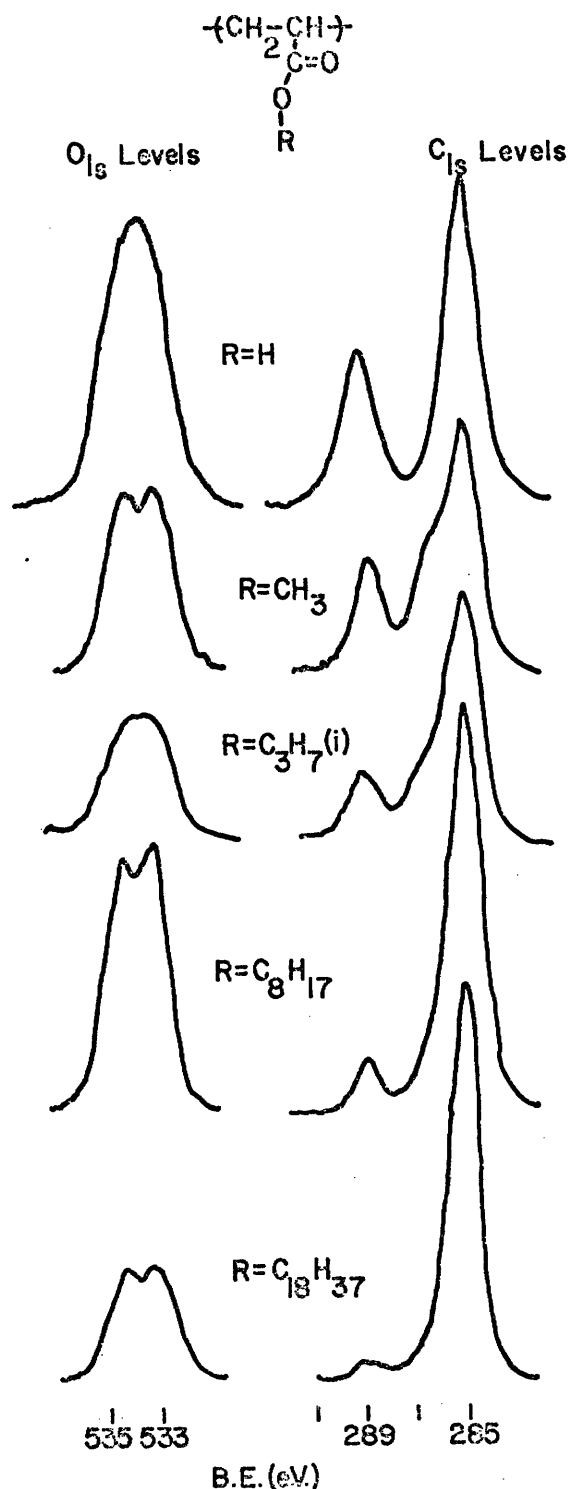


Figure 3.5. Core Level Spectra for a Series of Polyalkyl Acrylates.

the parent polyacrylic acid the  $C_{1s}$  spectrum consists of a doublet in a 1:2 ratio corresponding to the pendant carboxylate and backbone carbons respectively, the shift in binding energy being 4.1 eV in excellent agreement with that for model systems containing the corresponding structural features. In going to the methyl derivative the core levels corresponding to the methyl carbons are clearly apparent being shifted by  $\sim 1.6$  eV by the attached oxygen. This again is in excellent agreement with the data for the model compounds. As the alkyl group increases in complexity the shoulder arising from the carbon atoms directly attached to the ester oxygens becomes less well resolved but is still apparent even for the longest chain studied (C18). Deconvolution of the spectra in each case yields absolute and relative binding energies for the various structural features in excellent agreement with the data for the model systems and the data are shown in Table 3.5.

Considering now the  $O_{1s}$  levels it is clear that the overall band profiles arise from two peaks of equal intensity attributable to the carbonyl and ester type oxygens. This is most readily apparent for the methyl, 2-ethylhexyl and octadecyl systems and a similar pattern emerges from deconvolution of the spectra for the parent polyacrylic acid and for the isopropyl derivative. Again both the absolute and relative binding energies (Table 3.5) are in excellent agreement with the data previously described for the model systems.

As an initial test of the homogeneity of the samples on the ESCA depth profiling scale, a comparison was made to the measured  $O_{1s}/O_{2s}$  area ratios for these polymers with those

Table 3.5.

Experimentally Determined Binding Energies for Polyalkyl Acrylate

Samples

Molecule (-R)	Experimental Binding Energies in eV					
	1s Levels				2s Levels	
	--C--O--	C=O	C=O	-O-C	O <sub>2s</sub>	C <sub>2s</sub> <sup>†</sup>
H	534.3	533.0	289.1	-	26.6	15.5
C <sub>1</sub>	534.3	532.8	288.8	286.6	26.6	16
C <sub>2</sub>	534.3	532.8	288.9	286.5	26.6	16
C <sub>3</sub> (i)	534.1	532.7	288.8	286.6	26.6	16
C <sub>4</sub> (n)	534.3	532.8	288.9	286.6	26.4	16
C <sub>4</sub> (i)	534.0	532.8	288.9	286.6	27.2	16
C <sub>4</sub> (t)	534.5	532.7	288.9	286.6	26.8	16
C <sub>8</sub> (E-H)	534.5	533.1	289.1	286.8	26.4	15.5
C <sub>10</sub> (n)	534.4	532.9	289.0	286.5	26.2	15.5
C <sub>12</sub> (n)	534.4	533.0	289.0	286.2	26.4	15.5
C <sub>16</sub> (H-D)	534.2	532.7	288.7	286.5	26.4	15.5
C <sub>18</sub> (n)	534.2	532.8	288.9	286.6	26.4	15.5

† Centroid of relatively broad peak.

previously obtained for homogeneous thin films of the model systems; since, as previously indicated, the escape depth dependencies for the two levels are significantly different. It is fortunate in this respect that the  $O_{2s}$  levels are sufficiently core-like to be readily identifiable (Fig. 3.6) and also that the cross section for photoionization is large enough such that even for the long chain alkyl systems the signals arising from these levels have adequate intensity to be detected. The measured area ratios for the polymers fall within a narrow range ( $12 \pm 1$ ) which is within experimental error the same as that for the model compounds. As previously noted in Chapter 2, there are two essentially independent means of establishing the polymer compositions from the ESCA data. Firstly from the  $C_{1s}/O_{1s}$  area ratios employing the instrumentally dependent sensitivity factors for the core levels established from a study of model systems. Secondly from the area ratios for the relevant component peaks of the  $C_{1s}$  levels. The data pertaining to the first group of samples is shown in Fig. 3.7. For polyacrylic acid the measured areas for the various structural features for the  $O_{1s}$  levels and  $C_{1s}$  levels and  $C_{1s}$  levels and the overall ratios for the  $C_{1s}$  to  $O_{1s}$  levels (corrected for differing sensitivity factors) are 1.0, 2.0 and 1.6 respectively, in excellent agreement with the theoretical values of 1.0, 2.0 and 1.5 based on a statistical sampling of the polymer repeat unit. The area ratios for the individual components for the  $C_{1s}$  levels show an excellent correlation with the number of carbon atoms in the alkyl groups

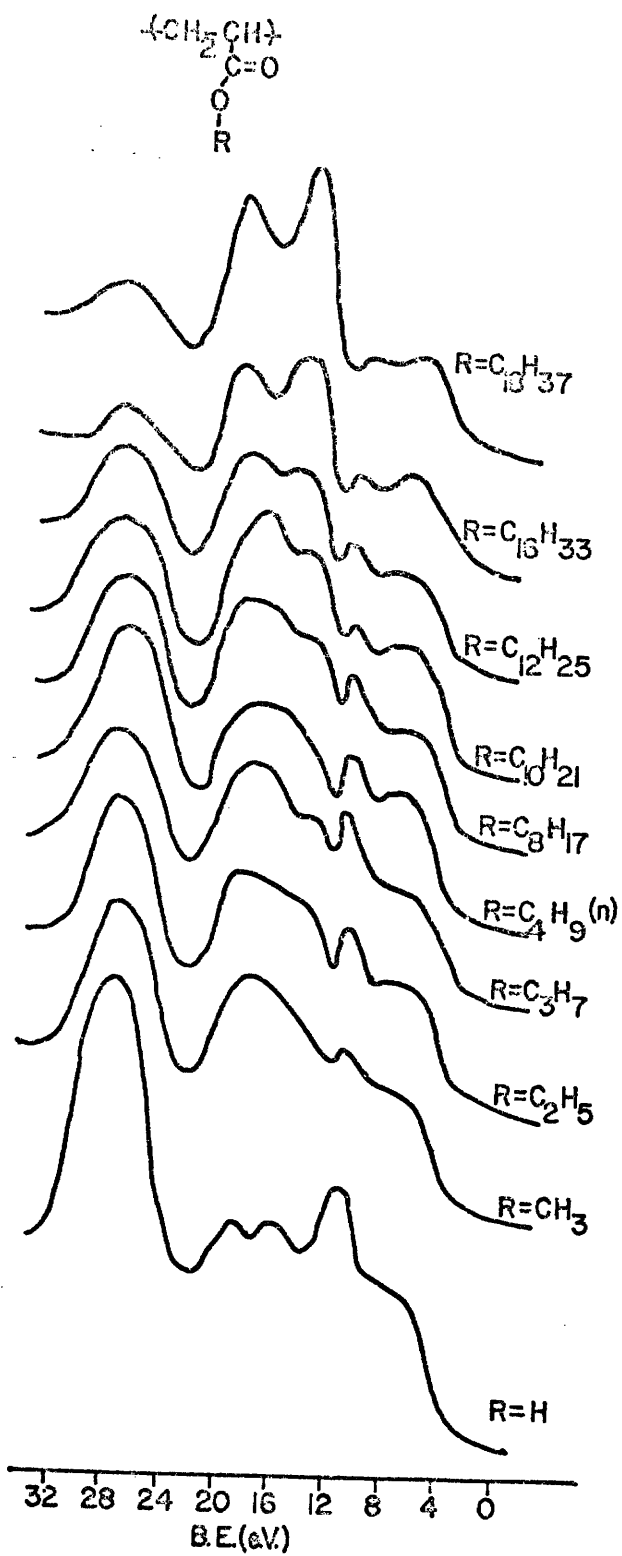


Figure 3.6. Measured Valence Energy Levels for a Series of Polyalkylacrylate.

(Slope; Experimental 1.03, Theoretical 1.0).\* By contrast the plot of Total  $C_{1s}/O_{1s}$  area ratios (corrected) against the chain length for the alkyl group falls on a smooth curve; however replotting the data in a different form as shown in Fig. 3.8 reveals the underlying linear correlation with the appropriately derived theoretical parameter. Within experimental limits the slope is unity as required by theory if the ESCA experiment statistically samples the repeat units of the polymers. In sum total therefore the ESCA data shows that for these systems the outermost few tens of Angstroms of the samples are representative of the bulk and that compositions, integrity of the immediate surface, and homogeneties may routinely be established.

(b) Theoretical Models for the Quantitative Interpretation of Absolute and Relative Binding Energies.

Having established the charge potential parameters  $E^{\circ}$  and  $k$  for the  $C_{1s}$  and  $O_{1s}$  levels of the model systems an investigation was made on both absolute and relative binding energies for models of the polymers discussed in the previous section. The objective of this investigation was twofold. First, with an unsymmetrical vinyl monomer the possibility exists for structural isomerism (viz. head to tail vs. head to head and tail to tail bonding). Second, for a given structural isomer the relative conformation of the pendant groups namely the carbonyl and ester functions,

---

\* It is convenient in this correlation to plot the area ratios for the two best resolved peaks, namely the carbonyl carbon which although of low relative intensity for the longer chain systems nonetheless is well removed from the main component arising from the backbone and carbons not directly attached to oxygen. This obviates any error due to deconvoluting the signal arising from the other carbons directly attached to oxygen (viz. of the ester group) since for the long chain systems it is obviously preferable to have a small error in a large rather than a small quantity. Since the area ratio does not therefore include the carbons of the ester group which are directly bonded to oxygen this leads to an obvious break in the curve for polyacrylic acid.

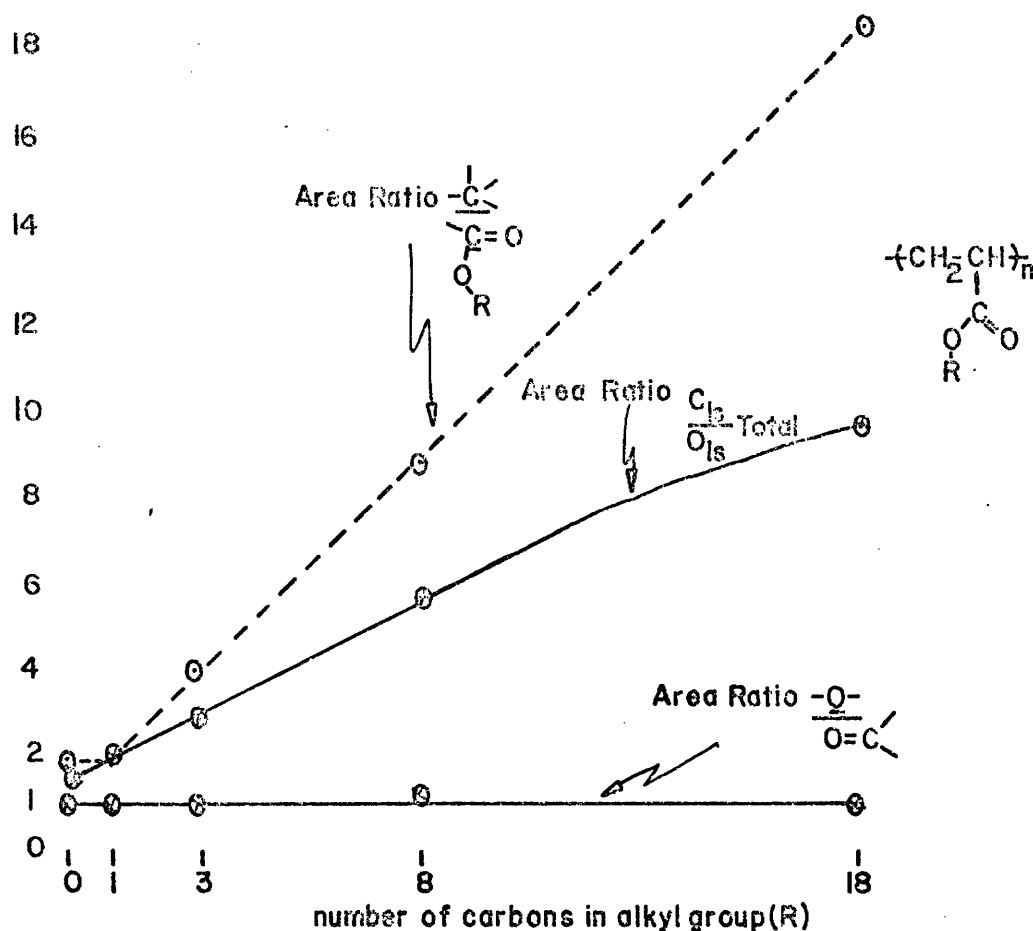


Figure 3.7. Plot of Area Ratios for the Core Levels Versus Number of Carbons on the Alkyl Group of a Series of Polyalkylacrylates. (These have been Corrected for Differences in Cross Section and Instrumental Sensitivity (see text)).

are of some interest. It has been shown<sup>17,35,37,39,42</sup> that the factors which determine differences in binding energies are relatively short range in nature and may therefore be quantitatively described by calculations on model systems incorporating a small number of monomer units such that all of the important short range interactions are quantified. In particular cases (e.g. nitroso rubbers<sup>39</sup>) it was shown that structural isomerisms may be investigated directly by ESCA; however in general for homopolymers based on simple unsymmetrical vinyl monomers both theory and

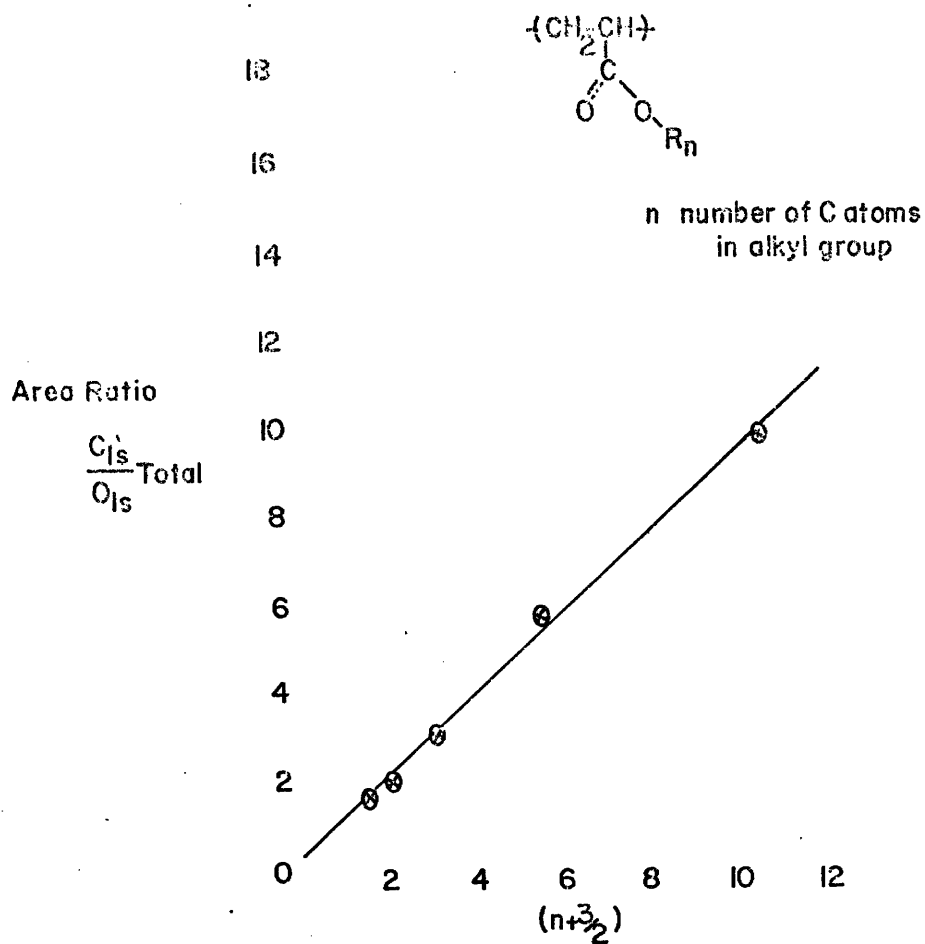


Figure 3.8. Plot of Area Ratios for the  $\text{C}_{1s}$  and  $\text{O}_{1s}$  Levels of a Series of Polyalkyl Acrylates as a Function of Chain Length of the Alkyl Group.

experiment agree that both absolute and relative binding energies are virtually the same for regular and irregular structures.<sup>35</sup>

Even at the semi-empirical all valence electron SCF MO CNDO/2 level, computations on model systems for the polymers studied in this work are extremely time consuming. Computing limitations therefore dictated that the central monomer unit of the model chains were linked to a single monomer unit at each end. Calculations reported in the literature show that such a

model incorporates all the important short range interactions with respect to the central unit.<sup>17,35,37,42</sup> The model systems chosen for study were polyacrylic acid and polymethyl acrylate. In all cases standard bond angles and lengths were employed for the various structural features.<sup>55</sup> The model systems studied are shown in Figs. 3.9 and 3.10.

For polyacrylic acid the models studied exemplified both structural isomerism and relative conformational preferences for the side chain. For a model system composed of three monomer units the two distinct structural isomers with respect to the central unit may be designated as head to tail (HT) or, head to head (HH) or tail to tail (TT). For the head to tail (regular) arrangement (HT-HT linkages) both the 'isotactic' and 'syndiotactic' forms were investigated. Calculations on simple model systems such as isopropyl acetate indicated that the most stable conformers involved an eclipsed arrangement for the carbon-oxygen double bond and the adjacent carbon hydrogen bond, and indeed experimental data on related systems supports this conclusion.<sup>56</sup> For the model systems therefore the carbonyl group was taken to eclipse the CH bond of the backbone and this is referred to as the  $\pi$  eclipsed arrangement. In particular cases calculations were also carried out on staggered conformers in which the carbonyl group was rotated through an angle of  $60^\circ$  (with respect to the eclipsed configuration) about an axis through the carbon-carbon bond linking the pendant group and backbone. Without exception such conformers were calculated to be significantly higher in energy than for those involving a  $\pi$  eclipsed arrangement. For a head to head (irregular) arrangement (HH-HT

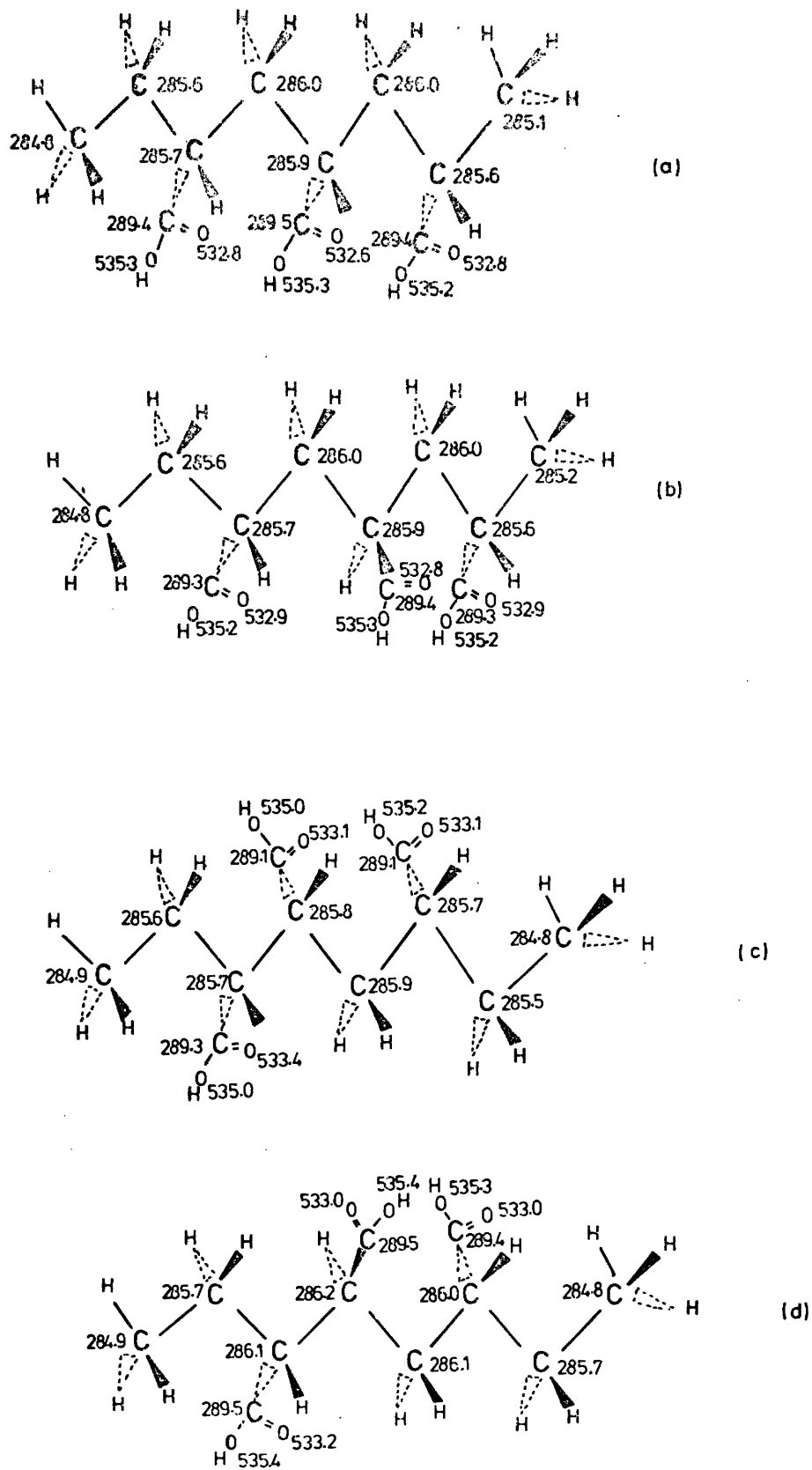


Figure 3.9. Conformational Models of Polyacrylic Acid with Calculated Binding Energies from the Charge Potential Model Shows for (a) HT-HT 'Isotactic' Model, (b) HT-HT 'Syndiotactic' Model, (c) HT-HT 'Isotactic' Model and, (d) HT-HT 'Syndiotactic' Model.

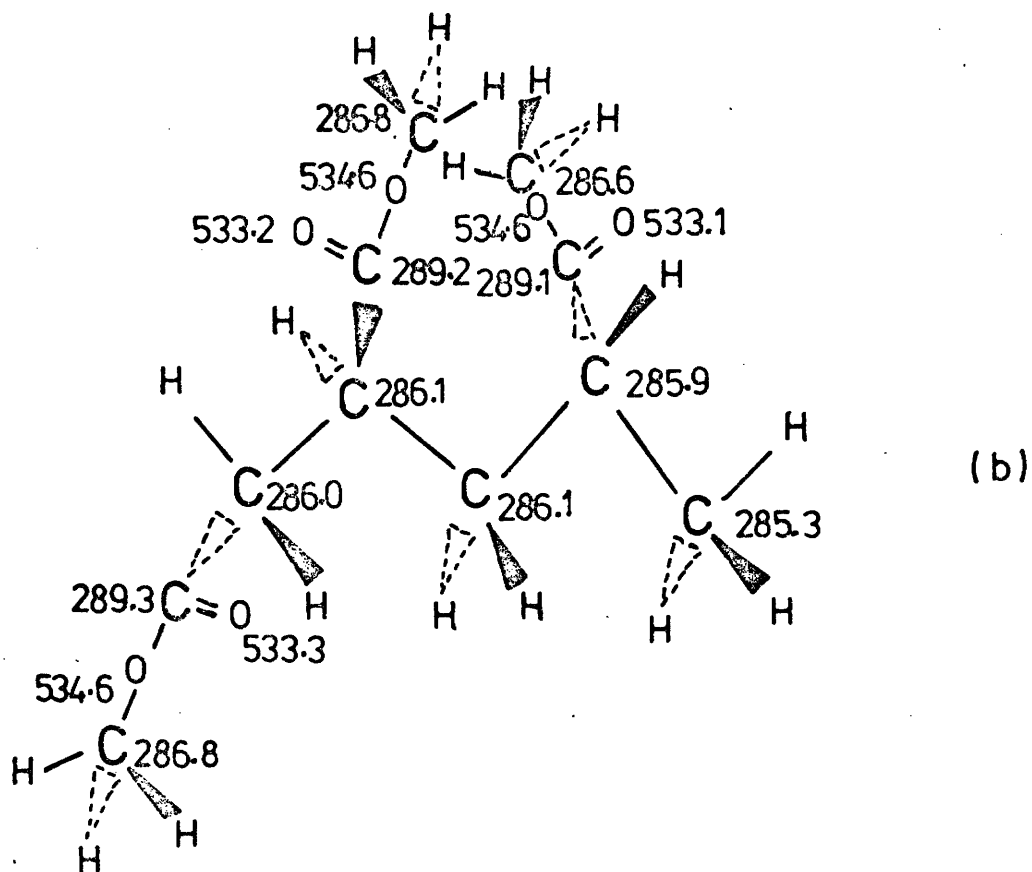
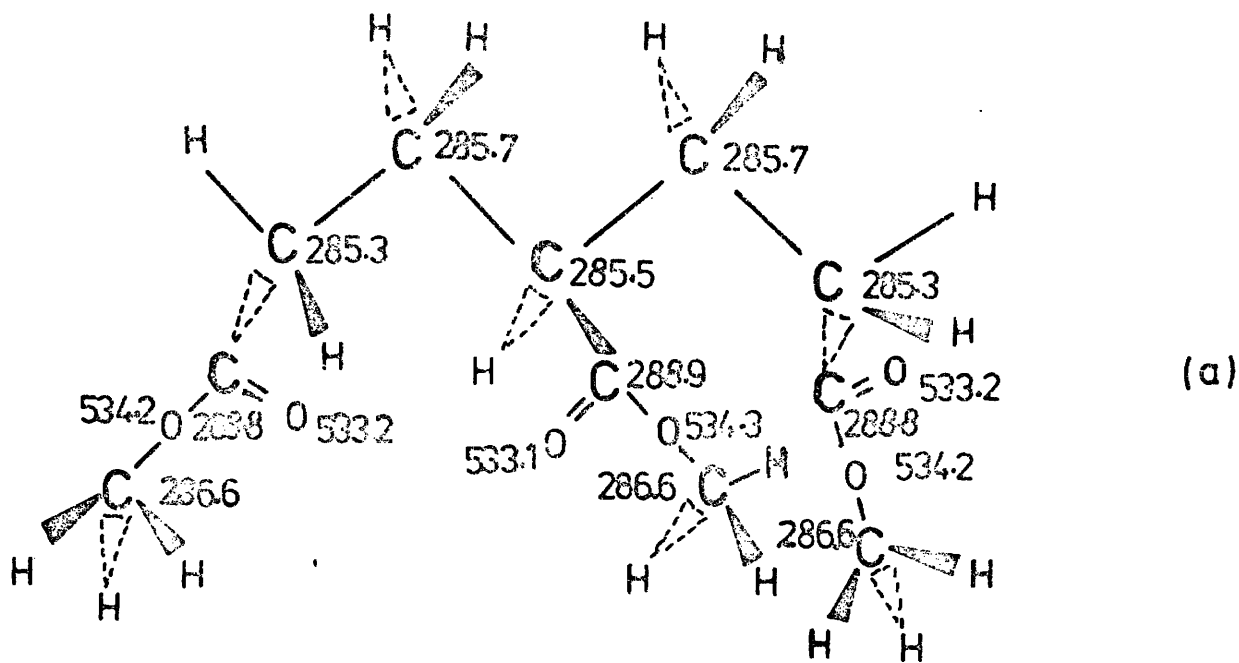


Figure 3.10. Conformational Models of Polymethyl Acrylate with Calculated Bond Lengths from the Charge Potential Model Similar to (a) [198] 'Syndiotactic' Model and, (b) [195-197] 'Syndiotactic' Model.

linkages) the side chains were again taken in the  $\pi$  eclipsed conformations with the pendant groups either all being on the same side of a plane drawn through the backbone or in an alternating arrangement. These are analogous to the isotactic and syndiotactic arrangements in the regular head to tail model system. Similar calculations were carried out on a model of polymethyl acrylate as prototype for the polyalkyl acrylates. In this case however computing limitations dictated that on one end of the model system the adjacent backbone carbons were simulated by taking a hydrogen atom rather than a methyl group. Since the calculated binding energies for such a model are taken with respect to the central unit this further approximation has virtually no effect as will become apparent in the discussion of the results.

The results for the models of polyacrylic acid are displayed in Fig. 3.9 where the absolute binding energies have been computed using the charge potential parameters derived from the study of simple model systems as described in a previous section. Considering first the regular head to tail arrangement ((a) and (b) Fig. 3.9) it is clear that the factors determining both the absolute and relative binding energies are insensitive to the overall stereochemistry of the system. Comparison with the corresponding data for the staggered (with respect to the carbon-oxygen double bond, conformers reinforces this conclusion since the calculated binding energies are in exact correspondence with those for the eclipsed conformers shown in Fig. 3.9. A comparison of the central monomer units with the adjacent units, effectively demonstrates the short range nature of the factors determining

absolute and relative binding energies in these systems. A comparison with the experimental data (Table 3.5) reveals the overall adequacy of the theoretical model in respect of both absolute and relative binding energies for both the  $O_{1s}$  and  $C_{1s}$  levels. For the regular models the second methylene group in the chain linked directly to the methyl group provides an indication of the likely binding energy for methylene groups appropriate to a tail to tail structural arrangement. This is also apparent from the corresponding irregular HH-HT models ((c) and (d) Fig. 3.9). For the two possibilities considered it is evident that the calculated binding energies show a small dependence on stereochemistry arising from the significant interaction between carbonyl groups oriented cis to one another on adjacent carbon atoms. For both models the backbone carbons are predicted to have closely similar binding energies a feature common to the regular models alluded to previously. The shifts in binding energy for the  $O_{1s}$  levels range from 2.7 eV for the HT-HT 'isotactic' model to 1.9 eV for the HH-HT 'isotactic' model. This compares with the experimentally determined value of 1.3 eV. The discrepancy is largely accounted for by the effect of inter and intra chain hydrogen bonding which has somewhat of a levelling effect on the relative charge distribution about the two types of oxygen. This effect has been noted in the literature and is manifest in a distinctly increased linewidth for the individual components of the  $O_{1s}$  levels.<sup>36</sup> In going from polyacrylic acid to polymethyl acrylate such interactions disappear with a concomitant decrease in linewidth for the individual components of the  $O_{1s}$  levels. The two models chosen for this system are shown in Fig. 3.10. The calculated

absolute and relative binding energies for the  $O_{1s}$  levels are seen to be in excellent agreement and bracket the experimental data. The calculations suggest that whereas the  $O_{1s}$  levels and  $C_{1s}$  levels for the  $\overset{O}{\parallel}C=O$  and  $\frac{1}{2}\overset{O}{\parallel}C-O$  structural features should fall within a narrow range ( $\pm 0.2$  eV) for an atactic material the  $C_{1s}$  levels for the backbone carbons should span a much larger range ( $\pm 0.4$  eV) with the extremes being represented by tail-to-tail and head-to-head arrangements. All of the polymer samples studied in this work were synthesized by free radical processes at relatively high temperature and should therefore be predominantly atactic.<sup>57</sup>

The theoretical models suggest that this would be manifest in the ESCA data by a somewhat larger linewidth for the  $C_{1s}$  signal arising from the backbone carbons than from the pendant groups. Since the signal arising from the carbons of the alkyl group (other than that directly attached to oxygen) falls on the same region as that for the backbone carbons one corollary of the theoretical analysis is that as the alkyl chain becomes longer and therefore proportionally provides a larger contribution to the low binding energy region of the  $C_{1s}$  spectra, the FWHM should approach that appropriate to the alkyl chain and hence be largely independent of the tacticity of the polymer system. Analysis of the experimental data provides evidence for this. Thus while the FWHM for the deconvoluted components of the  $C_{1s}$  and  $O_{1s}$  levels for polymethyl acrylate are 1.55 eV, 1.4 eV, and 1.55 eV for the  $\underline{CH}$ ,  $\overset{O}{\parallel}C=O$  and  $C=\underline{O}$  structural features, for polyoctadecyl acrylate the corresponding figures are 1.35 eV, 1.35 eV and 1.5 eV.

(c) Valence Levels of Polyacrylates.

The model systems previously discussed together with literature data pertaining to ultraviolet photoelectron spectroscopic studies of related compounds<sup>53</sup> provides a sound basis for the overall interpretation of the main features of the valence bands of the polymers studied. For convenience, samples which are known to be surface oxidized, from studies of the core levels, are also included in the discussion, since the escape depth dependence for electrons photoemitted from the valence levels is sufficiently large that the surface features contribute significantly less to the overall band profiles than is the case for the core levels.<sup>36</sup>

The measured valence energy levels for the polyacrylates are shown in Fig. 3.6. It is clear that the overall band profiles are 'fingerprints' for each particular polymer system and this is dramatically illustrated by the data for the isomeric polybutyl acrylates shown in Fig. 3.11.

It has previously been discussed that with a high energy photon source the cross sections for photoionization are such that for first row elements valence orbitals with a high degree of 2s character are relatively more intense than those predominantly of 2p character and this is clearly evident from the spectra shown in Figs. 3.6 and 3.11. Comparison of the two extremes ( $R=H$ ,  $R=C_{18}H_{37}$ ) in terms of the overall band profiles leads to a ready identification of the band centred around  $\sim 27$  eV as arising from molecular orbitals which derive predominantly from  $O_{2s}$  atomic orbitals. The region between  $\sim 12$  and 21 eV similarly derives largely from orbitals of  $C_{2s}$

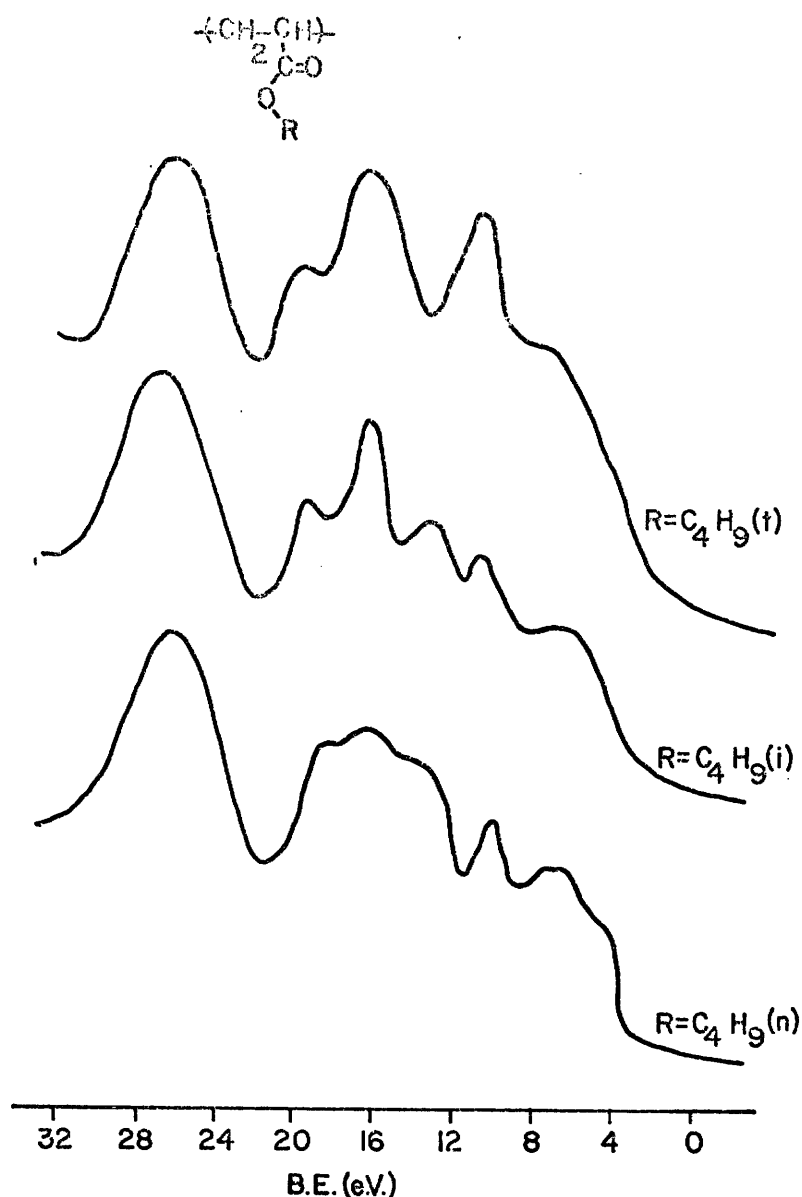


Figure 3.11. Measured Valence Energy Levels of Poly-n-iso- and tert-butylacrylates.

character. The region below 12 eV derives largely from molecular orbitals which are linear combinations involving  $C_{2p}$  and  $H_{1s}$  functions. It is interesting to compare the valence bands for the longer chain polyalkyl acrylates with those previously published for polyethylene.<sup>36</sup> The spectra are strikingly similar and are largely superimposable apart from the relatively intense peak at higher binding energy attributable to the  $O_{2s}$  levels of the carboxylate groups.

(vi) Polyalkyl Acrylates for which the Surface Composition is Different from the Bulk.

In a previous section it was shown that by an appropriate calibration with respect to model compounds for 'apparent' cross sections, the compositions for polyalkyl acrylates on the ESCA depth sampling scale may be established by two independent means. In several cases however it was apparent from such an analysis that the compositions differed from that appropriate to the bulk and further the variation in the intensity ratios for the  $O_{1s}$  with respect to  $O_{2s}$  levels indicated inhomogeneties in surface compositions. The experimental data for these samples is shown in Fig. 3.12. A distinctive feature clearly evident in all of the spectra is the obvious inequality in intensity of the two component peaks of the  $O_{1s}$  levels. A similar analysis to that presented in a previous section provides the following information. Fig. 3.13 for example shows a plot of the ratio of intensities for the individual components of the  $O_{1s}$  levels and also the total  $O_{1s}/O_{2s}$  ratios. For comparison purposes the dotted lines indicate the correlations expected for samples which on the ESCA depth profiling scale correspond to a statistical sampling of the appropriate repeat unit in the polymer. It is clear that there are considerable deviations from such correlations in a direction which overall suggests that the samples are oxidized. Considering the polydecyl acrylate for example, the  $O_{1s}/O_{2s}$  ratio is significantly higher than for the reference compounds suggesting that since the mean free path for the  $O_{1s}$  levels is considerably shorter than for the  $O_{2s}$  levels<sup>17,42</sup> that the oxidation is largely confined to the surface. The absolute binding energies in each case for the

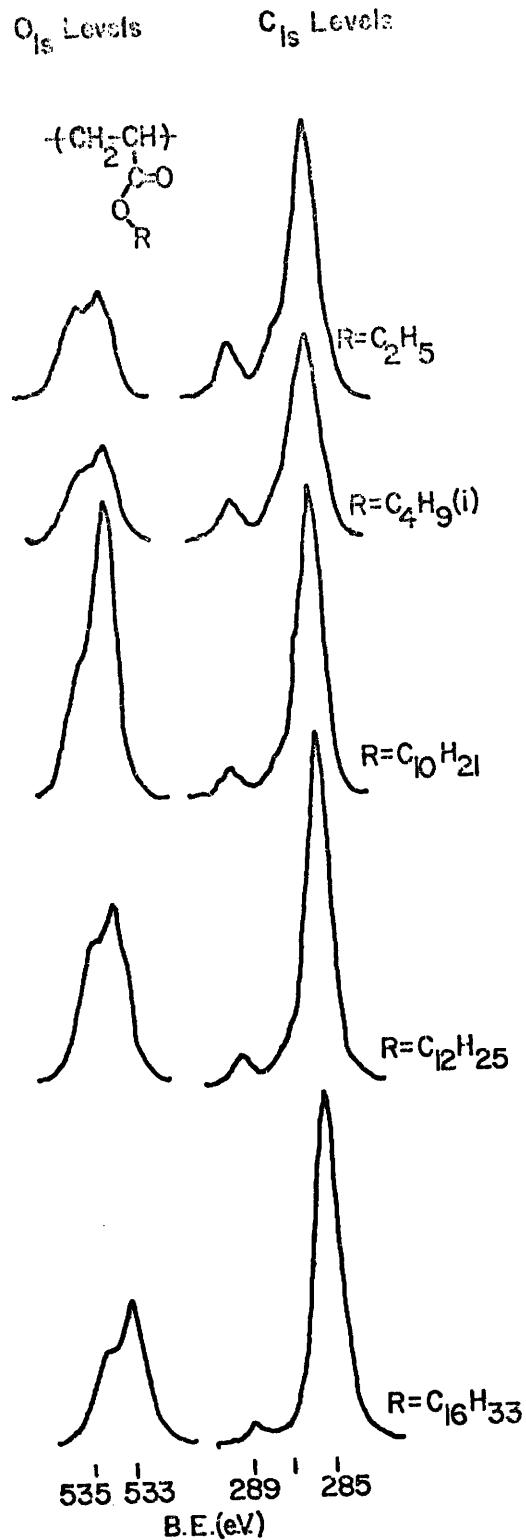


Figure 3.12. Spectra for  $O_{1s}$  and  $C_{1s}$  Core Levels for a Series of Surface Oxidized Polyalkyl Acrylates.

$O_{1s}$  component levels which have apparently increased in intensity correspond to  $C=O$  structural features as is apparent from a comparison with data for the model systems. It is interesting to

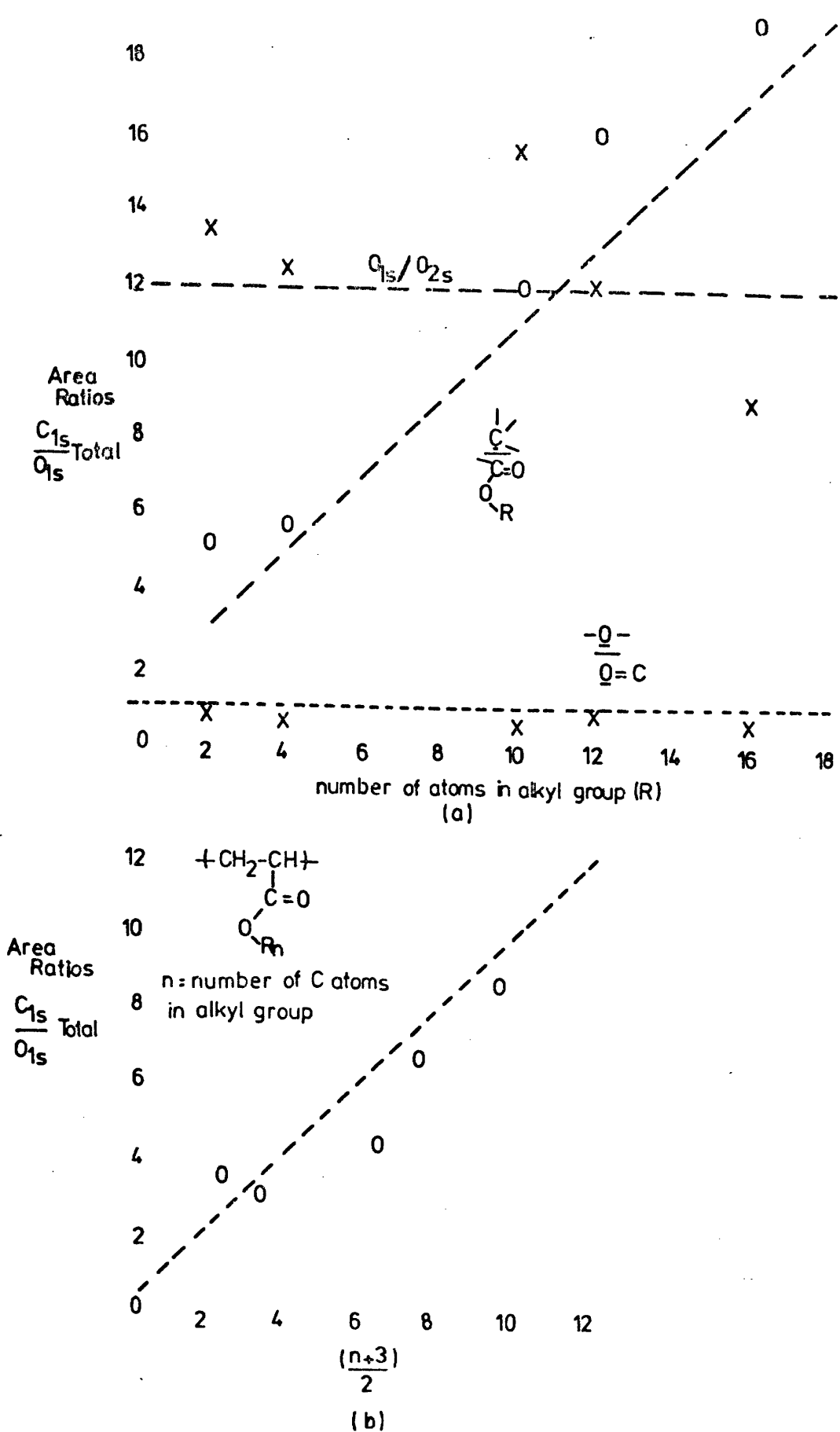


Figure 3.13. (a) Plot of the Intensity Ratios for the Individual Components of the  $O_{1s}$  Levels and also the  $O_{1s}/O_{2s}$  Ratios for a Series of Polyalkyl Acrylates. (b) Plot of the  $C_{1s}$  and  $O_{1s}$  Area Ratios Versus the Number of Carbons in the Alkyl Group.

note that high resolution infrared studies revealed no major distinction of the type clearly evident from the ESCA spectra and the carbonyl region for all of the samples showed only a single peak in the range  $1734 \pm 6 \text{ cm}^{-1}$  consistent with  $\begin{array}{c} \text{O} \\ \parallel \\ \text{-C} \\ \backslash \\ \text{O-R} \end{array}$  structural features.<sup>58</sup> This is readily understandable since the infrared data pertains essentially to the bulk. Further evidence for the oxidized nature of the poly-n-decyl acrylate surface is provided by the greatly increased wettability with respect to water compared with polyisopropyl acrylate as a representative example of the unoxidized samples. This was immediately apparent from the relative contact angles assessed from the photographs for the two samples. A comparison was also made with poly-2-ethylhexyl and polyoctadecyl acrylates the latter having a contact angle closely similar to that of polyisopropyl acrylate whilst the former showed a wettability intermediate between that of polyisopropyl acrylate and poly-n-decyl acrylate. It is interesting to note that although the data for the poly-2-ethylhexyl acrylate generally fits well into the overall analysis previously presented as is evident from Figs. 3.7 and 3.8, a close inspection of the relative intensities of the component peaks of the  $\text{O}_{1s}$  levels reveals some evidence for a small extent of oxidation (cf. Fig. 3.5).

If the surface oxidation inferred from the inequality of the component peaks of the  $\text{O}_{1s}$  levels is attributable to surface carbonyl features then this should also be manifest in the carbon 1s levels. It should, however, be emphasized that since the escape depth dependence for photoemitted electrons in the energy range considered is such that the mean free path increases

with increasing kinetic energy then any surface feature will be relatively more prominent for the more tightly bound  $O_{1s}$  levels than for the  $C_{1s}$  levels.<sup>17</sup> As a simple model for a system containing both structural features viz. ketonic carbonyl group and ester group ethyl acetoacetate was chosen. The  $C_{1s}$  levels are shown in Fig. 3.14 which also details expansion of the  $C_{1s}$  levels for isobutyl acetate, an polyisopropyl acrylate film which had been heated in air ( $\sim 150^{\circ}\text{C}$  for 30 mins.) and for comparison purposes a sample of polyisobutyl acrylate whose  $O_{1s}$  spectrum also showed evidence for surface oxidation (Fig. 3.12). Considering firstly the isobutyl acetate and polyisopropyl acrylate spectra the deconvolution into the component peaks associated with  $-\overset{\text{O}}{\underset{\text{O}}{\text{C}}}$ ,  $\text{O}-\overset{\text{O}}{\text{C}}-$  and  $-\overset{\text{O}}{\text{C}}-$  structural features with characteristic binding energies is straightforward as noted before. By comparison the spectrum of ethylacetoacetate shows that the carbonyl carbon at 287.2 eV (Table 3.2) has the effect of 'filling in' the valley between the high and low binding energy regions. This effect is clearly evident for both polyisobutyl acrylate and for a polyisopropyl acrylate sample heated in air. A detailed examination of the  $C_{1s}$  spectra for the series of surface oxidized samples (Fig. 3.12) shows that the overall line profiles can only be quantitatively fitted with the addition of a small peak in the  $C_{1s}$  spectrum appropriate to isolated carbonyl groups. This work is regarded as an important preliminary investigation of this interesting aspect of the surface oxidation of polymers and more detailed investigations are needed.

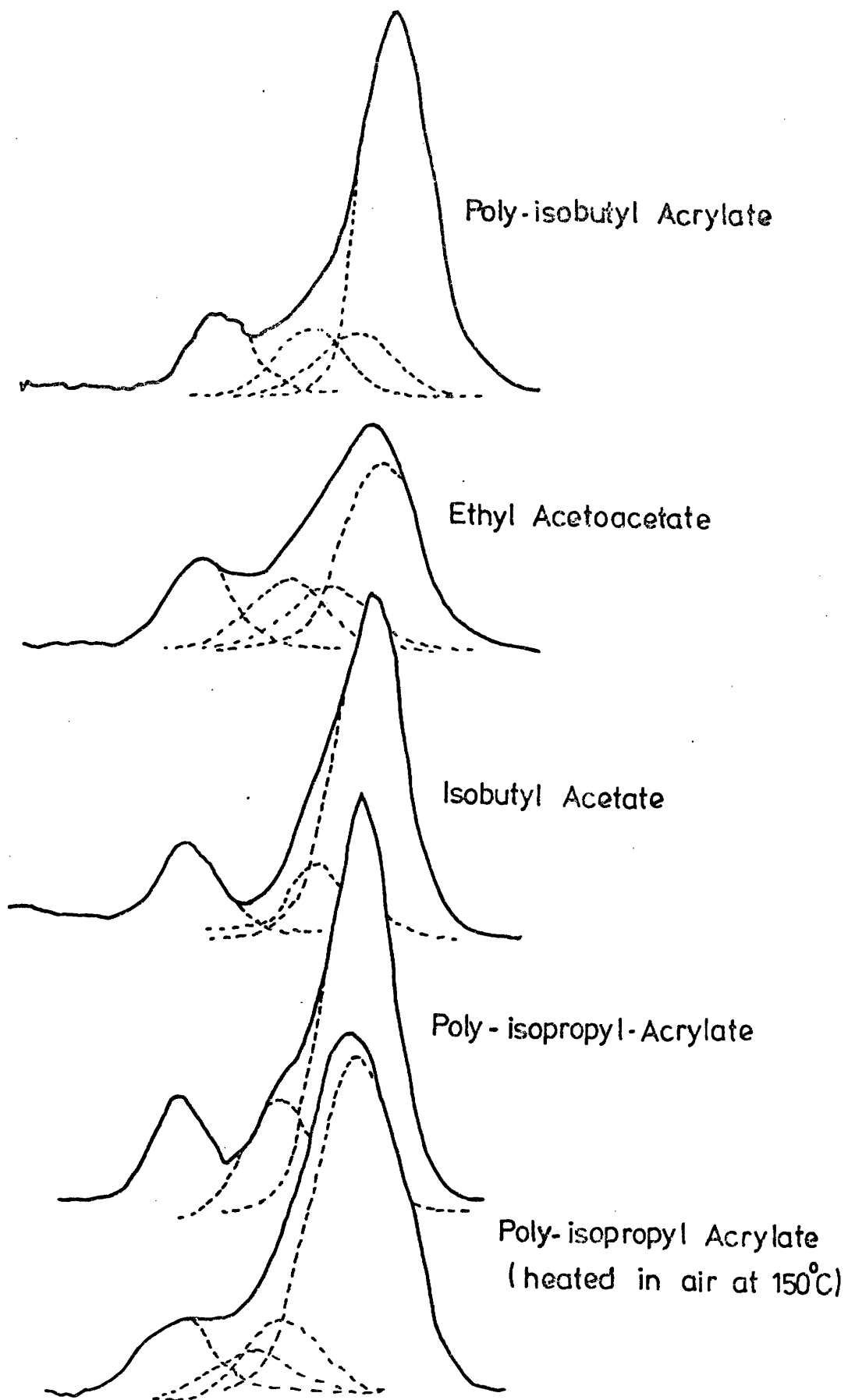


Figure 3.14. C<sub>1s</sub> Core Level Spectra on a Series of Acetates and Polyacrylates Illustrating the Effect of Oxidation of a Polymer Sample on the Core Level Spectrum.

In the particular case of polyethyl acrylate, in addition to the surface oxidized nature of the sample, the data in Fig. 3.12 also provides evidence for a certain amount of hydrocarbon contamination at the surface.<sup>37</sup> Clearly a more detailed study of these oxidized samples is required to elaborate the relevant surface structures and work is currently in progress on the ESCA examination of the initial stages of the oxidation of a variety of solid polymer systems.

In the particular case of the sample of polymethyl acrylate the ESCA data for the sample as received did not correspond with that expected for a statistical sampling of the repeat unit. However benzene extraction of the original material provided samples (solution cast onto gold) whose spectra were entirely consistent with the data presented in the previous section. The major differences in composition on the ESCA depth sampling scale between the original and extracted sample are clearly apparent both in terms of the overall intensity ratios of the  $C_{1s}/O_{1s}$  levels and also from the area of the individual components of the  $C_{1s}$  levels, Fig. 3.15. It is also apparent however from the overall band profiles that the original sample is not surface oxidized. The fact that an insoluble residue remains after extraction whose spectrum is identical to that of the original material strongly suggests that the original sample is crosslinked and that only the linear polymer (representing a relatively small amount of the total) is extracted. For comparison purposes the relevant intensity ratios as measured are shown in Table 3.6 where a comparison is also drawn with the theoretical values. The large relative intensity of the low

Table 3.6.

Comparison of Calculated Versus Experimental Area Ratios for Linear and Crosslinked Polymethyl Acrylate

	$C_{1s}$ Total		Area Ratios			
	$\frac{O_{1s}}{C_{1s}}$ Total		$\frac{O_{1s}}{-O- / C=O}$		$\frac{C_{1s}}{-C- / C=O}$	
	Calc.	Exptl.	Calc.	Exptl.	Calc.	Exptl.
Original Sample	2.0	5.7	1.0	1.0	2.0	5.8
Soluble Material	2.0	2.0	1.0	1.0	2.0	2.2

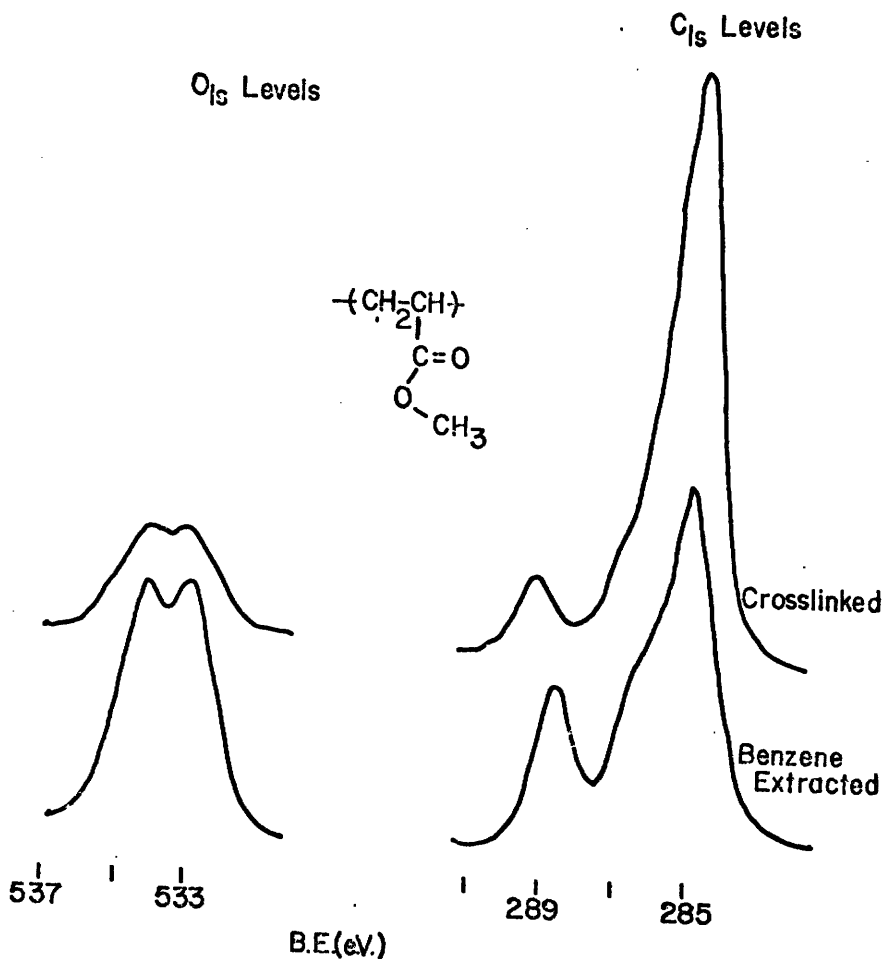


Figure 3.15. Comparison of  $C_{1s}$  Core level Spectra of Linear and Crosslinked Polymethyl Acrylate.

binding energy peak in the  $C_{1s}$  spectra of the original sample and extracted residue, characteristic of -C- structural features, suggests that this is due in part at least to hydrocarbon type contamination. However it is evident that this is not appreciably soluble in benzene since the extracted sample shows no evidence of the contaminant. At this stage only speculation on the likely nature of such a contaminant hydrocarbon layer is offered since it clearly does not correspond to that often revealed by ESCA examination of a wide variety of samples and which is readily removed by an appropriate solvent treatment.<sup>35,37</sup> The hydrocarbon type material whatever its origin, is clearly distributed throughout the bulk of the sample since a comparison of the infrared spectra of the original and extracted materials shows substantial changes in the overall integrated intensity ratios for the C-H and C=O stretching regions.

(vii) ESCA Studies of Adsorption at Surfaces.

It has been shown<sup>17</sup> that the great surface sensitivity of ESCA may be used to considerable advantage in studying the hydration of surface features on polymers capable of participation in hydrogen bonding. Such studies are likely to be of some considerable importance in unravelling the complexities of for example triboelectric charging and various aspects of tribochemistry. In the particular case of low density polyethylene the adsorption of  $H_2O$  on surface carbonyl features manifests itself in terms of the appearance of a shoulder to the high binding energy side of the  $O_{1s}$  levels associated with the carbonyl oxygen and attributed to the hydrogen bonded water.<sup>17</sup>

Careful double beam infrared studies reveals no evidence for such interactions since they are localized at the surface.

An investigation into the interaction of hydrogen bonding species with the surface of polyisopropyl acrylate films, being prototypes for a system which is unoxidized at the surface, was performed.

Fig. 3.16 shows the  $O_{1s}$  and  $C_{1s}$  levels for samples of polyisopropyl acrylate that were exposed to  $NH_3$ ,  $H_2O$ , and  $HF$ .

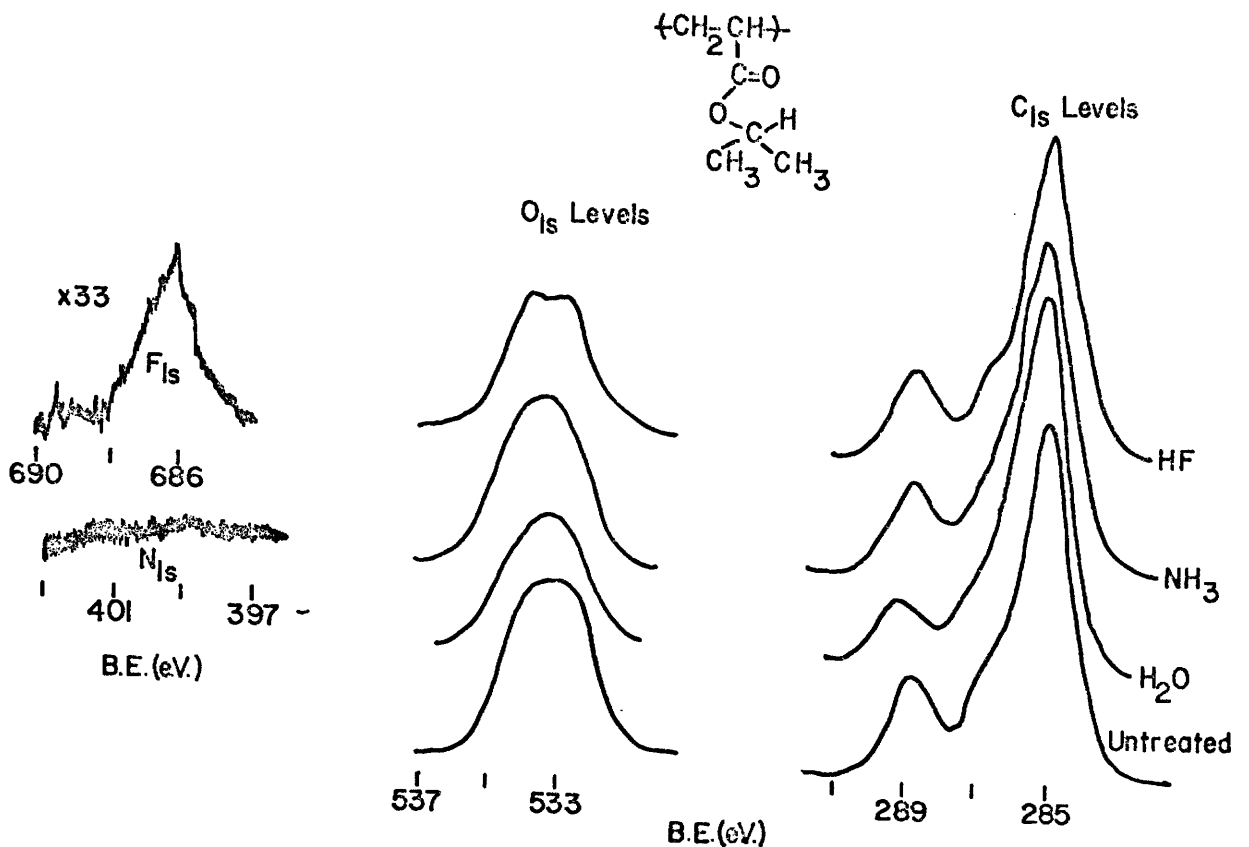


Figure 3.16.  $O_{1s}$  and  $C_{1s}$  Core Level Spectra for Samples of Polyiso-propyl Acrylate Surface Tested with  $H_2O$ ,  $NH_3$  and  $HF$ .

These represent an order of increasing hydrogen bond strength and it is clear from the spectra that only in the case of the  $HF$  treatment is there any substantial change in the overall spectra. The hydrogen bonding almost certainly involving

primarily the carbonyl oxygen of the ester group leads to a sharpening of the  $O_{1s}$  levels such that the two components are now more readily apparent without recourse to line shape analysis. The overall signal intensity for the  $O_{1s}$  and  $C_{1s}$  levels is also attenuated due to the adsorbed HF which is identified by the low absolute binding energy for the  $F_{1s}$  levels. The propensity for hydrogen bonding of the carbonyl group of an ester is considerably less than that for a ketonic carbonyl group and in addition for these particular polymer samples as the bulk of the alkyl group increases the hydrophilic 'carbonyl region' is increasingly shielded by the hydrophobic portions of the polymer system. In contrast, therefore, to the clear-cut detection of surface hydrogen-bonding to ketonic type carbonyl groups in polyethylene the net effect of surface treatment of poly-isopropyl acrylate with  $H_2O$  is a small change in linewidth which can be attributed to a very small degree of hydrogen bonding. It is interesting to note that for  $NH_3$  which might be expected to form the weakest hydrogen bonds the spectra show little evidence for any interaction since the  $N_{1s}$  signal is barely discernible above the background and the overall band profiles for the  $O_{1s}$  and  $C_{1s}$  levels within the statistical limits of the data are superimposable on those for the untreated sample.

CHAPTER 4

Core and Valence Energy Levels of a Series of Poly-  
alkyl and -aryl Methacrylates

CHAPTER 4

Studies of Structure and Bonding in a Series of Poly-alkyl, and -aryl Methacrylates through the Application of ESCA.

(i) Introduction.

Clark et al.<sup>17,35,37,42</sup> have shown how a detailed consideration of the absolute and relative binding energies and relative intensities of peaks corresponding to the direct photoionization of core levels in polymeric systems can provide valuable data on structure and bonding in general in the surface regions of polymeric systems. The investigations reported to date have largely pertained to fluorocarbon based polymers where the large electronegativity of the fluorine substituents gives rise to a substantial span in binding energies for  $C_{1s}$  levels corresponding to substituted carbon atoms in widely differing electronic environments.<sup>17,35,37</sup> For systems in which the shifts in core binding energies are insufficiently large to be well resolved, (e.g. solely hydrocarbon based polymers), it has been shown that it is still possible to derive information on the structure and bonding in these systems from observations of the relative intensities and separation from the direct photoionization peak of the satellite peaks arising from shake-up transitions.<sup>40,41</sup>

In the preceding chapter it was shown that for polymeric systems not possessing either a very large range in absolute binding energies, or an extended conjugated pi-electronic system (as exemplified by polyalkyl acrylates), that nonetheless, from a careful study of both core and valence levels ESCA may routinely be used in such systems to investigate structure, bonding, and

composition of the outermost 'surfaces'.\*

For fluorocarbon based polymers it was shown<sup>42</sup> that surface modifications may readily be detected by ESCA and quantitative data obtained from an investigation of changes in relative peak intensities for core levels which cover a wide range in binding energies, giving rise to substantial differences in escape depth dependencies and hence sampling depth. ESCA as a spectroscopic tool is becoming increasingly important in establishing whether structure and bonding at surface of polymer samples is the same or different from the bulk and also in monitoring chemical and physical modifications which are initiated at the surface.<sup>42</sup>

In the preceding chapter an ESCA investigation was reported on the core and valence energy levels of an extensive series of polyalkyl acrylates and in continuance of this work this chapter details with a study of a series of polyalkyl-, and -aryl methacrylates. Since the range of substituent effects is somewhat smaller than for the previously studied fluorocarbon based polymer series, and the span in escape depth dependencies encompassed by the core levels is also somewhat less, these materials fit logically into a systematic study of polymer systems by ESCA. Although there has been a considerable amount of time and effort spent on the study of structure and bonding in the polyalkylmethacrylate systems by a wide variety of analytical techniques, it is quite clear from a review of the literature that little effort has been expended to a study of the surface and subsurface structure of the solid polymeric systems,

---

\* 'Surface' taken in the terms described by Clark.<sup>17</sup>

since most of the work refers to the polymers in solution.<sup>44-46</sup> As has been discussed by Clark,<sup>42</sup> this is an area of some importance, more particularly since ESCA is one of the few techniques which allows the direct study of polymeric films in-situ in the original form in which they are used. In this chapter the following points were considered.

From studies of the absolute and relative binding energies of the core levels and the relative peak intensities one can establish the compositions of these materials and draw comparisons with data pertaining to the bulk. This is obviously of relevance, as in the study of the polyalkyl acrylates, in establishing whether specific orientation of alkyl groups, studied as a function of the length of the side chain, occur at the surface, and if surface oxidation or cross-linking are apparent in the ESCA core level spectra. The data obtained from these studies has also proven quite useful in discussing the distinctive features of the valence levels of the polyalkyl-methacrylate series.

(ii) Experimental

(a) Samples.

The polymers, listed in Table 4.1 were commercially available samples obtained from Cellomer Associates, Inc., P.O. Box 311, Webster, N.Y. and were used directly in preparing samples for the ESCA investigations. Infrared analyses confirmed the overall purity of the samples and where comparisons were available, agreed with spectra in the literature. (See Appendix B for the reproductions of the infrared spectra of the poly-alkyl- and -aryl methacrylates).

Table 4.1.

Poly-alkyl- and -aryl-methacrylate Samples Studied in this Work  
Showing their Typical Glass Transition Temperature (Tg).

<u>Polymethacrylate Homopolymers</u>	<u>Typical Tg's</u>
Polymethyl methacrylate (low $\bar{M}_w$ )	+105
Polymethyl methacrylate (med $\bar{M}_w$ )	+105
Polymethyl methacrylate (high $\bar{M}_w$ )	+105
Polymethyl methacrylate (very high $\bar{M}_w$ )	+105
Polyethyl methacrylate	+ 65
Polyisopropyl methacrylate	+ 82
Poly-n-butyl methacrylate	+ 20
Polyisobutyl methacrylate	+ 56
Poly-sec-butyl methacrylate	+ 60
Poly-tert-butyl methacrylate	+107
Polyhexyl methacrylate	- 5
Poly-2-ethylhexyl methacrylate	- 10
Polyauryl methacrylate	- 65
Polyhexyldecyl methacrylate	+ 15
Polyoctadecyl methacrylate	> + 60
Polybenzyl methacrylate	+ 54
Polyphenyl methacrylate	+120

(b) Sample preparation.

The poly-alkyl- and -aryl-methacrylate samples in the form of fine powders were coated onto double sided Scotch tape directly attached to the spectrometer probe, while the polyalkyl methacrylates with low Tg's were prepared for investigation as thin films coated directly onto gold substrates. The gold substrate was attached directly to the sample probe by means of double sided Scotch tape. One of the samples, polyhexyldecyl-methacrylate, was received as a 20% solution in benzene which was coated onto a gold substrate and the solvent evaporated before analysis, leaving a thin film of polymer on the surface of the gold. The polyoctadecyl methacrylate was applied neat onto a gold substrate and the temperature was slowly raised to  $\sim 40^{\circ}\text{C}$  to allow for the sample to spread evenly onto the substrate as a thin film.

(c) Post-treatment of Polyisopropyl Methacrylate.

The study of the adsorption of a series of 'hydrogen bonding species' at the surface of polyisopropyl methacrylate was accomplished by exposing the polymer film, (which had been previously coated onto a gold substrate to about 100  $\mu$  thick), to the appropriate material. In this study the compounds selected were HF, H<sub>2</sub>O and NH<sub>3</sub> in the order of decreasing propensity for hydrogen bonding. The polymer samples were exposed to a stream of HF at atmospheric pressure for several minutes and the samples then transferred to the spectrometer, the spectra being recorded after pump down to the required operating base pressure (an operation requiring about 5 minutes).

The H<sub>2</sub>O treatment was accomplished simply by wiping the surface of the polymer with a wet tissue and the sample then inserted into the spectrometer for analysis. The NH<sub>3</sub> treatment was accomplished by exposing the polymer sample to an atmosphere of NH<sub>3</sub> in a closed container of .88% ammonia for half an hour. The sample was then removed from the container and introduced into the spectrometer for analysis.

In the particular cases of polymethyl-, polylauryl- and polyoctadecyl-methacrylates, qualitative studies were made of wettabilities. Contact angles for sessile drops of water on the polymer films were measured from enlargements of photographs taken with rear illumination.<sup>47</sup> No attempt was made to quantify the results because of the crude nature of the experiments.

(d) Instrumentation.

The details of the instrumentation employed in this study on the polymethacrylates have been given in the preceding chapter on the polyacrylate systems.

(iii) Theoretical.

In the previous chapter on the polyalkylacrylates a discussion of the model compounds used to interpret the polymer systems was presented. These same model systems also form the basis for the interpretation of data pertaining to the polyalkyl-methacrylates.

(iv) Results and Discussion for Polyalkylmethacrylates.

(a) Experimental.

The core level spectra for the polyalkyl methacrylates, and in addition, for a few samples of polyaryl methacrylates are

shown in Fig. 4.1 and 4.2 respectively. Considering first the

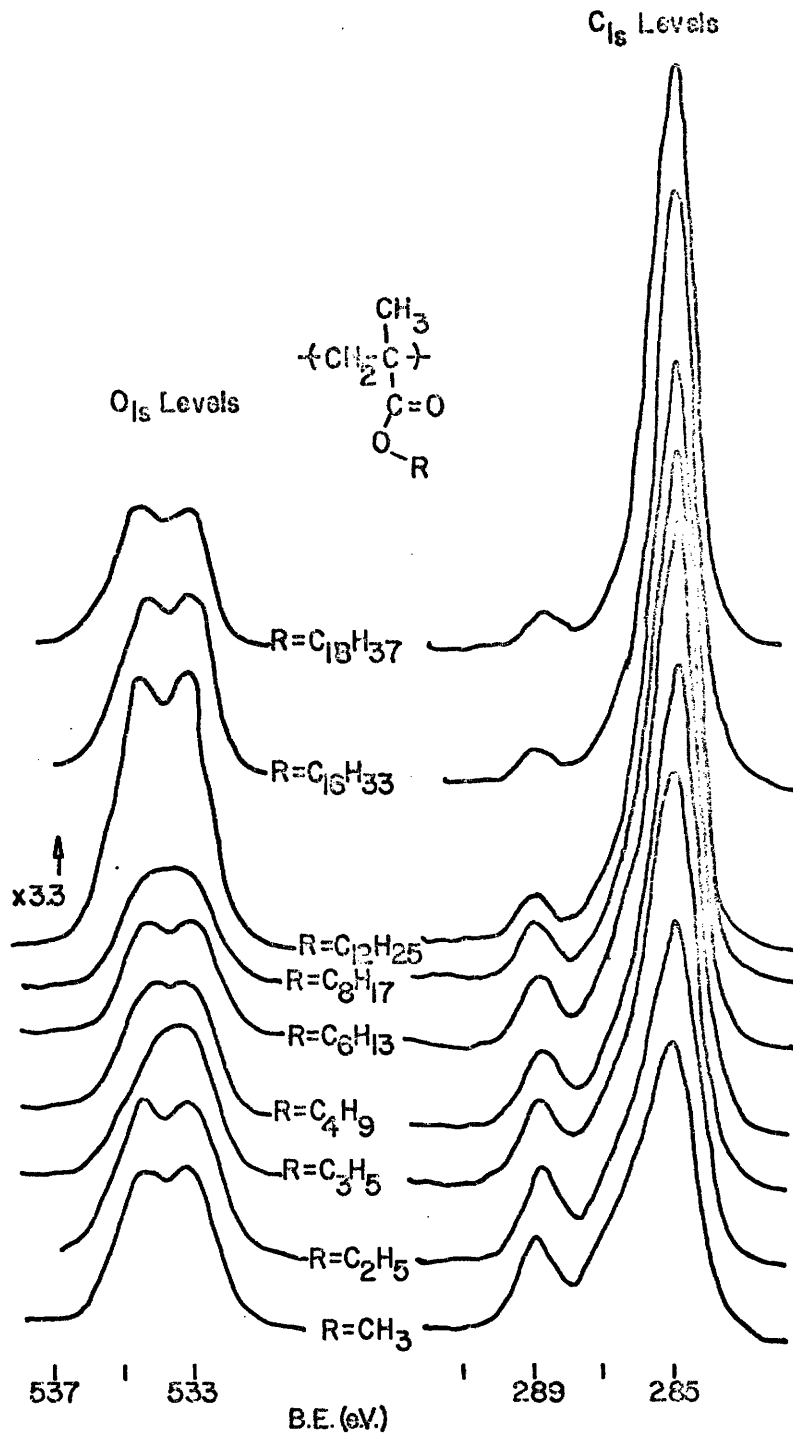


Figure 4.1. Core Level Spectra for a Series of Polyalkyl Methacrylates.

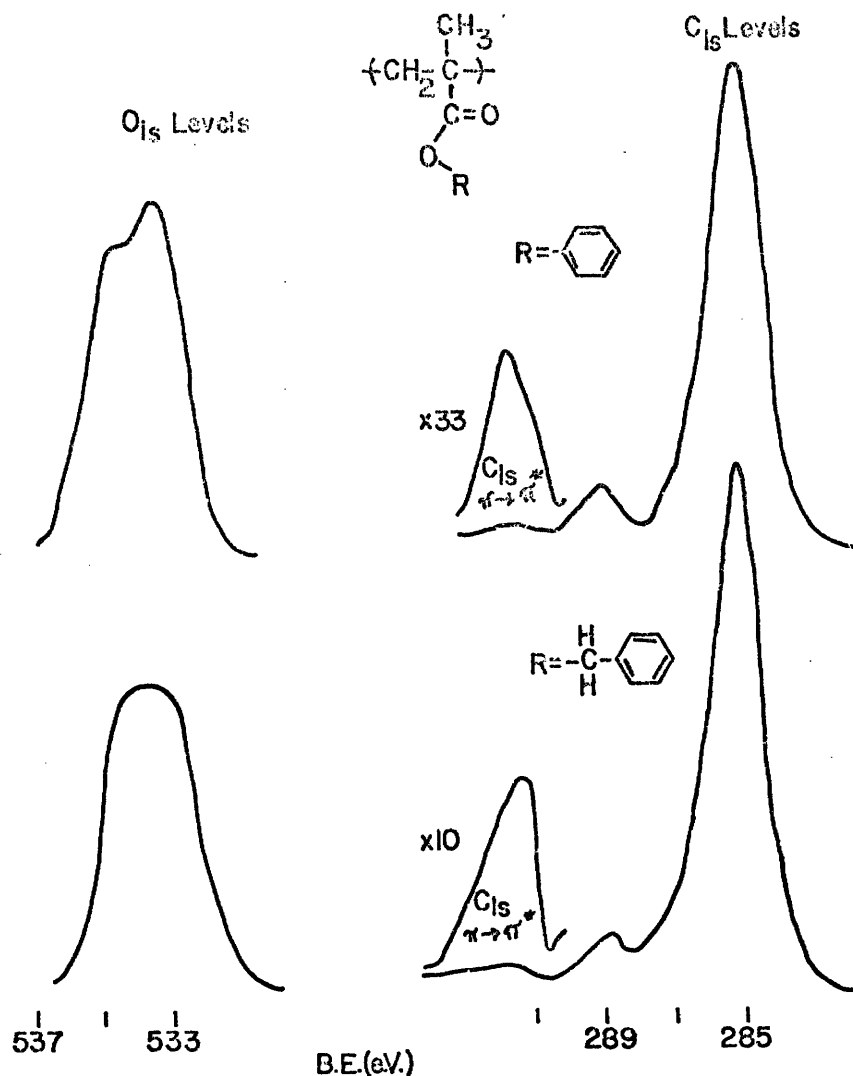


Figure 4.2. Core Level Spectra for Polybenzyl- and Polyphenyl-Methacrylates.

simplest of the alkylmethacrylates, namely polymethyl methacrylate, the  $C_{1s}$  spectrum consists of a doublet with an apparent shoulder on the higher binding energy side of the main backbone carbon peak. The doublet appears as one peak to the highest binding energy, corresponding to the pendant carboxylate carbon, (shifted by  $\sim 4.1$  eV from the lowest B.E. peak), and the peak appearing as a shoulder on the main backbone carbon peak, shifted by about 1.6 eV by the attached singly bonded oxygen. This data is in excellent agreement with the data from the model

compounds and that for polymethyl acrylate. As the alkyl group increases in length the shoulder arising from the carbon atoms directly bonded to the ester oxygens becomes less well resolved, but is still quite apparent for polyoctadecyl methacrylate. Deconvolution of the spectra for each of the alkylmethacrylates studied yields absolute and relative binding energies for the various structural features, in good agreement with the data for the model systems, and is shown in Table 4.2. The average of the binding energies and shifts for the characteristic structural features for the polyalkyl methacrylates are shown in Table 4.3.

In observing the  $O_{1s}$  levels for the polymer systems it is apparent that the overall band profiles arise from two peaks of equal intensity, separated by  $\sim 1.4$  eV, assigned to the carbonyl and ester type oxygens. This is quite apparent for most of the polymer systems and deconvolution of the  $O_{1s}$  levels for the polyisopropyl-, poly-2-ethylhexyl- and polybenzyl-methacrylates reveals a similar assignment. The absolute and relative binding energies, Table 4.2 are in excellent agreement with the data described previously for the model systems and for the polyalkyl-acrylates in Chapter 3.

The homogeneity of the polymer samples can be investigated on the ESCA depth profiling scale by comparing the  $O_{1s}/O_{2s}$  area ratios for the polymers with the ratios previously obtained for the homogeneous thin films of the model compounds, since the escape depth dependencies for the two levels are significantly different.<sup>42</sup> In Fig. 4.3. the valence levels for the alkyl-methacrylates are shown and it is readily seen that the  $O_{2s}$  levels

Table 4.2.

Experimentally Determined Binding Energies for Polyalkyl  
Methacrylate Samples.

Molecule (-R)	Experimental Binding Energies in eV					
	1s Levels				2s Levels	
	<u>-C-O-</u>	<u>C=O</u>	<u>C=O</u>	<u>-O-C</u>	O <sub>2s</sub>	C <sub>2s</sub>
C <sub>1</sub>	534.5	532.9	288.9	286.7	27.4	18
C <sub>2</sub> (n)	534.0	532.5	288.7	286.7	27.4	17
C <sub>3</sub> (iso)	534.2	532.9	288.9	286.8	26.8	16
C <sub>4</sub> (n)	534.3	532.9	288.9	286.6	27.0	16
C <sub>4</sub> (iso)	534.3	532.7	288.8	287.0	27.2	16
C <sub>4</sub> (sec)	534.1	532.7	288.9	286.8	26.8	16
C <sub>4</sub> (tert)	533.9	532.6	288.8	287.0	27.0	16
C <sub>6</sub> (n)	534.1	532.9	288.9	286.9	27.0	16
C <sub>8</sub> (2-EH)	534.3	532.9	288.9	286.9	27.0	16
C <sub>12</sub> (n)	534.2	532.7	288.8	286.7	27.0	16
C <sub>16</sub> (H-D)	534.5	533.0	289.0	286.8	26.8	15
C <sub>18</sub> (n)	534.2	532.6	289.0	286.7	28.6	15

Table 4.3.

Average  $O_{1s}$  and  $C_{1s}$  Absolute Binding Energies and Chemical Shifts  
for the Series of Polymethacrylates.

	$O_{1s}$	$\Delta$	FWHM
$\begin{array}{c} \text{CH}_3 \\   \\ (\text{CH}_2-\text{CH})_m \\   \\ \text{C}=\text{O} \\   \\ \text{O} \\   \\ \text{R}_n \end{array}$	534.4 ± .02	1.4 eV	1.7 ± .01
	533.0 ± .02		1.7 ± .01
$\begin{array}{c} \text{O} \\ // \\ \text{C} \\ \backslash \\ \text{O}-\text{R} \end{array}$	288.8 ± .02	3.8 eV	1.4 ± .01
	286.7 ± .02	1.7 eV	
	285.0 ± .02	0	1.6 ± .01

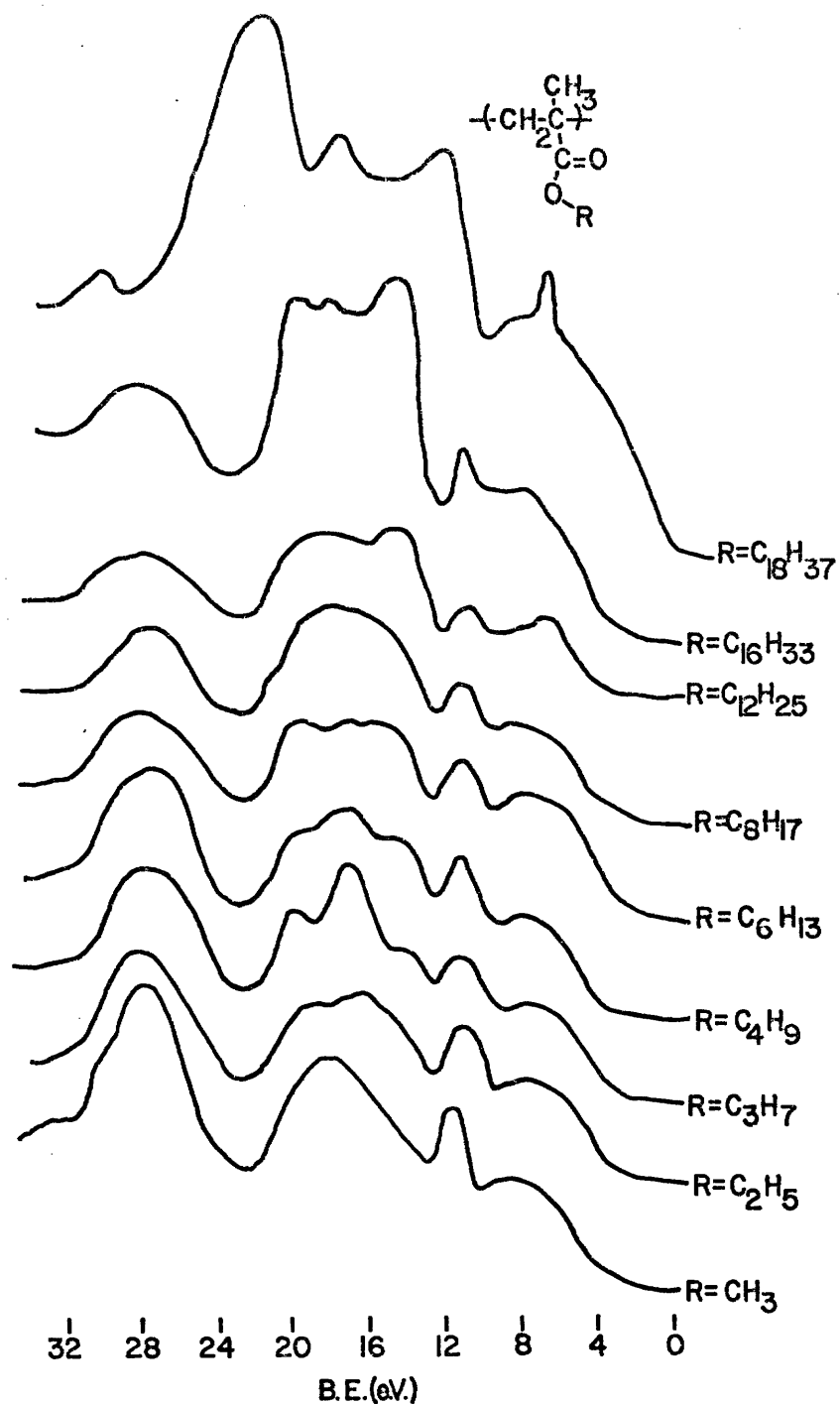


Figure 4.3. Valence Energy Levels for a Series of Polyalkyl Methacrylates.

are sufficiently core like in character to be readily identified, and also that the cross section for photoionization is such that even for the long chain alkyl systems the signals arising from the levels have adequate intensity to be detected. The measured

area ratios for these polymers of  $11 \pm 1$  is within experimental error the same as that for the model systems in the preceding chapter, indicating their homogeneity. As was discussed in Chapter 2 and 3 there are essentially two independent methods of establishing the polymer compositions from ESCA data. First, the  $C_{1s}/O_{1s}$  area ratios, by making use of the instrumentally dependent sensitivity factors; and such an analysis is shown in Fig. 4.4. An excellent correlation is obtained as a function

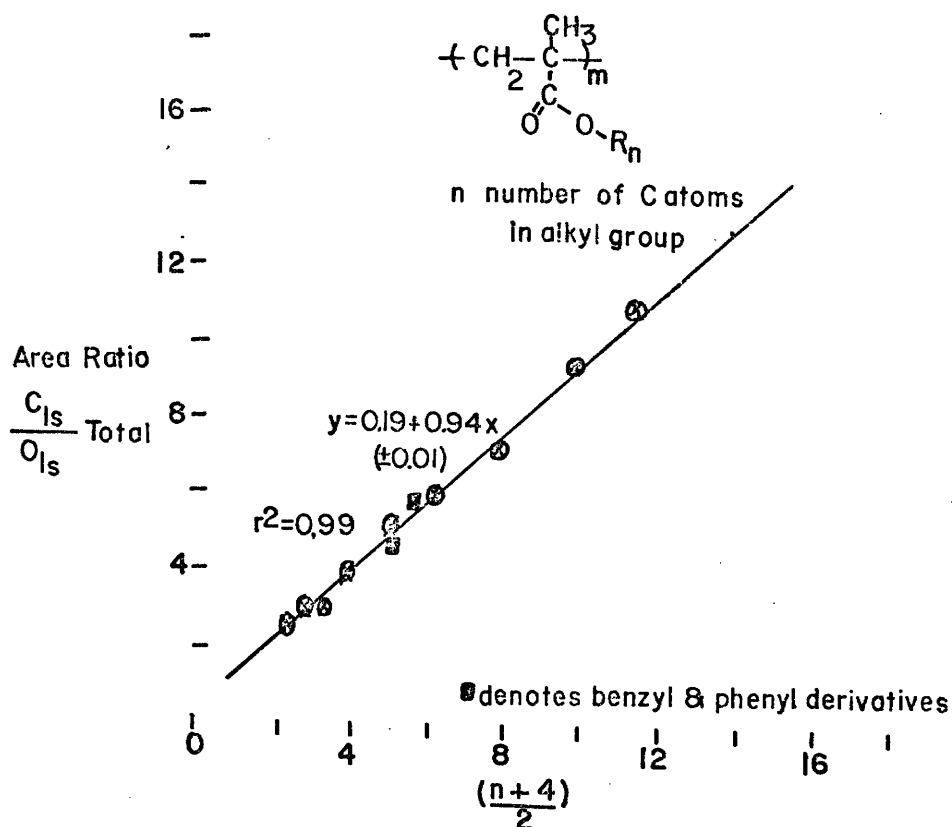


Figure 4.4. Plot of Area Ratios for the  $C_{1s}$  and  $O_{1s}$  Levels of a Series of Polyalkyl- and -aryl-methacrylates as a Function of Chain Length of the Pendant Ester Group.

of the chain length for the alkyl group. The slope of nearly unity (0.94) is in good agreement with theory if the ESCA experiment statistically samples the repeat units of the polymer with no evidence for specific orientation of the alkyl side chains. The second method involves the relevant component peaks of the  $C_{1s}$  levels using the area ratios for the individual components, corresponding to given structural features, and these again show an excellent correlation as is evident from Fig. 4.5.

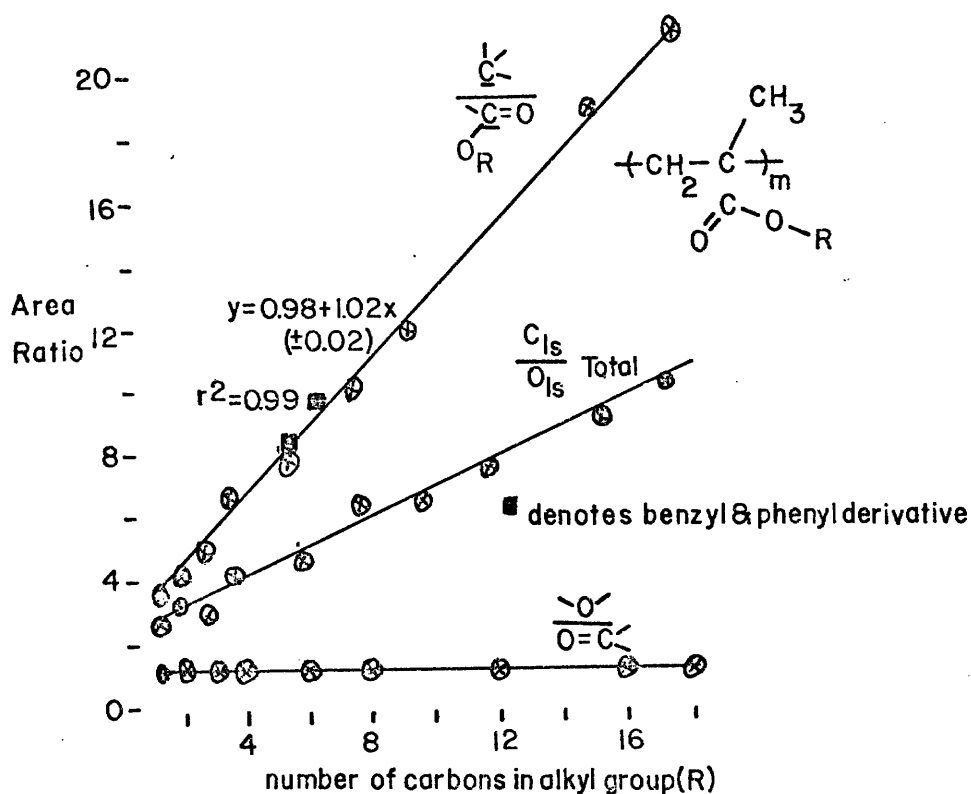


Figure 4.5. Plot of Area Ratios for the Core Levels Versus Number of Carbons on the Alkyl Group of a Series of Poly-alkyl- and -aryl-methacrylates. (These have been corrected for differences in cross section and instrumental sensitivity (see text)).

The  $C_{1s}$  spectra of the polyphenyl methacrylate and polybenzyl methacrylate samples both show, in addition to the characteristic peaks arising from the chemically shifted structural features, low intensity peaks to the high binding energy side of the main spectra arising from  $\pi \rightarrow \pi^*$  transitions accompanying core ionizations in the aromatic systems.<sup>40,41</sup> It is interesting to note that when due allowance is made for the shake-up processes the data for both of these samples yield an excellent correlation, as is evident from Figs. 4.4 and 4.5. The observation of shake-up phenomena therefore gives a straightforward means of distinguishing between samples which fit these two correlations identically, as is the case for polyhexyl- and polyphenyl-methacrylates. The ESCA data suggests, therefore, that the outermost few tens of Angstroms of the polymer films studied are representative of the bulk and that composition, integrity, and homogeneity of the immediate surface can routinely be established.

In the particular case of polymethyl methacrylate the four commercially available samples which were studied spanned a considerable range in molecular weights, all with MWD's of  $\sim 2$ . The spectra obtained from these samples however were identical, and this again is consistent with a statistical sampling of the repeat unit on the ESCA depth profiling scale. The method of synthesis<sup>57</sup> for all of the polymer samples would suggest that the materials are largely atactic, however as noted in Chapter 3 from the study of the model polyacrylate systems, ESCA is a relatively insensitive tool for investigating tacticities in the solid state.<sup>35,37,39</sup>

In the particular cases of polymethyl-, polylauryl- and polyoctadecyl methacrylates, spanning the range in side chain complexity, the measured contact angles were closely similar which is readily understandable in terms of the ESCA analysis.

(b) Valence Levels of Polymethacrylates.

The model systems discussed in Chapter 3 together with literature data pertaining to UPS studies on related compounds<sup>53</sup> provide a sound foundation for the overall interpretation of the main features of the valence bands of the polymers studied.

The measured valence energy levels for the polyalkyl methacrylates, in Fig. 4.3 show clearly that the overall band profiles are 'fingerprints' for each particular polymer system and this becomes much more evident from the data for the isomeric polybutylmethacrylates shown in Fig. 4.6, for which the core levels (Fig. 4.7) are closely similar. As might have been expected these results parallel those on the polyalkylacrylates and the main features of the assignment of levels follow along similar lines.

(v) ESCA Studies of Adsorption at Surfaces.

Clark has discussed<sup>42</sup> the great surface sensitivity of ESCA and it may be used to considerable advantage in studying the hydration of surface features on polymers capable of participation in hydrogen bonding. Such studies are likely to be of considerable importance in detailing the complexities of, for example, triboelectric charging and various aspects of tribochemistry. In the particular case of low density polyethylene the adsorption of H<sub>2</sub>O on surface carbonyl features

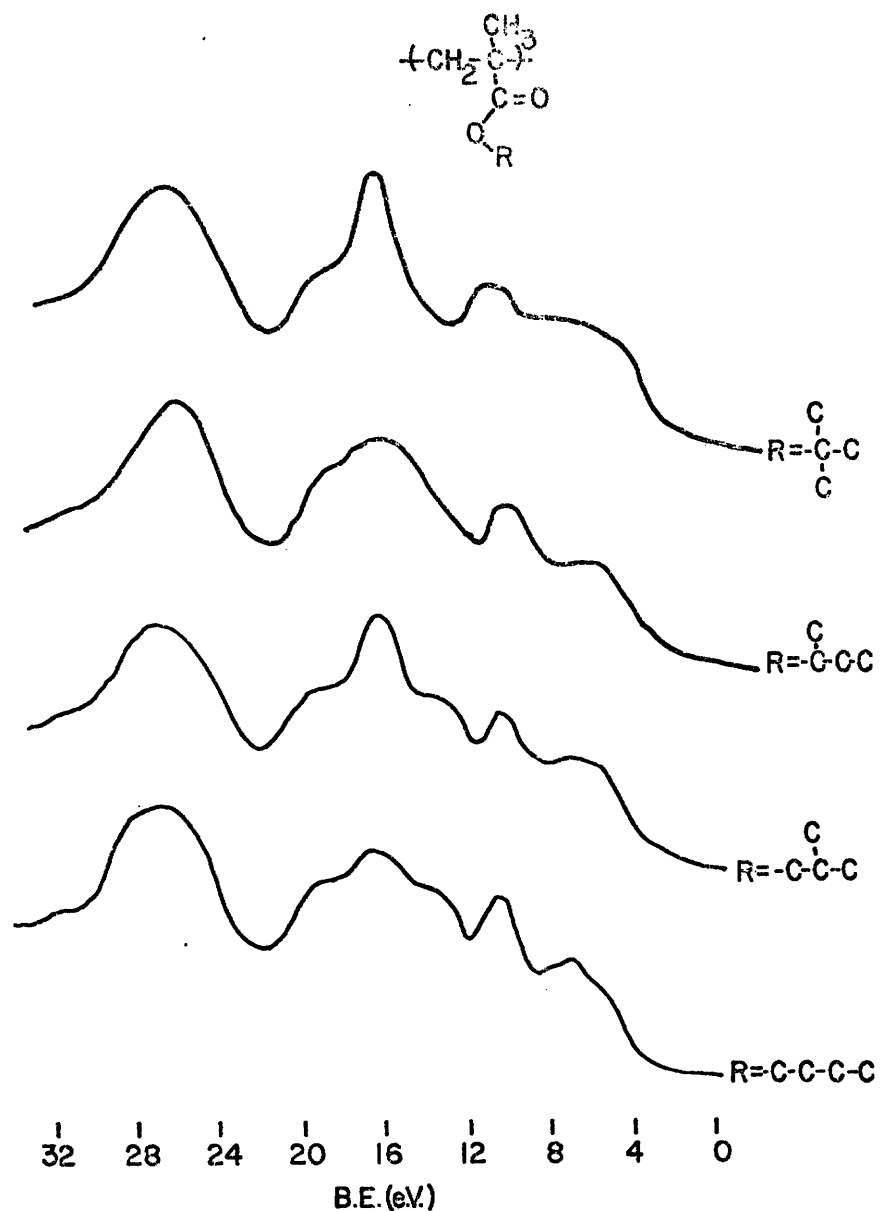


Figure 4.6. Measured Valence Energy Levels of Poly-n-, -iso-, -sec-, and -tert-butylmethacrylates.

manifests itself in terms of the appearance of a shoulder to the high binding energy side of the  $O_{1s}$  levels associated with the carbonyl oxygen and attributed to the hydrogen bonded water.<sup>42</sup> Careful double beam infrared studies revealed no evidence for such

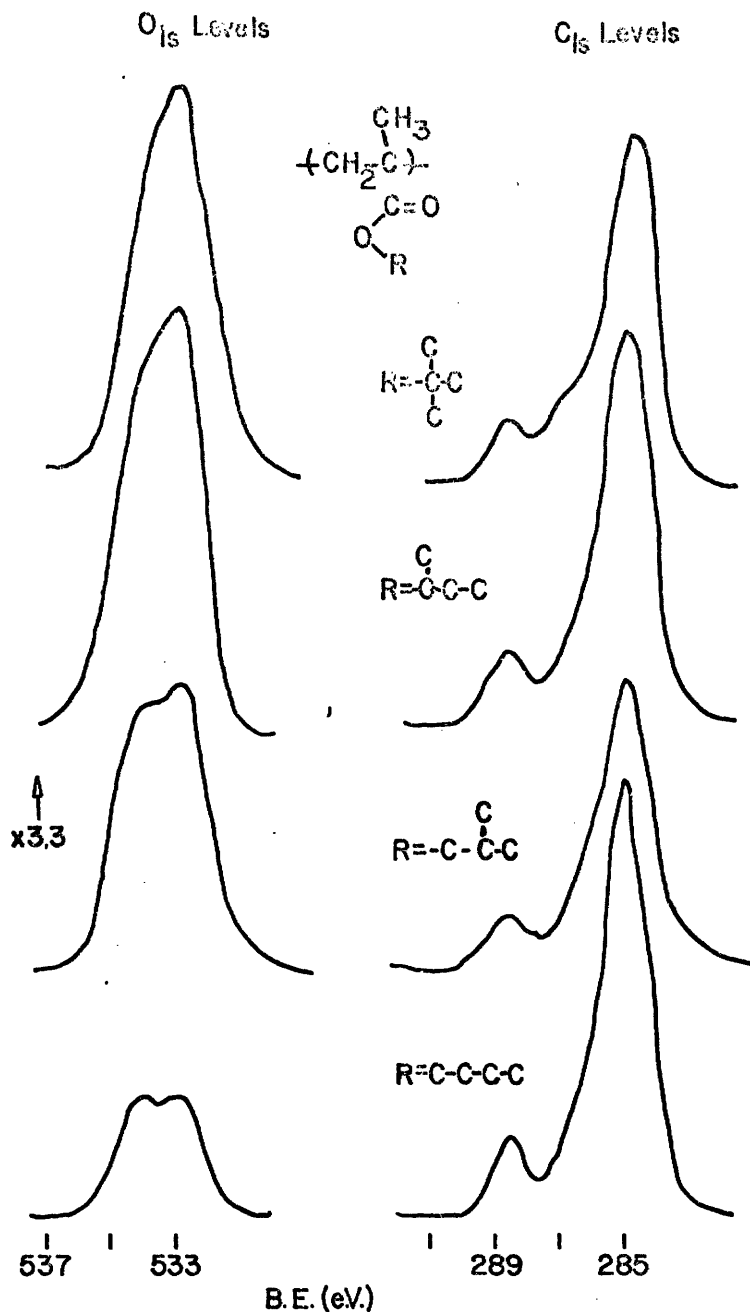


Figure 4.7. Core Level Spectra for Poly-n-, -iso-, -sec- and -tert-butylmethacrylates.

interactions since they are localized at the surface. In continuance of the work on the polyalkylacrylate systems the interaction of hydrogen bonding species with the surface of polyisopropyl methacrylate films has been investigated.

Fig. 4.8 shows the  $O_{1s}$  and  $C_{1s}$  levels for samples of polyisopropyl methacrylate that were exposed to  $NH_3$ ,  $H_2O$  and HF. These represent an order of increasing hydrogen bond strength, and it is apparent from the spectra that as in the case of the polyisopropyl acrylate, discussed in the last chapter, it is only in the case of the HF treatment that the spectra reveal any significant change.

A sharpening of the  $O_{1s}$  levels, such that the carbonyl and ester type oxygens are more distinguishable without recourse to line shape analysis, is apparent. The overall signal intensity for the  $O_{1s}$  and  $C_{1s}$  levels is also decreased due to the adsorbed HF on the surface of the film, which can be identified by the low absolute binding energy for the  $F_{1s}$  levels.

As has been discussed in the preceding chapter the overall effects of the absorption study are identical to the polyisopropyl acrylate with the  $H_2O$  and  $NH_3$  treatments showing little or no effects on the linewidths.

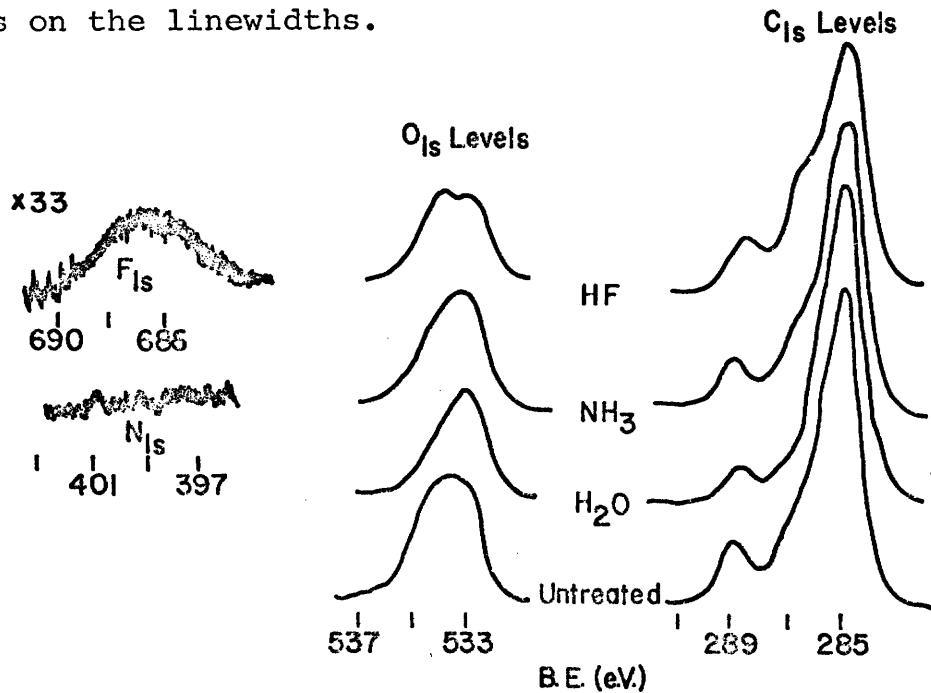
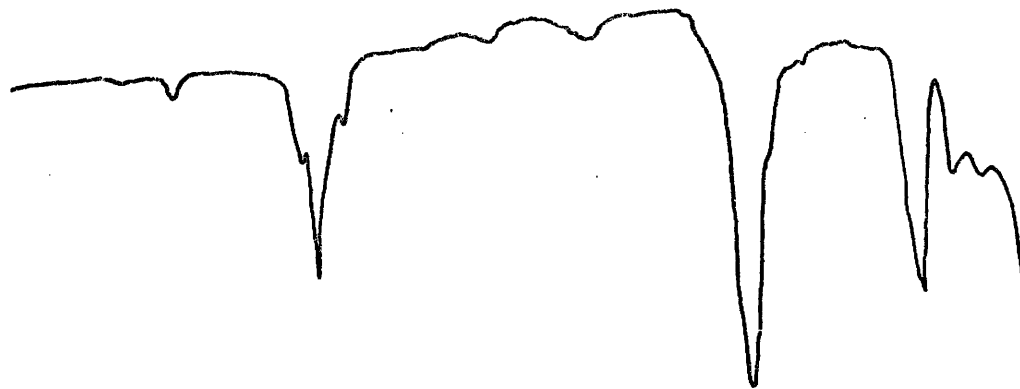


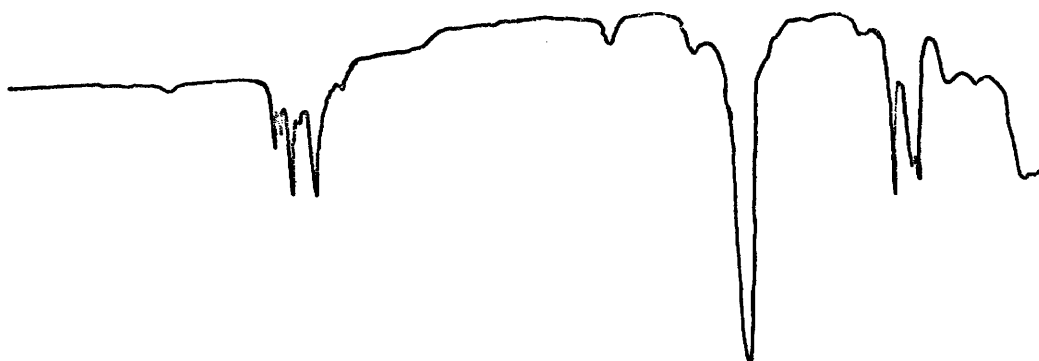
Figure 4.8.  $O_{1s}$  and  $C_{1s}$  Core level Spectra for Samples of Polyisopropyl Methacrylate Surface Treated with  $H_2O$ ,  $NH_3$  and HF.

APPENDIX A

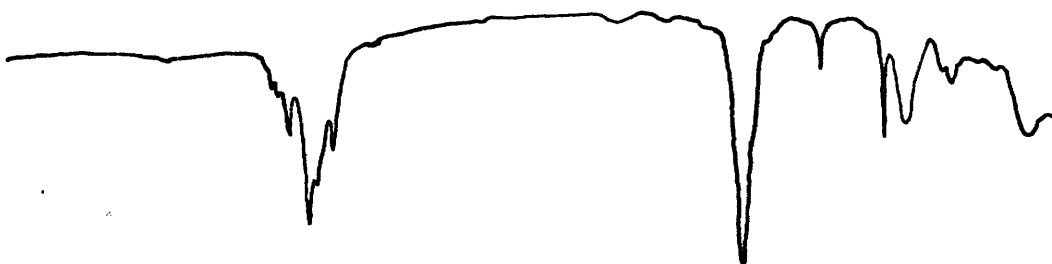
Infrared Spectra of Polyalkyl Acrylates and Ethyl Aceto-  
acetate



Polymethyl Acrylate (crosslinked)



Polymethyl Acrylate (extracted)

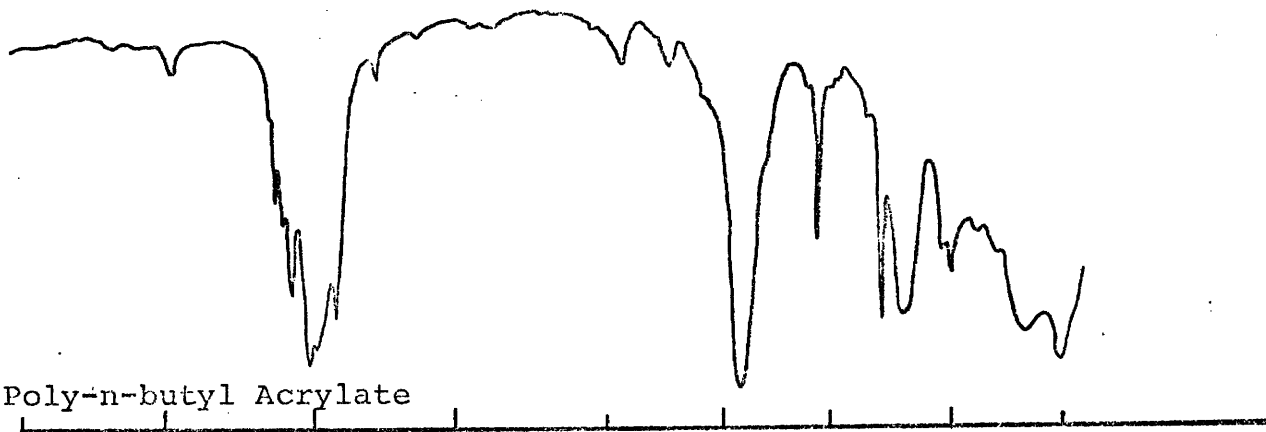


Polyethyl Acrylate

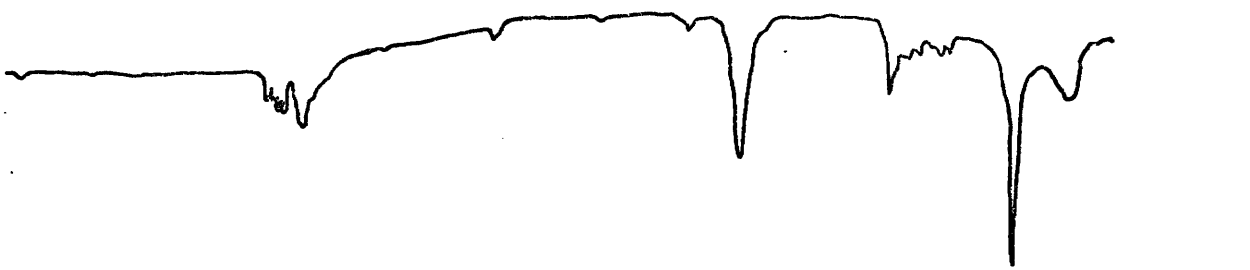


Poly Isopropyl Acrylate

4000 3500 3000 2500 2000 1800 1600 1400 1200  
wavenumber (cm.<sup>-1</sup>)



Poly-n-butyl Acrylate



Poly-iso-butyl Acrylate



Poly-tert-butyl Acrylate

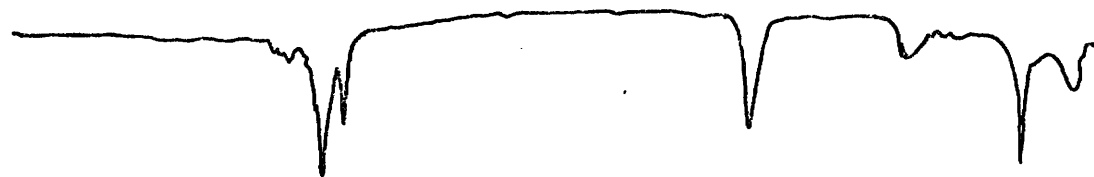


Poly-2-ethylhexyl Acrylate

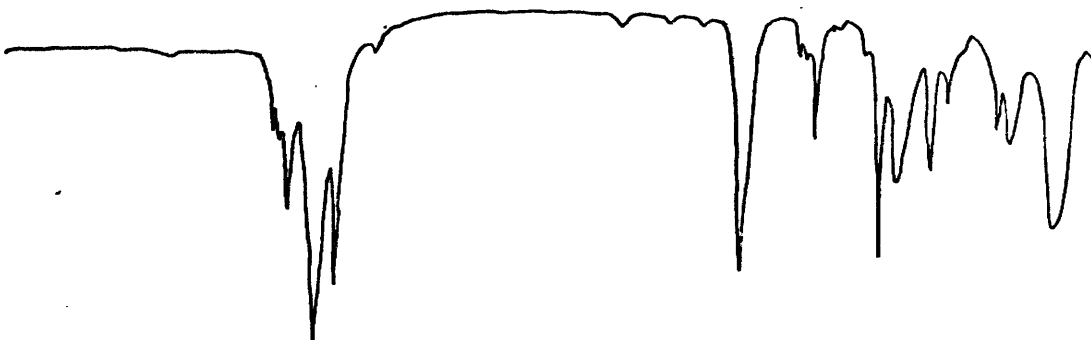
4000 3500 3000 2500 2000 1800 1600 1400 1200  
wavenumber (cm.<sup>-1</sup>)



Poly-n-decyl Acrylate



Poly-n-lauryl Acrylate

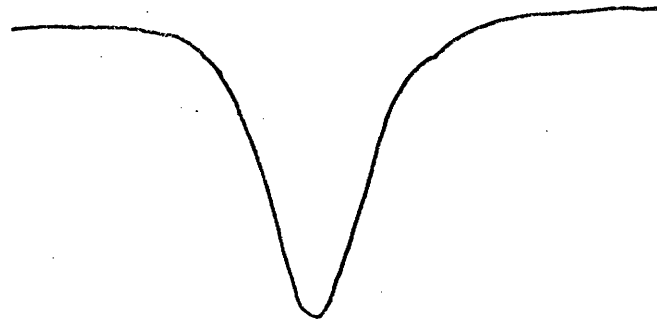


Poly-hexadecyl Acrylate



Polyoctadecyl Acrylate

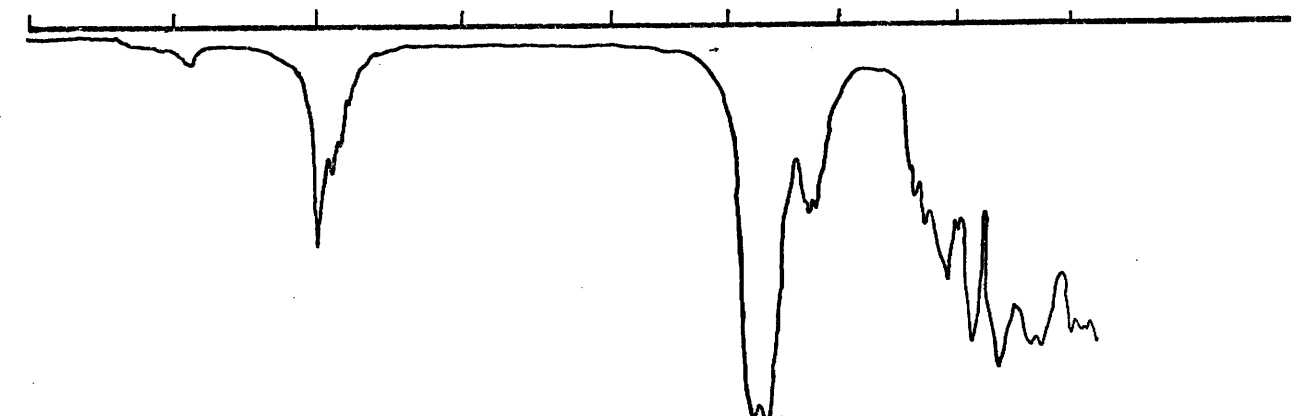
4000 3500 3000 2500 2000 1800 1600 1400 1200  
wavenumber (cm.<sup>-1</sup>)



Poly-isopropyl Acrylate [C=O region (Abscissa X5)]



Poly-n-decyl Acrylate [C=O region (Abscissa X5)]

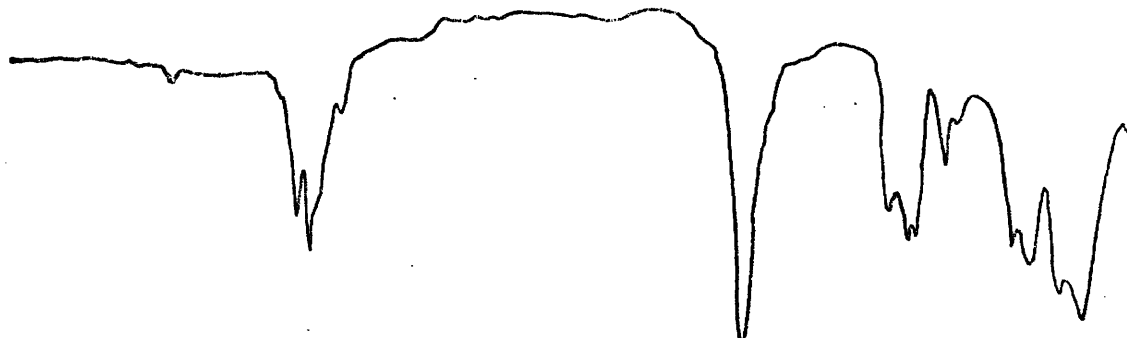


Ethyl Acetoacetate (C-H and C=O regions)

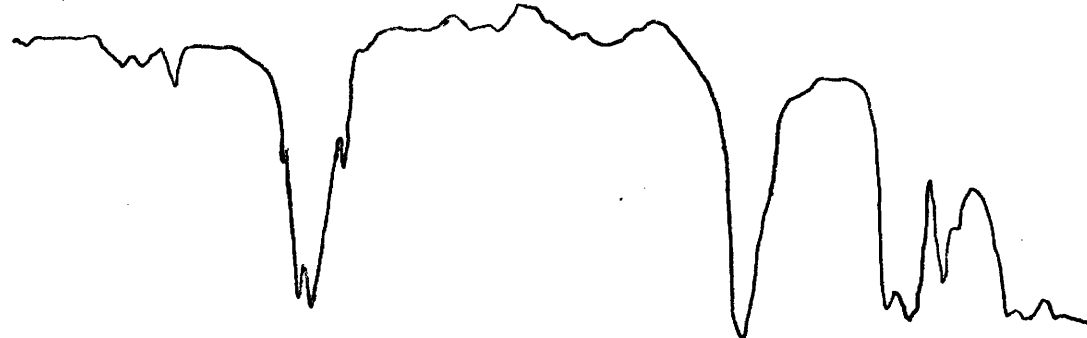
4000 3500 3000 2500 2000 1800 1600 1400 1200  
wavenumber (cm.<sup>-1</sup>)

APPENDIX B

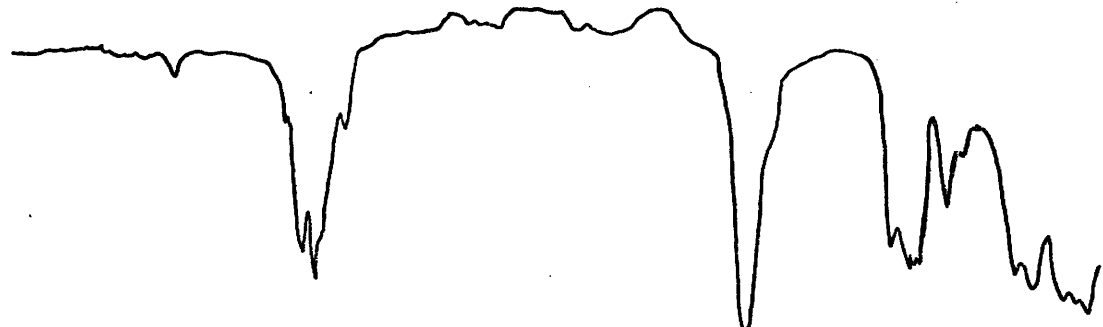
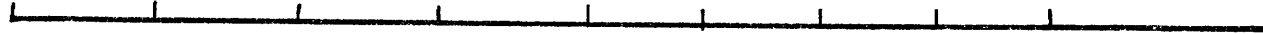
Infrared Spectra of Poly-alkyl- and -aryl-methacrylates



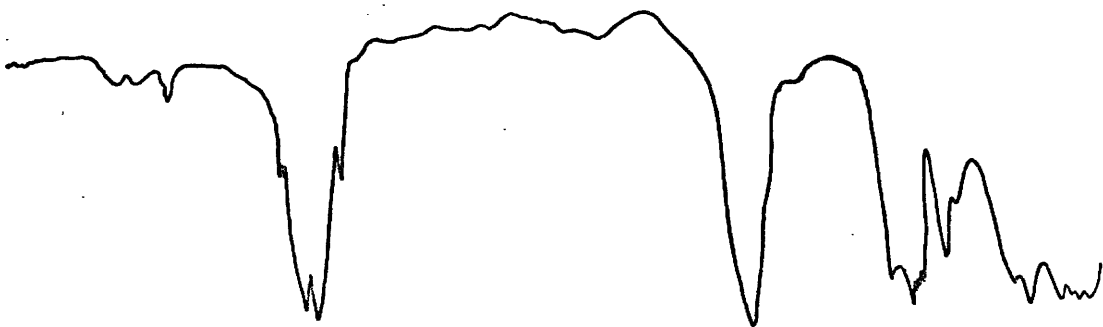
Polymethyl Methacrylate (low  $\bar{M}_w$ )



Polymethyl Methacrylate (med.  $\bar{M}_w$ )



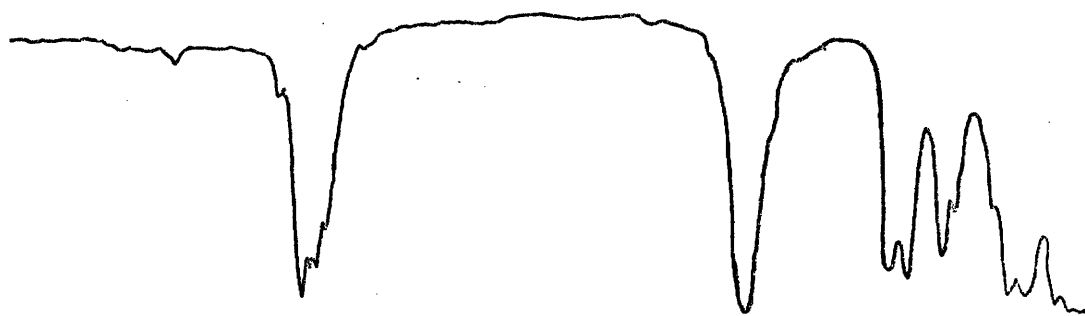
Polymethyl Methacrylate (high  $\bar{M}_w$ )



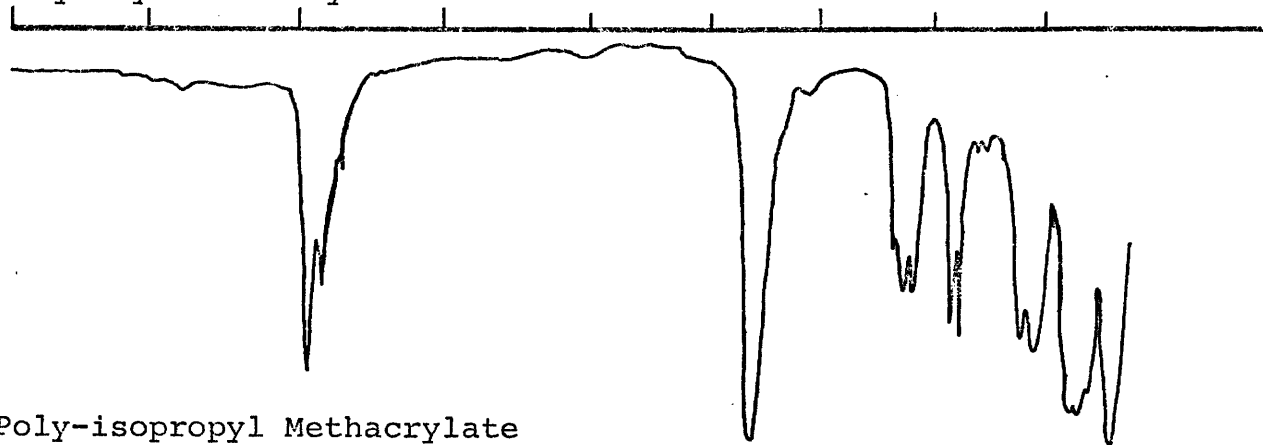
Polymethyl Methacrylate (very high  $\bar{M}_w$ )



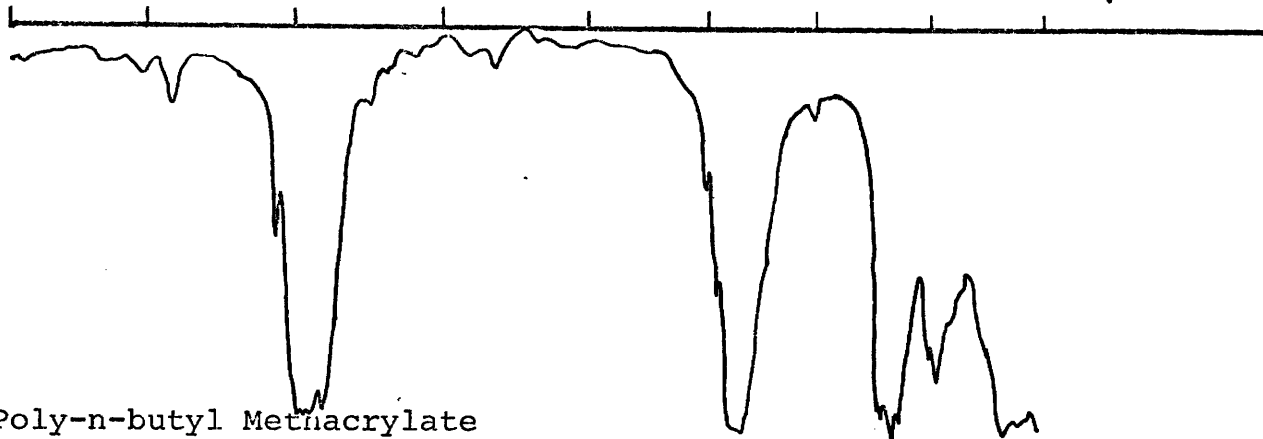
4000 3500 3000 2500 2000 1800 1600 1400 1200  
wavenumber ( $\text{cm.}^{-1}$ )



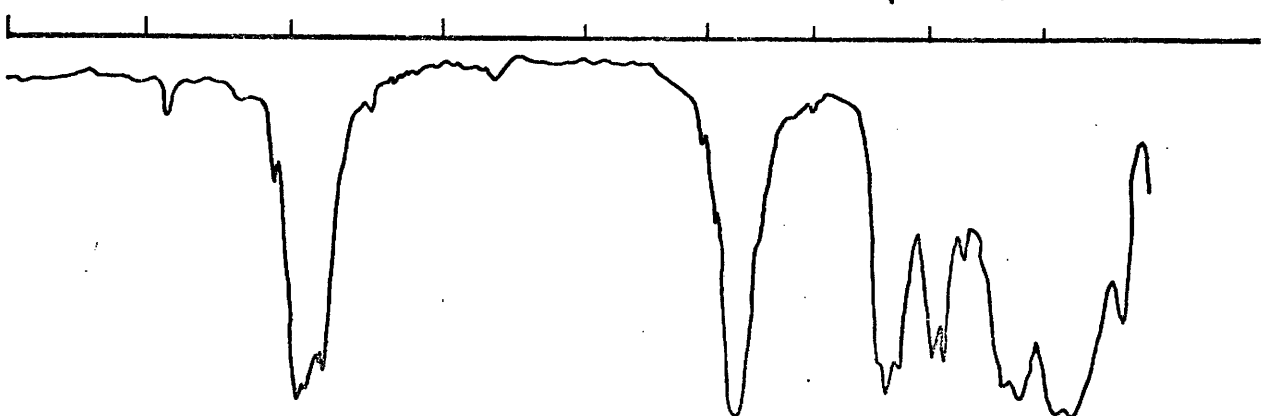
Polyethyl Methacrylate



Poly-isopropyl Methacrylate

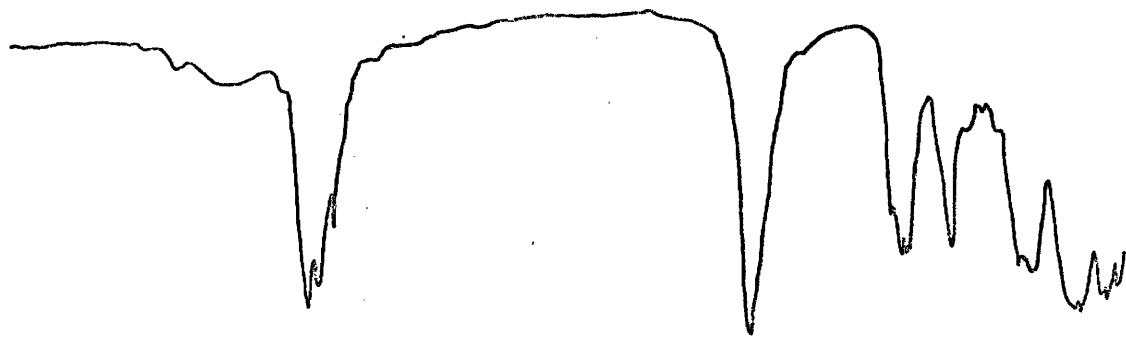


Poly-n-butyl Methacrylate



Poly-iso-butyl Methacrylate

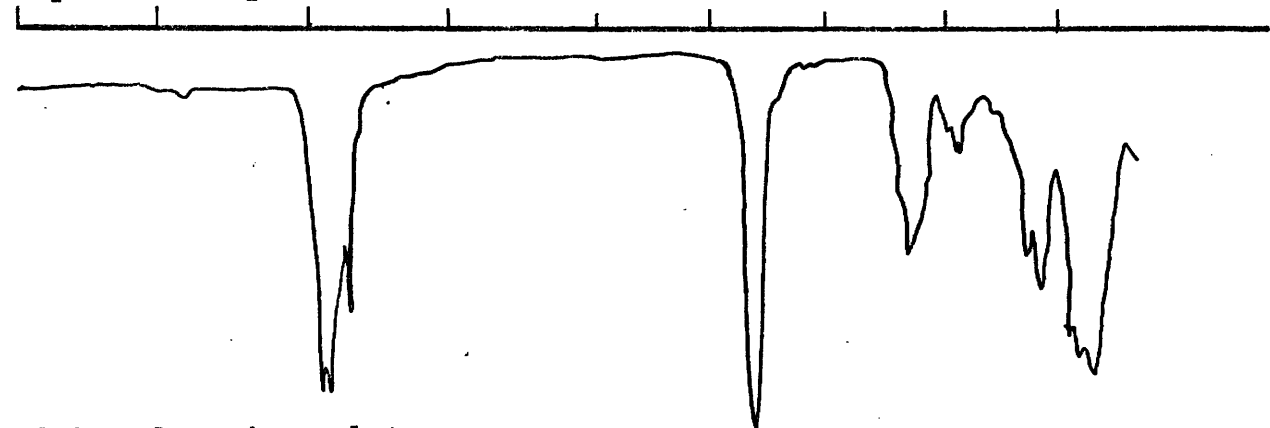
4000 3500 3000 2500 2000 1800 1600 1400 1200  
wavenumber (cm.<sup>-1</sup>)



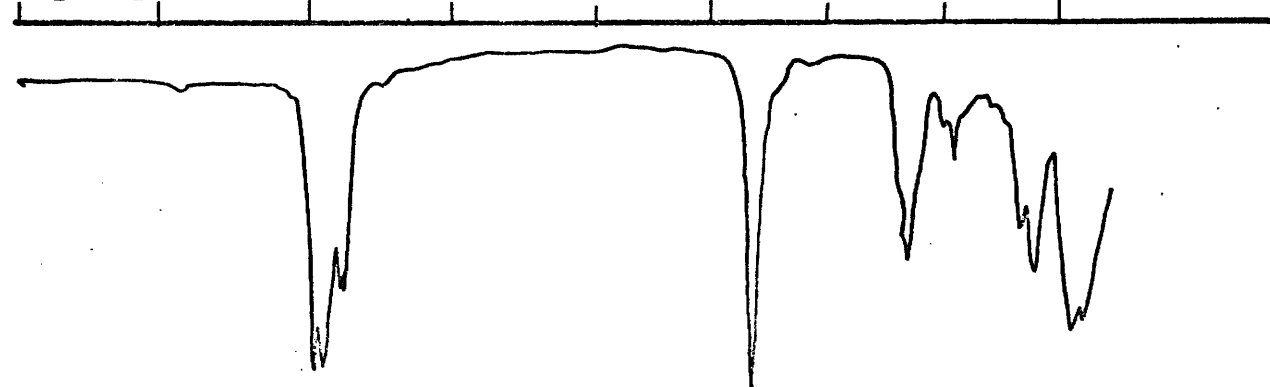
Poly-sec-butyl Methacrylate



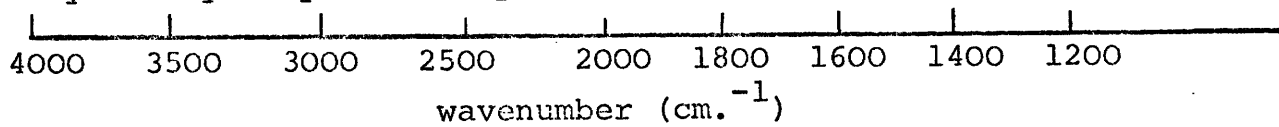
Poly-tert-butyl Methacrylate

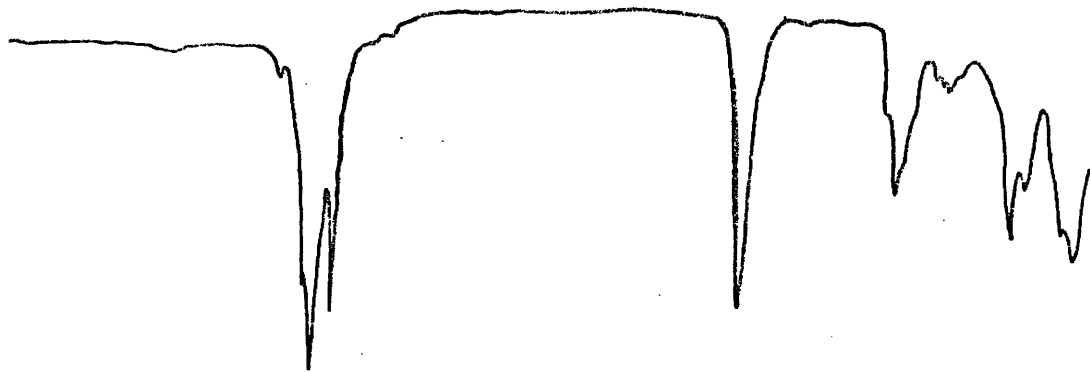


Polyhexyl Methacrylate

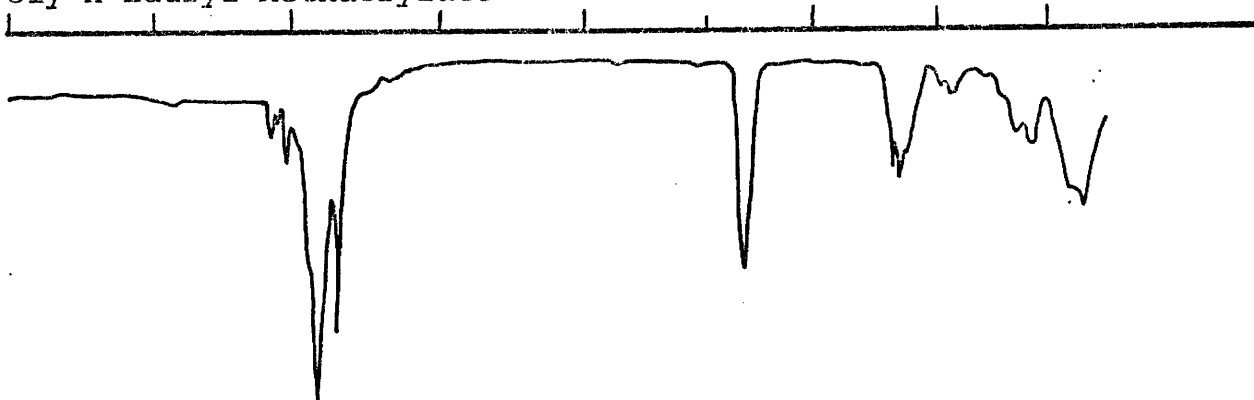


Poly-2-ethylhexyl Methacrylate

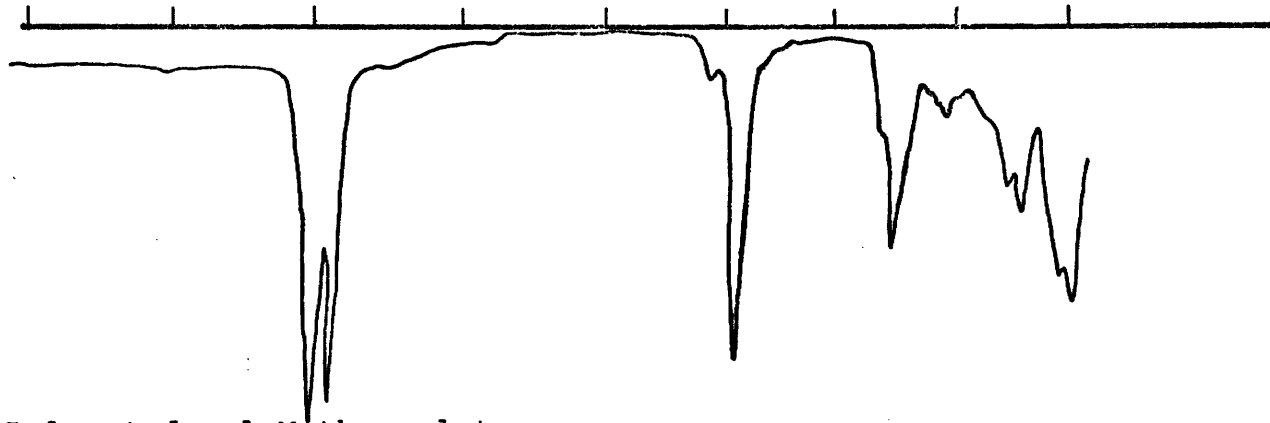




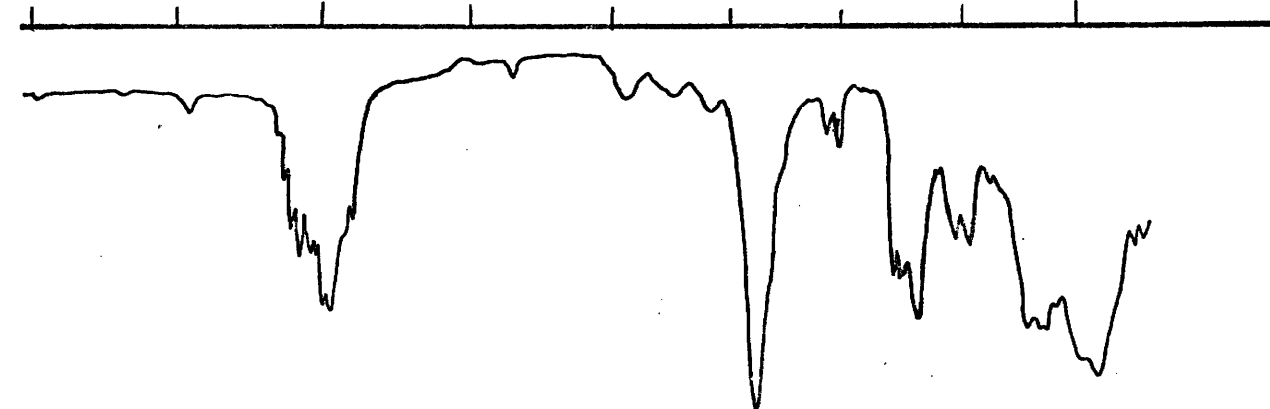
Poly-n-Lauryl Methacrylate



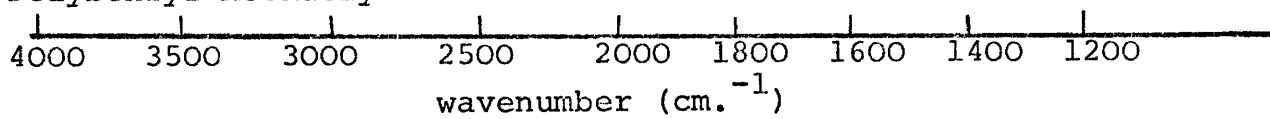
Poly-hexadecyl Methacrylate

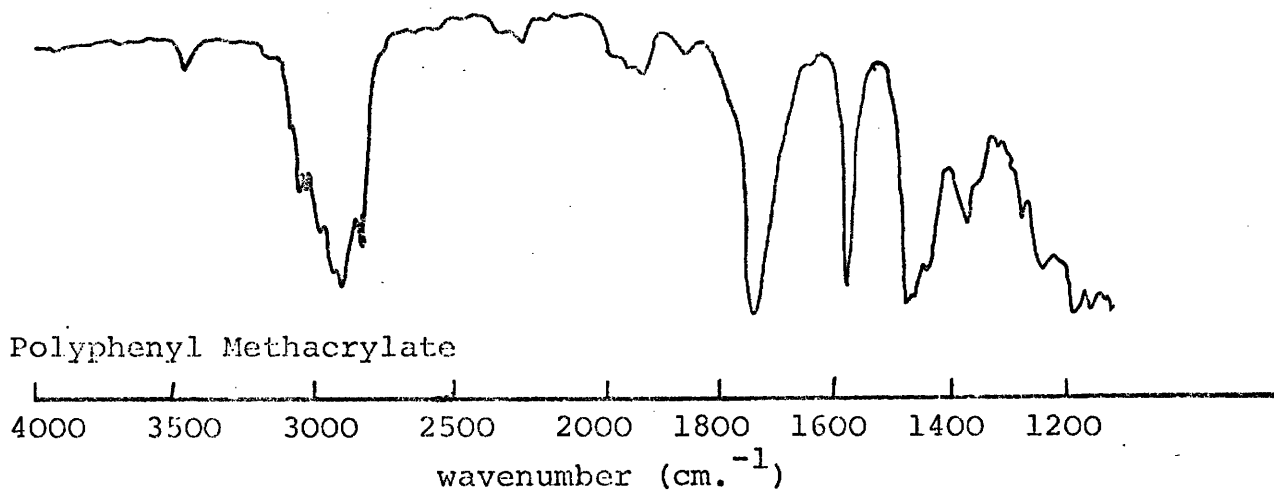


Polyoctadecyl Methacrylate



Polybenzyl Methacrylate





REFERENCES

1. D.W. Turner, C. Baker, A.D. Baker, C.R. Brundle 'Molecular Photoelectron Spectroscopy', Wiley-Interscience (1970).
2. D.E. Eastman, 'Photoemission Spectroscopy of Metals', in 'Techniques in Metals Research VI', ed. E. Passaglia, Wiley-Interscience (1972).
3. C.C. Chang, Surface Science, 25, 53-75 (1971).
4. J.P. Coad, M. Gettings and J.C. Riviere, Faraday Discussions, 60, Vancouver, July 1975, Paper 21.
5. K. Siegbahn, C. Nordling, G. Johansson, J. Hedman, P.F. Heden, K. Hamrin, U. Gelius, T. Berkmark, L.D. Werme, R. Manne and Y. Baer, 'ESCA Applied to Free Molecules', North-Holland Publ. Co., Amsterdam (1969).
6. K. Siegbahn, C. Nordling, A. Fahlman, R. Nordberg, K. Hamrin, J. Hedman, G. Johansson, T. Berkmark, S.E. Karlsson, I. Lidgren and B. Lindberg, 'ESCA, Atomic, Molecular and Solid State Structure Studied by Means of Electron Spectroscopy' Almquist and Wiksells, Uppsala (1967).
7. L. Asbrink, Chem. Phys. Lett., 7, 549 (1970)
8. L. Asbrink and J.W. Kabalais, Chem. Phys. Lett., 12, 182 (1972).
9. R.E. Weber and W.T. Peria, J. Appl. Phys., 38, 3320 (1967).
10. H.D. Hagstrum and G.E. Becker, Phys. Rev. Letts., 22, 1054 (1969)
11. A.E. Sandström, in S. Flügge, Handbook of Physics, Vol. XXX, X-Rays, p.164 (Springer-Verlag, Berlin, 1957).
12. C.D. Wagner, Faraday Discussion, 60, Paper 23 (1975).
13. J.F. McGilp and I.G. Main, J. Elect. Spect. and Related Phen., 63, 97-409 (1975).
14. P. Ascarelli and G. Missoni, Ibid., 5, 417-435 (1974).

15. G. Johansson, J. Hedman, A. Berndtson, M. Klasson and R. Nilsson, *Ibid.*, ref. 13, 2, 295-317 (1973).
16. J.P. Contour and G. Mouvier, *J. Elect. Spect. and Related Phen.*, 7, 85-90 (1975).
17. D.T. Clark, W.J. Feast, W.K.R. Musgrave and I. Ritchie, *J. Poly. Sci.*, 13, 857-890 (1975).
18. T.A. Koopmans, *Physica*, 1, 104 (1933).
19. U. Gelius, *Phys. Scripta*, 9, 133 (1974).
20. M. Barber and D.T. Clark, *J. Chem. Soc.*, D, 22 (1970).
21. D.B. Adams, D.T. Clark, *Theoret. Chim. Acta.* (Berl.), 31, 171 (1973).
22. D.T. Clark, I.W. Scanlan, J. Müller, *Theoret. Chim. Acta* (Berl), 35, 341 (1974).
23. U. Gelius, *Disc. Fara. Soc.*, 54 (1972).
24. R.E. Watson and A.J. Freeman, *Hyperfine Interactions* (Ed. A.J. Freeman and R.B. Frankel), Academic Press, New York (1967).
25. C.S. Fadley, D.A. Shirley, A.J. Freeman, P.S. Bagus and J.V. Mallow, *Phys. Rev. Lett.*, 23, 1397 (1969).
26. T. Novakov and J.M. Hollander, *Bull. Am. Phys. Soc.*, 14, 524 (1969).
27. T. Novakov and J.M. Hollander, *Phys. Rev. Lett.*, 21, 1133 (1968).
28. C.S. Fadley, Lecture Series, 'N.A.T.O. Advanced Study Institute on Electron Emission Spectroscopy', Ghent University, Ghent, Belgium, August 28 - September 8, 1972.
29. T.A. Carlson, W.E. Hunt and M.O. Krause, *Phys. Rev. Lett.*, 151, 41 (1966).

30. R. Manne and T. Aberg, Chem. Phys. Letts., 21, 1133 (1968).
31. R.M. Eisenberg, Fundamentals of Modern Physics, Ch. 14, John Wiley and Sons, Inc. (1961).
32. U. Gelius, E. Basilier, S. Svensson, T. Bergmark and K. Siegbahn, J. Elect. Spect. and Rel. Phen., 2, 405 (1973).
33. E.M. Purcell, Phys. Rev., 54, 818 (1938).
34. J.C. Helmer and N.H. Weichert, Appl. Phys. Lett., 13, 268 (1968).
35. D.T. Clark, D. Kilcast, W.J. Feast, and W.K.R. Musgrave, J. Polym. Sci., Polym. Chem. Ed., 11, 389 (1973).
36. D.T. Clark, 'Elect. Emission Spect!', W. Dekeyser, et al. (eds.), 373-507, D. Reidel Publishing Co., Dordrecht, Holland (1973).
37. D.T. Clark, W.J. Feast, I. Ritchie and W.K.R. Musgrave, J. Polym. Sci., Poly. Chem. Ed., 12, 1049 (1974).
38. D.T. Clark, J. Peeling and J.M. O'Malley, J. Poly. Sci. Polym. Chem. Ed., in press (1975).
39. D.T. Clark, D. Kilcast, W.J. Feast, and W.K.R. Musgrave, J. Polym. Sci., A-1, 10, 1637 (1972).
40. D.T. Clark, A. Dilks, J. Peeling, and H.R. Thomas, Trans. Faraday Soc., Faraday Disc., 60, No. 14 (1974), 000.
41. D.T. Clark and A. Dilks, J. Polym. Sci., Polym. Chem. Ed., in press (1975).
42. Cf. D.T. Clark, 'Advances in Polymer Friction and Wear', 5A, 241 (1974), Ed. L.H. Lee, Plenum Press, N.Y. (1974).
43. J. Brandrup and E.H. Immergut (Eds.), 'Polymer Handbook', Interscience Publishers, New York (1967).
44. 'Reactivity, Mechanism and Structure in Polymer Chemistry' eds. A.D. Jenkins and A. Ledwith, J. Wiley and Sons, London (1974).

45. P.L. Magagnini, A. Marchetti, F. Matera, G. Pizzirani, and G. Turchi, Eur. Poly. J., 10, 585-91 (1974).
46. A. Tanaka and Y. Ishida, J. Poly. Sci., 13, 431-36 (1975).
47. B. Arkles and W.R. Peterson, 'Advances in Polymer Friction and Wear', 5B, 453 (1974) Ed. L.H. Lee, Plenum Press, N.Y. (1974).
48. I.H. Hiller, V.R. Saunders, Atlas Computer Laboratory, (1972).
49. R.F. Stewart, J. Chem. Phys., 50, 2485 (1969).
50. E. Clementi, IBM J. Res. Develop. Suppt., 9, 2 (1965).
51. J.A. Pople and D.L. Beveridge, 'Approximate Molecular Orbital Theory', McGraw-Hill (1970).
52. D.T. Clark, D. Kilcast, and D.B. Adams, Farad. Disc. Chem. Soc., 54, 182 (1972).
53. A.W. Potts, T.A. Williams and W.C. Price, Disc. Farad. Soc., 54, 104 (1972).
54. Cf. K. Siegbahn, J. Elect. Spect., 5, 3 (1974).
55. L.E. Sutton, 'Tables of Interatomic Distances', Chemical Society, London, Special publication, No. 18, 1965.
56. D.T. Clark and D.M.J. Lilley, Tetrahedron, 29, 845 (1973).
57. Re. Cellomer Associates, Inc., private communication (1975).